Nf1-DEFICIENT MICE DISPLAY SOCIAL LEARNING DEFICITS THAT ARE RESCUED BY THE DELETION OF *PAK1* GENE

John Paul Spence

Submitted to the faculty of the University Graduate School
in partial fulfillment of the requirements
for the degree
Doctor of Philosophy
in the Program in Medical Neuroscience,
Indiana University

December 2010

Accepted by the Faculty of Indiana University, in partial
fulfillment of the requirements for the degree of Doctor of Philosophy.

_____

Anantha Shekhar, M.D., Ph.D., Chair

_____

D. Wade Clapp, M.D.

Doctoral Committee

_____

Philip L. Johnson, Ph.D.

August 9, 2010

_____

Feng-Chun Yang, M.D., Ph.D.

This work is dedicated to my daughter,

Mary Louise Spence,

who was born on October 6, 2009.

ACKNOWLEDGMENTS

First, I would like to thank Dr. Anantha Shekhar for his help and guidance throughout my graduate career. His advice and support has made these years not only a learning experience, but an enjoyable experience as well. In addition, I am sincerely grateful that he has made my education a priority in his busy schedule.

I would also like to thank the other members of my research committee: Dr. Wade Clapp, Dr. Philip Johnson and Dr. Feng-Chun Yang. With their input they have provided me with a broad, but focused perspective of the scientific process. Through their guidance and constructive criticism, I have developed substantially as a scientist.

I am also grateful for the help and financial support that I received from Dr. Shekhar's and Dr. Clapp's laboratories and Indiana Clinical and Translational Science Institute (CTSI). While many people helped me throughout my graduate career, I would like to specifically thank several individuals for their efforts that directly contributed to the completion of this dissertation. I would like to thank Matt Shew and Gracie Michels for animal breeding, and Amy Dietrich for helping me score the mouse social behavior tests. I also would like to thank Dr. Andrei Molosh for his efforts to complete the electrophysiology studies, and Dr. Weiguo Zhu for his help with Western blotting. Additionally, I would like to thank Dr. Rajesh Khanna for his help in dissection, cell culture, and Western blotting. I would also like to thank Dr. Yehia Mechref, Dr. Lang Li, Dr. Zaneer Segu, and Dr. Chirayu Goswami for their help with various aspects of the protein studies.

Finally, I would like to thank my family and friends for their support during this process. Their advice and inspiration has enabled me to navigate the ups and downs associated with academic research. Above all, I would like to thank my wife Bett who has stood by my side throughout my graduate career. I am eternally grateful for her love and patience.

ABSTRACT

John Paul Spence

Nf1-DEFICIENT MICE DISPLAY SOCIAL LEARNING DEFICITS THAT ARE RESCUED BY THE DELETION OF *PAK1* GENE

Neurofibromatosis type 1 (NF1) is a neurocutaneous disorder that affects roughly 1 in 3500 individuals. In addition to physical features (e.g., neurofibromas), developmental disorders are also common that can affect cognition, learning, attention and social function. The *NF1* gene encodes neurofibromin, a GTPase activating protein (GAP)-like protein that negatively regulates Ras GTPase activation. Mutation at the *NF1* locus increases the output of MAPK and PI3K signal transduction from the cellular membrane to the nucleus. Similar to humans, $Nf1^{+/-}$ mice show spatial learning abnormalities that are potentially correlated with increases in GABA-mediated inhibition and deficits in long-term potentiation in the hippocampus. Here, we demonstrate for the first time that $Nf1^{+/-}$ mice exhibit a selective loss of long-term social learning / memory and increased GABAergic inhibition in the basolateral amygdala, a critical brain region for regulating social behaviors. Next, utilizing a genetic intercross, we show that the co-deletion of p21-activated kinase type 1 ($Pak1^{-/-}$), which positively regulates MAPK activation, restores $Nf1^{+/-}$-dependent MAPK hyperactivation in neurons cultured from the frontal cortex. We found that the co-deletion of *Pak1* in $Nf1^{+/-}$ mice ($Nf1^{+/-}$ / $Pak1^{-/-}$) also restores the deficits in long-

term social learning / memory seen in *Nf1*$^{+/-}$ mice and normalizes the increases in GABA-mediated inhibition in the BLA, as compared to *Nf1*$^{+/-}$ mice. Together, these findings establish a role for *Nf1* and *Pak1* genes in the regulation of social learning in *Nf1*-deficient mice. Furthermore, proteomic studies identify dysregulation of F-actin and microtubule dynamics in the prefrontal cortex, and implicate proteins associated with vesicular release as well as neurite formation and outgrowth (e.g., LSAMP, STXBP1, DREB). In the BLA, disintegrin and metalloproteinase domain-containing protein 22 (ADAM22) was identified, and ADAM22 may play a role in the regulation of AMPA receptors. Finally, due to the increased co-occurrence of NF1 and autism, these findings may also have important implications for the pathology and treatment of NF1-related social deficits and some forms of autism.

Anantha Shekhar, M.D., Ph.D., Chair

TABLE OF CONTENTS

ABBREVIATIONS

AC	Adenylyl cyclase
ACSF	Artificial cerebrospinal fluid
ADHD	Attention deficit hyperactivity disorder
AKT	Protein kinase B
BLA	Basolateral Amygdala
cAMP	Cyclic adenosine monophosphate
CNS	Central nervous system
CPP	3-(2-carboxypiperazin-4-yl)propyl-1-phosphonic acid
DTT	Dithiothreitol
DNQX	Dinitroquinoxaline-2,3-dione
EPM	Elevated Plus Maze
EPSC	Excitatory postsynaptic current
ERK	Extracellular regulated kinase
F-actin	Filamentous actin
GABA	γ-Aminobutyric acid
GAP	GTPase-activating protein
GDP	Guanine diphosphate
Grb2	Growth factor receptor-bound protein 2
GTP	Guanine triphosphate
IPSC	inhibitory postsynaptic current
KO	Knockout
LTP	long-term potentiation
MAPK	Mitogen activated protein (MAP) kinases
MEK	MAPK/ERK kinase
MPNST	Malignant peripheral nerve sheath turmor
NF1-GRD	GAP-related domain
NF1	Neurofibromatosis type 1
Nf1	Locus that encodes neurofibromin
PAK1	p21-activated kinase 1
Pak1	Locus that encodes PAK1
PBD	p21-binding domain
PFC	Prefrontal cortex
PLSD	Fisher's protected least significant difference test
PI3K	Phosphatidylinositol triphosphate kinase
RAS	Guanosine triphosphate (GTP) binding proteins
RAC	Rho family, small GTP-binding protein
RAF	Raf serine/threonine kinase
RAL	Guanosine diphosphate (GDP)-dissociation stimulator
SCF	Stem cell factor
SI	Social interaction
SOS	RAS exchange protein
TTX	Tetrodotoxin
WT	Wild-type

INTRODUCTION

A. Background

While illustrations of neurofibromatosis-like characteristics date to the second century and the first clinical description of neurofibromatosis type 1 (NF1) is likely that of a man with a plexiform neurofibroma dating back to the sixteenth century (Hecht, 1989; Zanca and Zanca, 1980), the term “neurofibroma” was first coined in 1882 by the physician Friedrich Daniel von Recklinghausen in his landmark report entitled “On multiple cutaneous fibromas and their relationship to multiple neuromas”. However, the specific forms of von Recklinghausen’s disease were not clinically differentiated until the late 1970s. In addition to NF1, other neurocutaneous disorders include neurofibromatosis type 2, tuberous sclerosis, Von-Hipple Lindau syndrome and Sturge-Weber syndrome. NF1 represents the most frequent among the disorders that were previously defined as von Recklinghausen’s disease (see Ruggieri and Huson, 1999 for review).

1. Epidemiology of NF1

To date, the current epidemiological data compiled for NF1 has been largely generated from Caucasian and Japanese subjects; however, NF1 is observed world-wide and does not appear to be influenced by ethnicity (see Friedman, 1999 for review). NF1 is caused by mutation in one copy of the *NF1* gene ($NF1^{+/-}$), and affects roughly 1 in every 3000-4000 individuals world-wide. NF1 is a simple autosomal dominant disorder that displays full penetrance in adulthood. To date, the homozygous deletion of the *NF1* gene ($NF1^{-/-}$) is has not

yet been detected in humans suggesting that *NF1*$^{-/-}$ genotype is likely lethal (Messiaen et al, 2000). Likewise, rodents that encode null mutations in both copies of the *Nf1* gene (*Nf1*$^{-/-}$) die *in utero* at 12-14 days of gestation due to heart malformations (Jacks et al, 1994; Brannan et al, 1994). While most cases of NF1 can be diagnosed by eight years of age, nearly all cases are diagnosed by age 20 (DeBella et al, 2000).

The symptoms of NF1 are variably present between individuals as well as within families, and NF1 does not appear to be influenced by sex or race (Friedman and Birch, 1997). NF1 is a chronic disorder associated with lifelong morbidity and increased mortality. Likely due to the progressive nature of the disorder, the life expectancy of an affected individual is significantly lower than normal and ranges from 54-62 years of age compared to 70 in the general population (Rasmussen et al, 2001). This high mortality rate has been attributed to an increased incidence of brain tumors, malignant cancers as well as hypertension and cardiovascular disease (Rasmussen et al, 2001).

2. Physical features of NF1

Established in 1987 by the National Institute of Health (NIH) Consensus Conference on Neurofibromatosis, the diagnostic criteria for NF1 summarize common physical features associated with the NF1 phenotype (NIH, 1988). Neurofibromas represent the most commonly found NF1-related tumor occurring in more than 95% of NF1 patients (see Bader, 1986 for review). Usually seen during early adolescence, cutaneous neurofibromas appear as soft, purplish

bumps on the skin, while subcutaneous neurofibromas usually appear as palpations of the skin (Riccardi, 1980). Dermal and subcutaneous neurofibromas are often associated with cosmetic problems, pain, and pruritus (i.e., intense itching of the skin; Creange et al, 1999). Plexiform neurofibromas are highly vascular encasing major nerves, blood vessels as well as other vital structures (Schorry et al, 1997; see Korf, 1999 for review). Therefore, neurofibromas can significantly impact the quality of life of NF1 patients leading to significant morbidity due to gross disfigurement. In addition, plexiform neurofibromas can transform into malignant peripheral nerve sheath tumors (MPNSTs) leading to metastasis and premature death (Tucker et al, 2005).

NF1-affected individuals manifest a wide array of non-malignant physical features including café-au-lait spots, skin-fold freckling, optic gliomas, Lisch nodules and skeletal malformations (see Ferner et al, 2007 for review). Café-au-lait spots are frequently observed in NF1 patients (roughly 95%) at early stages of development and appear light to dark brown in color (North, 1993). Crowe's sign or skin-fold freckling are present in roughly 30% of NF1 patients often observed under the armpit, in the groin area and around the base of the neck (North, 1993). Gliomas are tumors that arise from glial cells and can occur in the optic pathways, brainstem and cerebellum of NF1 patients (Creange, 1999). Detected in 15-20% of patients, optic pathway gliomas can lead to vision loss (Zeid et al, 2006; see Listernick for review). Unique to NF1 patients, Lisch nodules are yellow to brown dome-shaped elevations projecting from the surface of the iris (Richetta et al, 2004). NF1 patients can also exhibit a variety of skeletal

problems including scoliosis, tibial bowing and pseudarthrosis or a false joint associated with abnormal skeletal movement (Crawford and Bagamery, 1986).

Other symptoms are also observed at an increased frequency in individuals with NF1. For instance, NF1 patients have an increased risk for developing epilepsy with an incidence of 4 to 6%, and epileptic seizures are often due to intracranial masses and other cytoarchitectural abnormalities (Vivarelli et al, 2003). Cardiovascular disorders are frequently observed in NF1 patients including vasculopathy, hypertension, and congenital heart defects (Friedman et al, 2002). Phaeochromocytomas or neuroendocrine tumors of glands in the adrenal medulla are detected in roughly 2% of NF1 patients, and approximately 12% of these tumors are malignant (Bausch, 2005). Macrocephaly is observed in 30-50% of patients diagnosed with NF1, and other minor features include short stature, angiomas as well as and thoracic abnormalities (Cnossen et al, 1998).

3. Genetics of NF1 pathogenesis

NF1 is a product of mutation in one copy of the *NF1* gene. Using linkage analyses, the chromosomal region responsible for NF1 was localized to chromosome 17 (Goldgar, 1989; Wallace et al, 1990). Shortly thereafter, the *NF1* locus was mapped to chromosome 17q11.2 by positional cloning (Cawthon et al, 1990). Utilizing cDNA walking strategies and DNA sequencing, the complete coding region of the *NF1* transcript was cloned revealing that the *NF1* gene encompasses over 300 Kb of genomic DNA with 60 exons (Xu et al, 1990; Marchuk et al, 1991). The chromosomal region linked to the *NF1* gene is

unstable and prone to rearrangements, and represents a “hot spot” for sporadic mutation (Van Roy et al, 2002). Germline mutations in the *NF1* gene were characterized utilizing DNA and RNA sequencing, and included nonsense, frame-shift, missense, and splice mutations as well as in-frame deletions and translocations (Messiaen et al, 2000). Accounting for roughly 30% of mutations, exons 10a-10c and 37 represent the most common regions for mutation (Messiaen et al, 2000). However, specific *NF1* variants have not yet been correlated with NF1-related features or severity in human studies of association (Castle et al, 2003).

4. Biochemistry of neurofibromin

The *NF1* gene encodes the protein product neurofibromin with 2818 amino acids (Xu et al, 1990; see Gutmann and Collins for review). Neurofibromin is a cytoplasmic guanosine triphosphatase (GTPase)-activating protein (GAP)-like protein that negatively regulates RAS-GTPase activity. The amino acid sequence of neurofibromin is highly homologous with mammalian GAP and yeast IRA proteins (Xu et al, 1990; Ballester et al, 1990). In yeast, the expression of neurofibromin leads to the inhibition of human RAS proteins that are coexpressed, and the deletion of neurofibromin is associated with increased RAS GTPase-stimulating activity (Ballester et al, 1990). Furthermore, a fragment of *NF1* cDNA encoding the GAP-related domain (NF1-GRD) was expressed *in vitro* and tested for its effects on RAS-GTPase activity, and found that the NF1-GRD, a region located between amino acids 1125 and 1537, is primarily responsible for the inactivation of RAS-GTPase activity (Martin et al, 1990). Kinetic

measurements indicate that neurofibromin regulates RAS-GTPase activity, particularly at low concentrations (Martin et al, 1990). Characterizing tumor cells isolated from NF1 patients, *in vitro* and *in vivo* studies found that neurofibromin negatively regulates RAS-GTPase activity, and demonstrate a "positive" growth role for RAS activity in NF1 tumorigensis (DeClue et al, 1992; Downward, 1992; Upadhyaya et al, 1997).

Due to its role as a negative regulator of RAS activation, neurofibromin acts as a key regulator in signal transduction from the cell membrane to the nucleus (see Le and Parada, 2007 for review; **Figure 1**). RAS is recruited when a growth factor(s) binds to a receptor on the extracellular matrix of the cell membrane, and RAS-GDP is then converted to RAS-GTP through its interaction with the GRB2 adapter and guanine nucleotide exchange factor SOS (see Margolis and Skolnik for review). The active form of RAS or RAS-GTP is, in part, responsible for the propagation of the classical RAS-RAF-MEK-ERK or MAPK. RAS-GTP binds to RAF serine/threonine kinase (RAF; Stokoe et al, 1994), and activated RAF leads to the phosphorylation and activation of MAP kinase/ERK kinase (MEK; Kyriakis et al, 1992). In turn, MEK (active form) phosphorylates and activates members of the extracellular signal-regulated kinase (ERK) family (Crews and Erikson, 1993). Activated ERK then phosphorylates various targets including other kinases as well as transcription factors.

In addition to the MAPK pathway, the active form of RAS or RAS-GTP propagates the phosphotidylinositol 3-kinase or PI3K cascades. RAS-GTP binds

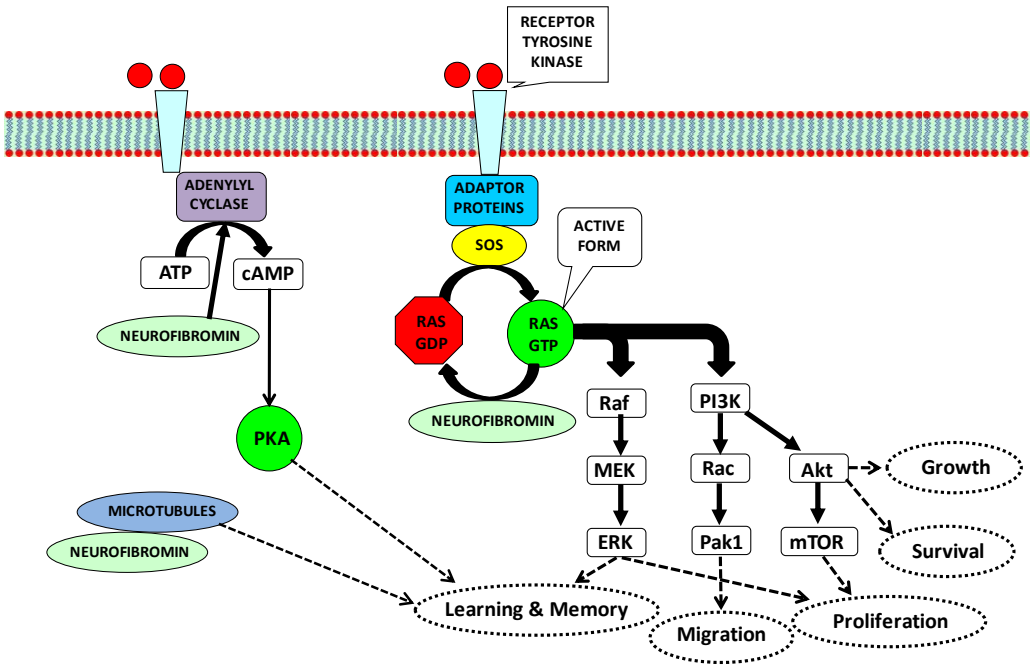

Figure 1. Neurofibromin is a key regulator of RAS and adenylyl cyclase signal transduction from the cell membrane to the nucleus. Neurofibromin, a cytoplasmic GAP-like protein, negatively regulates RAS activation by accelerating the conversion of RAS-GTP to RAS-GDP and increasing RAS signal transduction. The RAS-GTP activates both PI3K and the classical MAPK pathway propagating complex interactions of cellular signaling pathways that regulate cellular functions. Neurofibromin also binds to microtubules, and interacts with adenylyl cyclase to decrease cAMP levels in the central nervous system. Thereby, neurofibromin represents a key node in the regulation of multiple cellular functions.

to and activates the p110 catalytic subunit of PI3K, thereby, resulting in increased activity of lipid kinase (Kodaki et al, 1994). PI3K activation leads to the activation of downstream effectors including RAC (rho family) and RAL GDP-dissociation stimulator (RAL-GDS) (Stephens et al, 1996; Welch et al, 2003). Furthermore, the activated PI3K also binds to and phosphorylates protein kinase B (AKT), and AKT (active form) inactivates the TSC1-TSC2 complex and activates TOR or serine/threonine kinase target of rapamycin (Johannessen et al, 2005). Additionally, neurofibromin binds to adenylyl cyclase (AC) and negatively regulates cyclic AMP (cAMP) levels in the CNS in mice (Tong et al, 2002; Brown et al, 2010). Neurofibromin has been shown to associate with microtubules (Xu and Gutmann, 1997).

Together, these findings demonstrate that neurofibromin functions as a modulatory protein in the cell by accelerating the hydrolysis of RAS-GTP (its active form) to RAS-guanosine diphosphate (GDP), its inactive form (Ballester et al, 1990; Martin et al, 1990; DeClue et al, 1992). Thereby, neurofibromin reduces the strength and duration of RAS signal transduction. Unltimately, the *Nf1*$^{+/-}$ genotype results in dysregulation of MAPK and PI3K signal transduction and decreases in cAMP levels in the CNS.

5. *Pak1* regulation of *Nf1*-dependent pathways

McDaniel et al (2008) demonstrates that the co-deletion of *Pak1* in *Nf1*$^{+/-}$ mice restores MAPK hyperactivation and abnormalities in cellular proliferation and migration that are associated with the *Nf1*$^{+/-}$ genotype (**Figure 2**). PAK1 is a

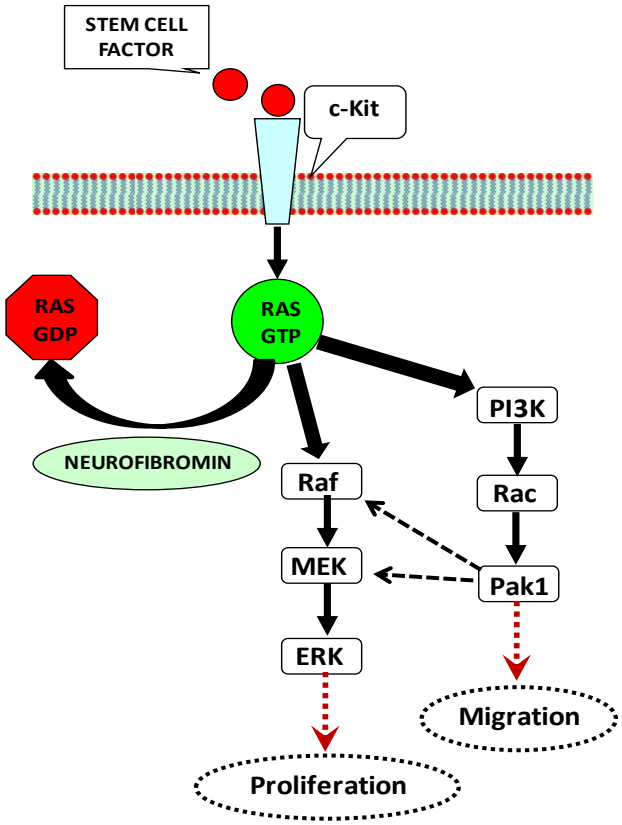

Adapted from McDaniel et al, Blood (2008)

Figure 2. *Pak1* inactivation corrects gain-in-function phenotypes seen in *Nf1* haploinsufficient mast cells. The illustration depicts a hypothetical mechanism(s) explaining how Pak1 may interact with MAPK to restore abnormalities in cellular proliferation and migration seen in *Nf1* haploinsufficient mast cells.

down-stream effector of the PI3K pathway, specifically Rac, and is abundantly expressed in the central nervous system (see Arias-Romero and Chernoff, 2008 for review). In humans, *PAK1* gene maps to 11q13-q14 (Bekri et al, 1997). *PAK1* encodes a protein product consisting of 545 amino acids that is 98% identical to mouse PAK1 and 52% identical to yeast Ste20 (Brown et al, 1996). PAK1 is enriched in neurons and oligodendrocytes and localized to pinocytic vesicles and cortical actin structures (Dharmawardhane et al, 1997). PAK1 is a member of a family of serine/threonine kinases and is highly homologous to PAK2 (γ-PAK) and PAK3 (β-PAK) (Brown et al, 1996).

PAK1 is a downstream effector regulated by the Rho family of GTPases that include RAC, RHO, and CDC42 (Manser et al, 1995; see Bishop and Hall, 2000 for review). The members of the Rho family of GTPases mediate diverse cellular functions that include cytoskeletal dynamics, vesicular transport, gene expression, and oxidant generation (see Nikolic, 2008 for review). Studies have established that the catalytic region in PAK1 (i.e., p21-binding domain or PBD) is located between amino acids 67 and 113 (Lei et al, 2000). To become biologically active, PAK1 and other PAK proteins interact with the active form or GTP-bound RAC or CDC42 (Manser et al, 1995). In its active state, the PBD of PAK1 dramatically increases the phosphotransferase activity of PAK1 on myelin basic protein (Knaus et al, 1995). In addition to the PBD in PAK1, an overlapping inhibitory switch regulates basal kinase activity, and amino acid domains in the N-terminus of PAK1 can bind to adapter proteins including NCK, GRB2, amng others (Bokoch et al, 1996). PAK1 can also be activated through mechanisms

that are GTPase-independent including lipid binding as well as autophosphorylation (Bokoch et al, 1998).

PAK1 has been shown to interact with a variety of downstream targets. For example, PAK1 mediates cytoskeletal dynamics through the regulation of actin organization and polymerizes filamentous actin into orthogonal networks at the membrane (Vadlamudi et al, 2002). Furthermore, PAK1 regulates LIM kinase activity, leading to the destabilization cofilin and the inactivation and aggregation of F-actin fibers (Ishibashi, 2008). The overexpression of *Pak1* leads to increases in cellular motility and actin polymerization, while the expression of dominant negative *Pak1* results in decreases in migration and organized actin structures (Sells et al, 1999). Thereby, PAK1 regulates cellular motility driven by the assembly and disassembly of actin filaments. PAK1 also mediates microtubule dynamics through the phosphorylation and inactivation of the microtubule-destabilizing protein stathmin (Daub et al, 2001).

More recent studies demonstrate that PAK1 can positively regulate MAPK activation. PAK1 has been shown to activate RAF-1 kinase by directly binding to and phosphorylating Ser338 (Zang et al, 2002). Additionally, PAK1 directly binds to and phosphorylates Ser298 in MEK1, leading to increased RAF-1 activity for Ser217/221 as well as increased MEK activation (Coles et al, 2002). Gene silencing of *Pak1* by small interfering RNA (siRNA) in cultured cells leads to significant decreases in ERK activation, and these decreases are associated with lower levels of activation in both RAF and MEK (Beeser et al, 2005). By binding to Ser338 on RAF-1 and Ser298 on MEK1, PAK1 increases the efficiency of ERK

for low-level stimuli, ultimately increasing the levels of ERK activation (Park et al, 2007).

Studies initially identified the existence of crosstalk between PI3K and MAPK, and implicated the PI3K downstream target RAC2 in the regulation of ERK1/2 activation (Ingram et al, 2001). For example, the genetic deletion of Rac restores MAPK hyperactivation associated with *Nf1*$^{+/-}$ genotype in mast cells (Ingram et al, 2001). These findings implicated *Nf1* haploinsufficiency in increased in mast cell proliferation, survival, and colony formation in response to the activation of receptor tyrosine kinase (RTK) c-kit by stem cell factor (SCF). SCF is a glycoprotein that is both soluble and membrane-bound, and acts as the ligand of the transmembrane receptor tyrosine kinase (RTK) c-kit (Besmer et al 1986). SCF/c-kit signal transduction is involved in the regulation multiple cellular functions including growth and development (Saito et al, 1994), cellular proliferation (Yee et al, 1994), cell survival (Iemura et al, 1994), and inflamatory response (see Reber et al, 2006 for review).

In addition to the periphery, SCF and c-kit receptor are abundantly expressed in the CNS of mice during early stages of development and in adulthood (Zhang and Fedoroff, 1997), and has been implicated in neural tube organization during embryonic development (Keshet et al, 1991). Similar to the inactivation of RAC2, McDaniel et al (2008) found that the inactivation of *Pak1* in *Nf1* haploinsufficient mast cells leads to the correction of *in vitro* and *in vivo* gain-in-function phenotypes that are mediated by SCF/c-kit signal transduction (see **Figure 2**). Based on these findings, the same genetic intercross (*Nf1*$^{+/-}$ / *Pak1*$^{-/-}$)

method was implemented in our experimental design in an attempt to restore the disruptions in MAPK signaling and learning abnormalities associated with the *Nf1*$^{+/-}$ genotype.

6. NF1 features associated with disruptions in higher CNS functions

While physical abnormalities represent the “hallmark” characteristics of NF1, the heterozygous *NF1* gene deletion also elicits significant effects on higher CNS function. When NF1 patients were assessed utilizing neuropsychological batteries, 80-90% of affected individuals show significant impairments including lower academic achievement, learning disabilities, attention, and social function (Hofman et al, 1994; North et al, 1997; Dilts et al, 1996; Brewer et al, 1997; Johnson et al, 1999; Kayl and Moore 2000; Noll et al, 2007). Similar to the physical manifestations associated with NF1, these CNS-related features exhibit a high level of variability between individuals, and do not appear to be correlated with sex, race or disease severity (North et al, 1995). Furthermore, these features also are independent of tumor predisposition (Moore et al, 1994).

While early studies report a high frequency of mental retardation or an IQ less than 70 (Samuelsson and Riccardi, 1989), more recent findings utilizing a battery of cognitive assessments suggest that the rate of mental retardation in the NF1 population is only slightly higher (4-10%) than the general population (Ferner et al, 1996). However, the average IQ is significantly lower than normal (around 90) in NF1-affected individuals (Ozonoff, 1999). Multiple studies have examined verbal and performance IQ in NF1 patients, and these studies indicate

that the heterozygous deletion of *NF1* (*NF1*$^{+/-}$) is not selective, but impacts both verbal and nonverbal aspects of cognition (North et al, 1997).

NF1 patients also exhibit learning disabilities associated with both visual-spatial and verbal aspects of learning, affecting roughly 30-65% of NF1-affected individuals (see Rosser and Packer, 2003 for review). Visual-spatial deficits are most often seen in NF1 patients, as measured by the Judgement of Line Orientation task (Hofman et al, 1994). For example, cognitive and neuropsychological batteries found that NF1 patients show impairments in spatial memory (Varnhagen et al, 1988), visual-motor integration (Dilts et al, 1996), visual-spatial skills, and mathematics (Eliason, 1986; Varnhagen et al, 1988; North, 1993). Furthermore, tests of academic acheivement also found significant impairment in spelling, reading and language skills (Dilts et al, 1996; Cutting et al, 2000).

Attention problems are observed in roughly 30-50% of NF1 children and adolescents (Keyhan et al, 2006; Koth et al, 2000; Mautner et al, 2002). As compared to controls, NF1 patients display significant deficits in attention including problems with concentration, attention, and hyperactivity (Eliason, 1986; Eliason, 1988; Coude et al, 2007). It has been suggested that these problems with attention may contribute to learning disabilities and lower academic achievement seen in the NF1 children (Brewer et al, 1997). A meta-analysis of 152 studies found that 75% of children with learning abnormalities also show problems with social skills, as compared to their peers (Kavale and Forness, 1996). Furthermore, psychological assessments found that the

presence of learning disabilities and attention problems were correlated with deficits in social skills, social competence, and other social problems (Barton and North, 2004).

NF1 patients manifest significant problems with social function compared to their unaffected siblings affecting roughly 50% of NF1-affected individuals. For example, NF1 children are often socially withdrawn, and show difficulty forming friendships and have fewer friends than their peers (Dilts et al, 1996, Johnson et al, 1999; Barton and North, 2004; Noll et al, 2007). In addition, NF1 children often show problems with social perception in that they inappropriately perceive and interpret social cues (i.e. facial expressions, body gestures, and tone of voice) (Eliason, 1986). Related to these problems with social function, NF1 shows a dramatically increased frequency in autistic patients with an estimated prevalence of 1.2% in autistic subjects (Martin et al, 2007), and human genetic studies found that the *NF1* locus is linked to autism (IMGSAC, 2001). However, the prevalence of autism in the NF1 population has not yet been determined, and the relationship between NF1 and autism is not clearly defined in the literature.

NF1 patients also display more emotional problems relative to their unaffected siblings and the general population (Johnson et al, 1999). For instance, Samuelsson and Riccardi (1989) found that 33% of NF1 patients showed increased rates of mental illness with the most commonly occurring psychiatric diagnoses being depression and anxiety. Another study found that roughly one-third of the NF1 subjects fulfilled the criteria for a psychiatric disorder, and diagnosed 21% of the NF1 cohort with the mood disorder

dysthymia (Zoller and Rembeck, 1999). Similarly, Belzeaux and Lançon (2006) observed mental illness in 33% of NF1 patients with dysthymia as the most frequent diagnosis (21% of patients). A higher prevalence of depressive mood (7%), anxiety (1-6%), and personality (3%) disorders were also observed, and the risk of suicide was four times greater than in the general population (Belzeaux and Lançon, 2006). Together, these findings indicate that anxiety and mood disorders (i.e., depression, dysthymia) are observed at a modestly higher frequency in NF1 patients.

7. Mouse models of NF1

Homologous recombination strategies were utilized to disrupt *Nf1*, the murine homolog of *NF1,* in an attempt to create an animal model of neurofibromatosis (Jacks et al, 1994; Brannan et al, 1994). In mice, the *Nf1* locus is highly conserved encoding an amino acid sequence that is 98% identical to human neurofibromin (Bernards et al, 1993). Similar to humans, the homozygous deletion of *Nf1* gene is lethal in mice. $Nf1^{-/-}$ mice die *in utero* at 12-14 days of gestation due to heart malformations (Jacks et al, 1994; Brannan et al, 1994). Heterozygous mice were developed that carry a null mutation at one copy of the *Nf1* locus ($Nf1^{+/-}$). While these $Nf1^{+/-}$ mice do not develop several features associated with the NF1 phenotype, $Nf1^{+/-}$ mice do show increased rates of myeloid leukemia and phaeochromocytomas or tumors of the neural crest-derived adrenal medulla (Jacks et al, 1994). Thus, other mechanisms also contribute to $Nf1^{+/-}$-related tumorigenesis including the inactivation of a second

allele, gene x gene interactions, NF1 hapolinsufficiency, and environmental factors.

The *NF1* gene functions as a classic tumor suppressor gene (Colman et al, 1995). In chimeric mice partially composed of $Nf1^{-/-}$ cells, the complete loss of *Nf1* gene leads to the development of neurofibromas (Chichowski et al, 1999). Furthermore, mice that have mutations in both *Nf1* and *p53* genes develop malignant peripheral nerve sheath tumors (MPNSTs), soft tissue sarcomas and abnormalities in neural crest formation, indicating that the development of malignant tumors can also result from gene x gene interactions (Chichowski et al, 1999; Vogel et al, 1999). By intercrossing $Nf1^{+/-}$ mice with c-kit mutant mice, Ingram et al (2000) demonstrates that *Nf1* haploinsufficiency leads to enhanced MAPK activity and increases in SCF-mediated mast cell proliferation, survival, and colony formation. Therefore, *Nf1* gene dosing effects alter the interactions between mast cells, Schwann cells, fibroblasts, and endothelial cells contributing to the tumor microenvironment and tumorigenesis (see Staser et al, 2010 for review).

In addition to the periphery, neurofibromin is abundantly expressed in the rodent CNS, and immunostaining of tissue sections localized neurofibromin expression to neurons, oligodendrocytes, and nonmyelinating Schwann cells (Daston et al, 1992). In the rat brain, neurofibromin is most abundantly expressed in large projection neurons including cortical and hippocampal pyramidal cells as well as cerebellar Purkinje cells (Nordlund et al, 1993). Neurofibromin is present in both cell bodies and axons, and is highly enriched in dendrites and associates

with smooth vesiculotubular elements, cisternal stacks as well as multivesicular bodies (Nordlund et al, 1993). Neurofibromin is not abundantly expressed in the plasma membrane, nucleus, nuclear envelope, Golgi apparatus, mitochondria, or rough endoplasmic reticulum (Nordlund et al, 1993).

Similar to humans NF1 patients, it has been well-established that *Nf1*$^{+/-}$ mice show spatial learning deficits, as measured by the Morris water maze (Silva et al, 1997). Costa et al (2002) found that *Nf1*$^{+/-}$ mice also display increases in inhibitory postsynaptic potentials (IPSPs) in *cornu Ammon* 1 (CA1) pyramidal cells of hippocampal slices (Costa et al, 2002). This increase in IPSPs is consistent with postsynaptic changes that decrease the likelihood of postsynaptic action potentials in CA1 pyramidal cells in the hippocampus. *Nf1*$^{+/-}$ mice also exhibit no differences in long-term potentiation (LTP), whereas LTP induced at the stimulation strength of 60mA is larger than LTP induced at 35mA in WT mice (Costa et al, 2002). For a review of IPSPs, refer to *Functions of the basolateral amygdala* section on page 28, and for a review of LTP mechanisms, refer to *Processes involved in learning and memory* section on page 21.

Pharmacological and genetic manipulations in *Nf1*$^{+/-}$ mice that restore RAS signaling can reverse the spatial learning abnormalities as well as the increases in IPSPs and deficits in LTP seen in CA1 pyramidal cells of hippocampal slices (Costa et al, 2002). For instance, mice heterozygous for mutations in both *Nf1* and *K-ras* genes (*Nf1*$^{+/-}$ / *K-ras*$^{+/-}$) show similar performance on the hidden water maze task as WT mice, and display restored IPSPs and LTP (Costa et al, 2002). These deficits can also be restored in the

Nf1$^{+/-}$ mutant mice by administering farnesyl-transferase inhibitors. Farnesyl-transferase inhibitors block the post-translational farnesylation of RAS protein, a process necessary for RAS activation (Costa et al, 2002; Li et al, 2005). Therefore, these findings demonstrate that *Nf1*$^{+/-}$-mediated deficits in spatial learning and associated abnormalities in IPSPs and LTP are mediated by RAS-dependent processes (see Costa and Silva, 2003 for review).

To further characterize the mechanism(s) underlying the spatial learning deficits seen in *Nf1*$^{+/-}$ mutant mice, Cui et al (2008) generated heterozygous Cre-mediated deletions of the *Nf1* gene in various cell types in the brain. The resulting mice expressed deletions of *Nf1* in the following cell types: both excitatory and inhibitory neurons (*Nf1*^{synI}; with synapsin I-Cre), forebrain GABAergic neurons (*Nf1*$^{Dlx5/6}$; with Dlx5/6-cre), forebrain pyramidal neurons (*Nf1*^{aCaMKII}; with aCaMKII-Cre), and most astrocytes (*Nf1*^{GFAP}; with GFAP-Cre). Cui et al (2008) found that only *synapsin I* and *Dlx5/6 Cre*-mediated deletions of the *Nf1* gene result in spatial learning deficits mice, thereby, implicating inhibitory interneurons in *Nf1*-related spatial learning deficits. These inhibitory interneurons branch locally and innervate other neurons, thereby, decreasing their likelihood of a postsynaptic action potential.

Using electrophysiological studies, Cui et al (2008) further demonstrates that these *Cre*-mediated deletions of *Nf1* gene result in increased miniature inhibitory postsynaptic current (mIPSC) frequency under periods of high-frequency stimulation (12.5 mM KCl) in CA1 pyramidal cells of hippocampal slices. Similar to previous findings (Costa et al, 2002), these *Cre*-mediated

deletions of *Nf1* gene also lead to deficits in LTP (Cui et al, 2008). Additionally, the pharmacological inhibition of MAPK using MEK inhibitors can reverse the increases in mIPSC frequency seen in $Nf1^{+/-}$ mice suggesting that these increases in mIPSC frequency are mediated by a MAPK-dependent mechanism (Cui et al, 2008).

In a separate study using a different animal model of NF1, Costa et al (2001) characterized the effect(s) of a spice variant of the *Nf1* gene in mice. The *Nf1* gene encodes mRNA with two alternative splices (Danglot et al, 1995). Exon 23a represents an alternatively spliced region of the *Nf1* gene that encodes 21 amino acids within the NF1-GRD domain (Martin et al, 1990). The type 1 isoform of NF1 excludes exon 23a, while the type 2 isoform includes this region. Compared to the type 1 isoform, the type 2 isoform has lower GAP activity, but greater affinity for Ras (Viskochil, 1999). Like the $Nf1^{+/-}$ mice, mice with a homozygous deletion of exon 23a in *Nf1* gene also exhibit impairments in spatial learning, as measured by the Morris water maze (Costa et al, 2001). Unlike the $Nf1^{+/-}$ mice, mice with the homozygous deletion of exon 23a are viable and do not show an increased tumor predisposition (Costa et al, 2001). Similar to the $Nf1^{+/-}$ mice, the $Nf1^{23a-/-}$ exhibit increases in IPSPs and abnormal LTP in the hippocampus that can be rescued by decreasing RAS function (Costa et al, 2001). These findings further implicate the NF1-GRD in the spatial learning deficits and abnormalities in IPSPs and LTP associated with the *Nf1* gene deletion in mice.

8. Processes involved in learning and memory

Learning and memory involves complex processes and the integration of multiple structures in the CNS (see Purves et al, 2004 for review). Encoding represents the initial process whereby sensory information induces cellular and molecular changes to neurons. Sensory inputs can generate either short-term memories that only last for seconds to minutes or long-term memories that can last for days or even indefinitely. During consolidation these cellular and molecular changes lead to persistent alterations in "synaptic strength" within neuronal circuits (i.e., memory storage and retention). Memories are encoded by modifications of synaptic strength in the CNS, and these changes to sypapses are defined as synaptic plasticity.

Long-term potentiation (LTP) is a cellular mechanism that is thought to contribute to memory storage underlying synaptic plasticity (see Tronson and Taylor, 2007 for review). In hippocampal slices, LTP results from a brief, high-frequency train of stimuli to the same axon (i.e., Schaffer collaterals) leading to a long-lasting enhancement in excitatory postsynaptic potentials (EPSPs) in CA1 neurons in the hippocampus (see Cooke and Bliss, 2006 for review). Mechanistically, LTP is triggered by the expolsion of the Mg^{2+} block from the NMDA channel in the postsynaptic neuron. If the postsynaptic neuron is sufficiently depolarized, Ca^{2+} ions freely enter the NMDA channel activating postsynaptic protein kinases, and these protein kinases insert new AMPA receptors into the postsynaptic spine increasing the sensitivity to glutamate (i.e., the major excitatory neurotransmitter in the brain), and ultimately defining the

number, size and shape of dendritic spines (see Bliss and Collingridge, 1993 for review).

Memory recall refers to the ability to retrieve stored information previously encoded from past experience. Memory has been categorized into two main constructs including declarative and procedural memories (see Fernald 1997 for review). Declarative memory is recalled by a deliberate and conscious effort, while non-declarative memory is retrieved automatically with no deliberate or conscious effort (e.g., procedural memory). Encoding new declarative memories requires an intact hippocampus and associated midline diencephalic and medial temporal lobes (Corkin, 1984; Corkin et al, 1997). In contrast, procedural memory is largely regulated by the premotor cortex, basal ganglia and cerebellum. Thereby, learning and memory processes enable an organism to process past experiences enabling a more effective adaptive response to environment stimuli.

Learning and memory requires morphological changes at the synapse, including the formation of new synapses or the strengthening of existing synapses (see Cooke and Bliss for review). In recent years, accumulating evidence has demonstrated that the MAPK signaling pathway plays an important role in the regulation of learning and memory (see Peng et al, 2010 for review). Studies have identified increases in ERK activation during long-term memory encoding and consolidation following training (Feld et al, 2005). In addition, increased ERK activation was detected for training in the Morris water maze (Blum et al, 1999) and following contextual fear conditioning learning (Atkins et al, 1998; Bozon et al, 2003). Merino and Maren (2006) measured the effects of a

Ras antagonist administered in the BLA on fear conditioning, and found that MAPK is required for the acquisition of long-term fear. Therefore, MAPK signaling is thought to play an important role in regulating memory encoding (see Giovannini for review).

9. Neural basis of social behavior

In humans, social behavior is mediated by complex processes involving multiple brain regions functioning in concert to coordinate a response to a social stimulus (**Figure 3**; see Insel and Fernald, 2004 for review). Cortical regions perceive socially relevant stimuli and communicate this information to the amygdala, orbitofrontal cortex, anterior and posterior cingulate cortices, and somatosensory-related cortices (see Adolphs, 2009 for review). These brain regions define the stimuli based on motivation or reward, emotions, and cognition, and then communicate this information to motor and emotional outputs (see Adolphs et al, 2002a-b for review). Therefore, the neural substrates that mediate social behavior consist of complex, integrated circuits within and between brain regions that perceive social stimuli (e.g., olfactory, visual, auditory), define their emotional valence (prefrontal cortex, amygdala, temporal cortex), evaluate social motivations (ventral tegmental area, nucleus accumbens, ventral pallidum), and ultimately provides this information to the appropriate brain regions that determine an adaptive social response (see Insel and Fernald, 2004).

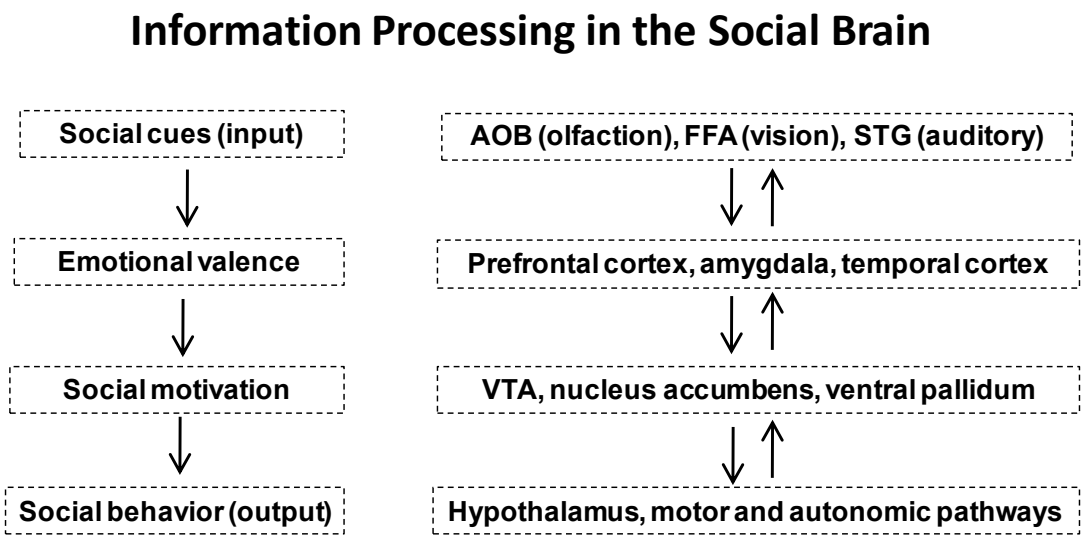

Adapted from Insel and Fernald, Annu Rev Neurosci (2004)

Figure 3. A simplified model of processes involved in social learning and memory. The figure above illustrates a theoretical model of the processes and brain regions involved in social learning and memory. Sensory information is initially processed by the accessory olfactory bulb, fusiform area or superior temporal gyrus. This sensory information is then defined by complex integrated networks in the CNS. Emotional valence is determined by projections to the prefrontal cortex, amygdala and temoporal cortex. Social motivation is processed by the VTA, nucleus accumbens, and ventral pallidum. These brain regions integrate sensory information, determine the appropriate emotional and/or motivational relevance, and then provide the information to the other brain regions affecting social behavior. AOB - accessory olfactory bulb; FFA - fusiform area; STF - superior temporal gyrus; VTA - ventral tegmental area

Facial recognition represents a core component of social behavior and social learning in humans. Prosopagnosia or “face blindness” is particularly relevant to understanding the neurosubstrates involved in social learning due to its selective impairment of facial recognition. In addition to other brain regions, functional imaging studies and lesion studies suggest that facial recognition is regulated by the frontal cortex (Hornak et al, 1996) and the amygdala (LeDoux, 1992; Luo et al, 2007). For instance, a functional imaging study that measured delayed matching to emotional expressions on human faces found that the prefrontal cortex and amygdala are recruited during working memory for social cues (LoPresti et al, 2009). Utilizing functional imaging studies and tractwise analyses, a recent study measured the effects of damage to the two tracts in the human CNS on facial recognition (Philippi, 2009). The findings demonstrate that damage to the tract connecting the occipital cortex with the anterior temporal lobe and amygdala, or damage to the tract connecting the occipital cortex, the temporal cortex, and the orbitofrontal cortex leads to impairment in facial recognition (Philippi, 2009). Therefore, these findings implicate the prefrontal-amygdala circuit in facial recognition processing (Philippi, 2009).

The prefrontal-amygdala circuit defines a primary processing center for emotional aspects of social response, and its dysregulation can have profound effects on social function in humans (see Blair, 2008 for review). For example, individuals with damage to the frontal cortex can show blunted affect, impaired goal-directed behavior and inappropriate social conduct (Barrash et al, 2000). Additionally, lesion studes demonstrate that damage to the frontal cortex impairs

the ability to react to emotionally charged pictures (Damasio et al, 1990). Similarly, damage to the amygdala leads to impairment in the facial recognition that are associated with emotions (Adolphs et al, 2003). While amygdala-dependent learning is often associated with fearful or negative emotional response, the amygdala also actively processes cues associated with a positive emotional valence (see Bachevalier and Malkova for review). For instance, the amygdala is activated when a child is presented with his mother's face (Todd et al, 2010). The amygdala is also essential for the regulation of social perception in that humans with amygdala lesions lack any sense of personal space during face-to-face interactions (Kennedy et al, 2009; Todd et al, 2009). Together, these findings demonstrate that the prefrontal-amygdala circuit is critical for processing cues during social encounters.

10. Social behavior and social learning in mice

In the natural environment, social behavior in mice is necessary for reproduction, territoriality, and the establishment of dominance. Dyadic social interactions represent a core component of social behaviors, and these interactions are defined by both innate and learned responses to social cues. In a laboratory setting, social interaction can be characterized by measuring the approach verses avoidance of a mouse toward a conspecific (Brodkin et al, 2004; Sankoorikal et al, 2006; Crawley et al, 2007). Social approach verses social avoidance is thought to be a product of multiple, sometimes opposing motivations that drive social behavior in mice (Sankoorikal et al, 2006). For

example, motivations that lead to social approach might include social investigation, play, reproduction, or offensive aggression, while social avoidance can potentially be a product of generalized anxiety, social anxiety, or fear of the other mouse.

In addition to innate response, mouse behavior is influenced by the ability to learn and then remember cues associated with individual conspecifics (Crawley et al, 2007; see Silverman et al, 2010 for review). Behavioral tests have been designed to test various aspects associated with social learning and memory utilizing approach and avoidance paradigms (Crawley et al, 2007). In the present dissertation, the amount of time the "test" mice spent sniffing (i.e., nose pointed toward cage and within one inch of cage) novel verses familiar conspecifics were determined in order to generate a quantitative measure of social approach, as defined by "preference for social novelty" (Nadler et al, 2004; Crawley et al, 2007). Thereby, short-term and long-term social learning / memory in mice were assessed based on their ability to discriminate between social cues associated with different conspecifics (Crawley et al, 2007). While three main stages contribute to memory formation including acquisition, consolidation, and retrieval (see Purves et al, 2004 for review), learning and memory is presented as a single construct throughout this body of work.

Social learning and the motivations that underlie social approach and avoidance to a conspecific are mediated by multiple brain regions (see **Figure 3**). However, these brain regions do not process social information exclusively, but process sensory information that is independent of a social context. The

amygdala has been implicated in both anxiety and fear-based learning (see LeDoux, 1993 for review). For instance, both electrical and pharamacological stimulation of the amygdala induces an enhanced cardiovascular response and behavioral arousal consistent with a fight-or-flight response (Kapp et al, 1982; Maskati and Zbrozyma, 1989). Likewise, when presented with a conspecific, social avoidance behavior can reflect anxiety or fear of the other mouse. By selectively targeting the basolateral amygdala (BLA) using pharmacological manipulation, previous studies demonstrate that the amygdala also regulates social aspects of anxiety and fear-based learning (Sanders and Shekhar, 1996; Sajdyk and Shekhar, 2000; Shekhar et al, 2001; Sajdyk et al, 2008). Thereby, learning and memory processes and brain regions that mediate social memory overlap with those that mediate anxiety and fear memory.

11. Functions of the basolateral amygdala

NF1 is associated with a higher incidence of learning disabilities, attention deficits, social problems and psychiatric disorders, including anxiety and depression (see *NF1 features associated with disruptions in higher CNS functions* section for review). Due to its role in regulation and processing of emotional information, the amygdala network represents a brain region of particular interest to these NF1-related features (see McGaugh, 2002 for review). The amgydala is composed of multiple sub-nuclei that work in concert to coordinate a response to emotional information (**Figure 4**). These sub-nuclei include the basolateral (BLA), lateral (LA), medial (ME) and central (CE). The LA

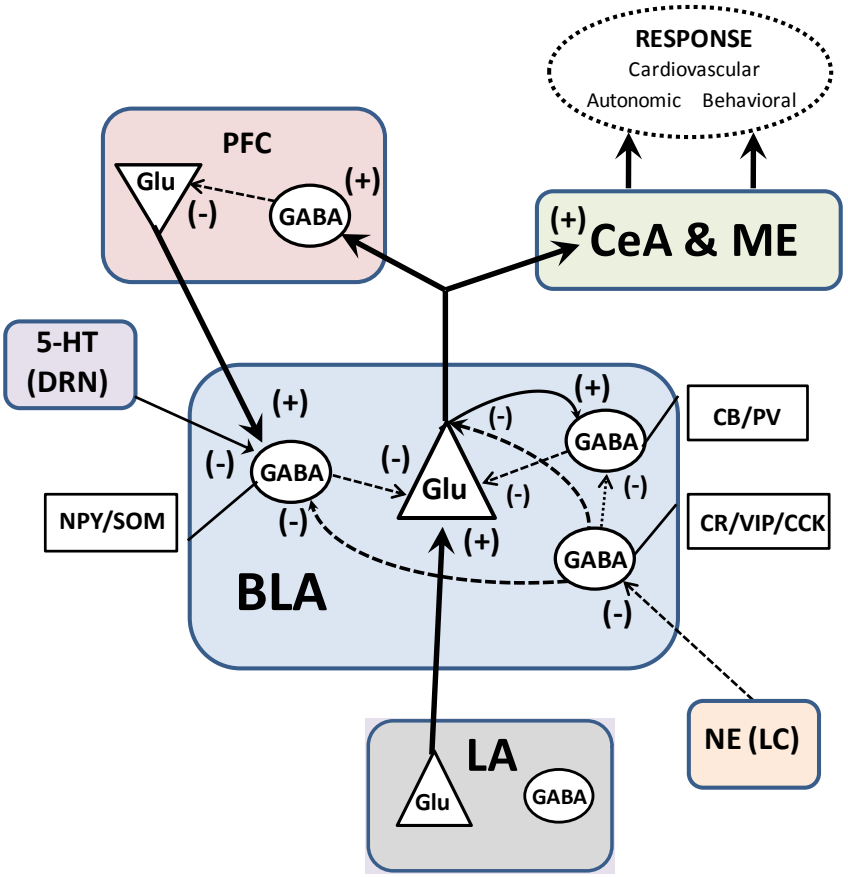

Adapted from Shekhar et al, Stress (2005)

Figure 4

Figure 4. A simplified schematic representation of the neurochemical circuitry within the BLA and its connectivity to the PFC involved in the regulation of emotional response. Glutamatergic projection neurons within the BLA are regulated by excitatory input (+) from the LA and other cortical regions (direct sensory information) and by inhibitory input (-) from local inhibitory interneurons. These inhibitory neurons process input from the PFC regarding the predicted ability to cope with sensory inputs. Additionally, serotonin from the dorsal raphe nucleus and norepinephrine from the locus coeruleus provide modulatory input to the BLA that mediates the balance of the stimulus and coping inputs from these cortical regions. Therefore, the BLA functions utilizing multiple feedback loops containing many neurotransmitters (i.e., Glu, GABA, 5-HT, NE) and neuropeptides (i.e., CB, CCK, CR, NPY, PV, SOM, VIP) to regulate cardiovascular, autonomic and behavioral response. 5-HT - serotonin; BLA, basolateral amygdala; CB - calbindin; CCK - cholecystokinin; CeA - central nuclelus of the amygdala; CR - calretinin; DRN - dorsal raphe nucleus; GABA - gamma-aminobutyric acid; Glu - glutamate; LA - lateral amygdala; LC - locus coeruleus; ME - medial nucleus of the amygdala; NE, norepinephrine; NPY - neuropeptide Y; PFC - prefrontal cortex; PV - parvalbumin; SOM, somatostatin; VIP - vasoactive intestinal peptide

and BLA sub-nuclei are the major sites of afferent inputs, while the ME and CE are the major efferent areas (Amaral et al, 1992). The BLA is hypothesized to play a central role in the mediation of amygdala-dependent response integrating a wide range of sensory information, determining the appropriate emotional valence, and then providing the information to the relevant brain regions (LeDoux, 1993).

The BLA is comprised of large spiny pyramidal (i.e., glutamatergic projection neurons) and non-pyramidal neurons while the non-pyramidal cells are predominantly GABAergic (McDonald, 1984). Similar to cortical structures, these glutamatergic projection neurons in the BLA are tonically inhibited by local GABAergic interneurons (Rainnie et al, 1991a,b). In the BLA, glutamatergic projection neurons are regulated by excitatory inputs from cortical and subcortical centers (largely sensory information) and inhibitory inputs from local GABAergic interneurons (Truitt et al, 2007). Glutamate and GABA are the main exicitatory and inhibitory neurotransmitters in the CNS, respectively. In addition to glutamate and GABA, other neurotransmitters are localized to the BLA including serotonin from the dorsal raphe (Norita and Kawamura, 1980) and norepinephrine from the locus coeruleus (Fallon et al, 1978). Other minor neurotransmitters include epinephrine, dopamine, and acetylcholine.

Neuropeptides are also abundantly expressed in the basolateral amygdala. The most common neuropeptides include somatostatin (SOM; Amaral et al, 1989), neuropeptide Y (NPY; Gustafson et al, 1986), and cholecystokinin (CCK; Kritzer et al, 1988). In the basolateral and lateral amygdala, SOM and

NPY are extensively colocalized with GABA (McDonald and Pearson, 1989), and CCK is also found to be colocalized with GABA in these subnuclei as well (McDonal and Pearson, 1989). Neuropeptides observed at a lower abundance in the BLA include vasoactive intestinal peptide (VIP; McDonald and Pearson, 1989), substance P (Cassell and Gray, 1989), galanin (Kohler et al, 1989), and neurotensin (Quirion, 1987), and other neuropeptides observed in the BLA include calbindin (CB), calretinin (CR), and parvalbumin (PV; see Shekhar et al, 2005 for review).

Electrophysiological recordings were previously conducted in order to characterize the interactions between excitatory amino acid (EAA) induced EPSPs (i.e. postsynaptic potential changes that depolarize the cell increasing the likelihood of initiating a post-synaptic action potential) and GABA-mediated IPSPs (i.e., postsynaptic changes that decrease the likelihood of a postsynaptic action potential) in the BLA (Rainnie et al, 1991a,b). Even without stimulation, single vesicles can occasionally be released into the synapse generating miniature EPSPs (mEPSPs) and IPSPs (mIPSPs), and can be characterized by amplitude (i.e., quantal size) and frequency (i.e, number of vesicles) defining the synaptic response to the release of neurotransmitter in response to a nerve impulse (see Purves et al, 2004 for review).

The electrical stimulation of afferent neurons to the BLA leads to EPSPs that are mediated by glutamate, and these EPSPs can be blocked by the administration of NMDA antagonists (i.e., AP5) and AMPA and Kainate receptor antagonists (CNQX; Rainnie et al, 1991a). In addition, the stimulation of afferents

to the BLA also elicits IPSPs that are mediated by GABA, and these IPSPs can be blocked by the administration of $GABA_A$ antagonists (i.e., BMI) and $GABA_B$ antagonists (i.e., 2-hydroxy-saclofen; Rainnie et al, 1991b). Therefore, the BLA is regulated by multiple feedback loops containing many neurotransmitters and neuropeptides that mediate the balance of excitatation and inhibition associated with inputs defined by largely sensory inputs and coping inputs from cortical regions (see Shekhar et al, 2005 for review).

B. Rationale and Objectives

Developmental disorders are seen at a higher frequency in NF1 patients, and can impact cognition, learning, attention and social function. To date, the treatment options for NF1-related learning disabilities and social dysfunction are lacking at best. The identification of behavioral markers in rodents that are relevant to sequelae of a human disease like NF1 represents an important first step in advancing this medical research. Understanding the biological mechanism(s) that contribute to these gene x phenotype associations can provide important targets for developing pharmaceutical treatments as well as other forms of clinical intervention.

The *overall hypothesis* of this thesis proposal is that mutation at the *NF1* locus leads to disruptions in social and emotional learning with unique disruptions in *Pak1*-dependent cellular processes in key CNS structures that are crucial for the development of normal rodent behaviors. The *objectives* for this thesis were to first screen for behavioral deficits in *Nf1*$^{+/-}$ mice that are associated with social dysfunction, anxiety-like behavior and depression-associated response and (2) then to characterize the biochemical and cellular mechanism(s) that may underlie these deficits. The following five hypotheses were generated in light of these *main objectives*:

Hypothesis 1: *Nf1*$^{+/-}$ *mice,* as compared *to WT, will show deficits in either general sociability and social learning, anxiety, and / or behavioral despair and learned helplessness, but not olfaction or locomotion.*

Rationale: Previous studies indicate that NF1 patients display problems with social function (Johnson et al, 1999; Barton and North, 2004; Noll et al, 2007), and studies have found that NF1 patients display a higher frequency of anxiety and mood disorders, including dysthymia and depression (Samuelsson and Riccardi, 1989; Zoller and Rembeck, 1999). ***Objective(s):*** The first series of experiments were designed in order to screen *Nf1*$^{+/-}$ and WT mice for differences in sociability, anxiety, locomotion and olfactory sensory habituation. Due to the high rate of emotional learning disabilities associated with NF1, emotional learning and memory components were also incorporated to assess short-term and long-term social learning and behavioral despair / learned helplessness. Olfaction and locomotion were also measured as experimental controls. In rodents, olfaction is the primary sensory input for social interactions; therefore, olfaction habituation was measured, and locomotor activity was also montitored in order to identify differences in movement that could potentially affect measures of social behavior and anxiety.

Hypothesis 2: *The co-deletion of Pak1 in Nf1*$^{+/-}$ *mice (Nf1*$^{+/-}$ */ Pak1*$^{-/-}$*) will restore the deficits in long-term social learning seen in Nf1*$^{+/-}$ *mice, but will not affect preference for social interaction, short-term social learning, anxiety, behavioral despair / learned helplessness, olfactory sensory habituation or locomotor activity.*

Rationale: PAK1 is a down-stream effector of PI3K that has been shown to activate MAPK signaling and mediates crosstalk between PI3K and MAPK pathways (Ingram et al, 2001). The *in vitro* and *in vivo* inactivation of *Pak1*

normalizes *Nf1*-related abnormalities seen in cellular proliferation that are MAPK-dependent and differences in migration seen in mast cells (McDaniel et al, 2008; see **Figure 2**). While no differences were detected in anxiety or behavioral despair / learned helplessness between *Nf1*$^{+/-}$ mice and WT, these phenotypes were also characterized to control for potential *Pak1*-dependent effects on these behavioral measures. ***Objective(s):*** This series of experiments was designed to determine whether the genetic intercross (*Nf1*$^{+/-}$ / *Pak1*$^{-/-}$) would restore the deficits in long-term social learning seen in *Nf1*$^{+/-}$ mice. Behavior tests were performed on *Nf1*$^{+/-}$, *Nf1*$^{+/-}$ / *Pak1*$^{-/-}$, and *Pak1*$^{-/-}$ genotypes to assess their preference for social interaction, short-term social learning, anxiety, behavioral despair / learned helplessness, olfactory sensory habituation and locomotor activity.

Hypothesis 3: *Nf1*$^{+/-}$ *mice, as compared to WT, will show increases in MAPK activation (ERK / p-ERK) in neuronal cells cultured from the frontal cortex. The co-deletion of Pak1 in Nf1*$^{+/-}$ *mice (Nf1*$^{+/-}$ / *Pak1*$^{-/-}$*) will normalize the hyperactivation in MAPK associated with the Nf1*$^{+/-}$ *genotype.*

Rationale: Previous studies have implicated MAPK hyperactivation in learning abnormalities seen in *Nf1*$^{+/-}$ mice (Cui et al, 2008; see Le and Parada, 2007 for review). Utilizing a genetic intercross to disrupt both *Nf1* and *Pak1* in all cells, it was shown that co-deletion of *Pak1*, which positively regulates MAPK activation, normalizes MAPK hyperactivation in *Nf1*$^{+/-}$ mast cells (McDaniel et al, 2008). ***Objective:*** To establish that *Pak1* co-deletion restores MAPK hyperactivation associated with *Nf1*$^{+/-}$ genotype in neurons in the CNS as it does

in mast cells, neuronal cells were cultured from the frontal cortex for each respective genotype (WT, *Nf1*$^{+/-}$, *Nf1*$^{+/-}$ / *Pak1*$^{-/-}$, *Pak1*$^{-/-}$), and Western blotting was used to quantify the relative activation of ERK (ERK vs. p-ERK) at basal levels and following SCF stimulation.

Hypothesis 4: *Nf1*$^{+/-}$ *mice, as compared to WT, will show increases in inhibitory synaptic currents (IPSCs) in the BLA, and the co-deletion of Pak1 in Nf1*$^{+/-}$ *mice will restore these differences.*

Rationale: Using electrophysiological measures of inhibitory synaptic currents, previous studies demonstrate increases in miniature IPSCs (mIPSCs) frequency under periods of high-frequency stimulation (12.5 mM KCl) in the hippocampus from *Nf1*$^{+/-}$ mice (Cui et al, 2008). Because the BLA is critical for emotional processing of social behavior, abnormalities in IPSCs in the BLA could affect processes involved in social learning by reducing neurotransmission from glutamatergic projection neurons to various brain regions, including the PFC. ***Objective:*** In this experiment the whole-cell patch-clamp was used to measure isolated spontaneous and miniature inhibitory synaptic currents (IPSC) recorded from glutamatergic projection neurons in the BLA of WT, *Nf1*$^{+/-}$, *Nf1*$^{+/-}$ / *Pak1*$^{-/-}$, *Pak1*$^{-/-}$ mice.

Hypothesis 5: *Nf1*$^{+/-}$ *mice, as compared to WT, will show dysregulation in proteins in the frontal cortex and BLA that are associated with cellular mechanisms involved in social learning, and increases in IPSCs observed in the BLA. The co-deletion of Pak in Nf1*$^{+/-}$ *mice will restore these differences in protein expression.*

Rationale: The BLA interacts with the frontal cortex to mediate emotional processing and the saliency to sensory cues that are thought to underlie various aspects of social behavior, including social learning (see *Neural basis of social behavior section* for review). ***Objective:*** To identify potential down-stream targets that contribute to the deficits seen in long-term social learning in $Nf1^{+/-}$ mice, mass spectrometry was utilized to screen for differences in protein expression associated with the heterozygous *Nf1* gene deletion ($Nf1^{+/-}$) in the frontal cortex and the BLA.

ADDENDUM

To measure inhibitory synaptic currents (IPSCs) in glutamatergic projection neurons dissected from WT, $Nf1^{+/-}$, $Nf1^{+/-}$ / $Pak1^{-/-}$ and $Pak1^{-/-}$ mice, I worked with Dr. Andrei Molosh who is an expert in the field of electrophysiology. While we worked closely together during this experiment, Dr. Molosh was the primary investigator for these electrophysiological studies. The results from these proposed studies are included as an addendum to this dissertation in order to better represent and define the scope of this body of work.

MATERIALS AND METHODS

The experimental protocols in this section were designed to address the five main hypotheses that are outlined in the Rationale and Objectives section. The following section provides a detailed summary of the animals, behavioral tests, electrophysiological procedures and protein studies (i.e., Western blotting, mass spectrometry) that were utilized in each respective experiment.

A. Animals

All of the mouse strains tested in these experiments were bred on a C57BL/6J background and included the following: (1) Wild-type (WT), (2) *Nf1*$^{+/-}$, (3) *Nf1*$^{+/-}$ / *Pak1*$^{-/-}$ and (4) *Pak1*$^{-/-}$ mice. The *Nf1*$^{+/-}$ mice were obtained from Tyler Jacks at the Massachusetts Institute of Technology (Cambridge, MA). The *Nf1* allele was genotyped as described previously (Zhang et al, 1998). The *Pak1*$^{-/-}$ strain was obtained from Dr. Jonathan Chernoff (Philadelphia, Pennsylvania). To generate the *Nf1*$^{+/-}$ / *Pak1*$^{-/-}$ mice, *Pak1*$^{-/-}$ mice were intercrossed with the *Nf1*$^{+/-}$ strain as previously described (McDaniel et al, 2008). All mice used in these experiments were bred in the Indiana University Laboratory Animal Research Center.

B. Behavioral Testing

For all behavioral experiments, adult mice were tested at approximately ten weeks of age. To minimize confounds for the behavior studies, the mice were male, age-matched and experimentally naïve. Upon arrival at the animal facility,

the mice were individually housed in a temperature controlled room (72˚F), and were given food and water *ad libitum*. The housing room was maintained on a 12 hour light-dark cycle (7:00 am / 7:00 pm). Before testing began, the mice were acclimated to the animal facility for six days, and behavioral testing was conducted between 8:00 am and 5:00 pm. A battery of behavioral assessments were performed including tests of general sociability, social learning / memory, anxiety, locomotion, behavioral despair and olfactory sensory habituation (**Figure 5**). All procedures were reviewed and approved by the Indiana University School of Medicine Institutional Animal Care and Use Committee.

1. Tests of social behaviors and social learning / memory:

Utilizing a three-chambered apparatus (Sankoorikal et al, 2006), the following tests were conducted: (1) preference for social interaction, (2) short-term social learning / memory, and (3) long-term social learning / memory (see **Figure 6**). The three-chambered apparatus consisted of a rectangular box (20 inches length x 10 inches width x 9 inches height) that was constructed entirely of black Plexiglas. For our experiments, the Plexiglas was lightly sanded to minimize reflection. The apparatus was open both on top and bottom, and had three interconnecting chambers. The chambers at opposite ends of the apparatus were equal in size (7.5 inches x 10 inches), while the middle chamber was slightly smaller (4.75 inches x 10 inches).

Two identical cylinders (3 inches diameter, 5 inches height) constructed of black wire were used to house “stimulus” mice (i.e., novel vs. familiar). For these

Figure 5. Timeline for behavioral testing

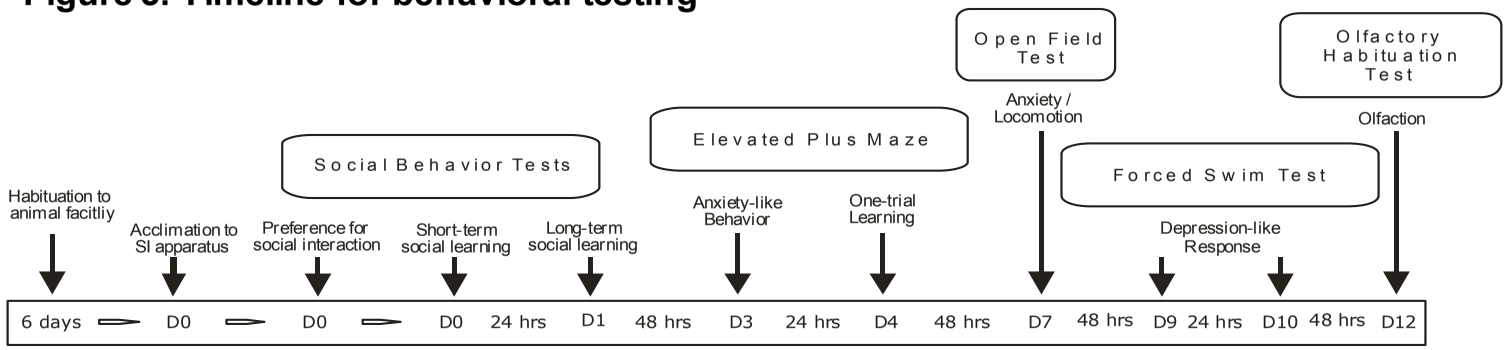

Figure 5. Timeline for behavioral testing. A battery of behavioral assessments was performed to measure sociability, social learning, anxiety, locomotion, behavioral despair and olfactory sensory habituation. The mice were acclimated to the animal facility for six days before testing began, and were followed by the social behavior tests. Four ten minute sessions were conducted that included acclimation, preference for social interaction, short-term learning, and long-term learning (performed 24 hours later). The elevated plus maze was then utilized to measure anxiety-like behavior and then one-trial learning in the EPM (performed 24 hours later), and the open field test was employed to measure both anxiety-like behavior and locomotor activity. Next, the forced swim test was used to measure behavioral despair and learned helplessness over two days of testing. Finally, the olfactory habituation test was utilized to control for differences in olfaction and olfactory learning. Each behavioral component was separated by 48 hours.

(**a**) Acclimation period

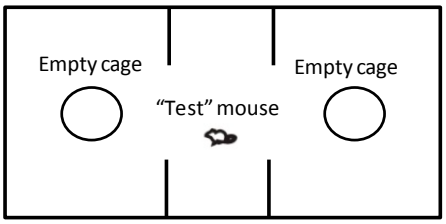

(**b**) Preference for social interaction

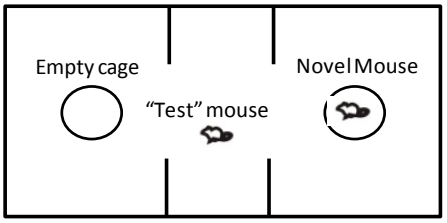

(**c**) Short-term social learning

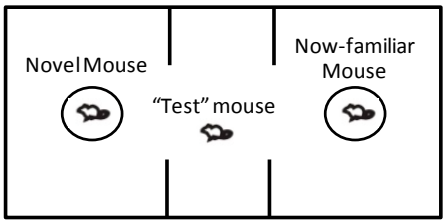

(**d**) Long-term social learning

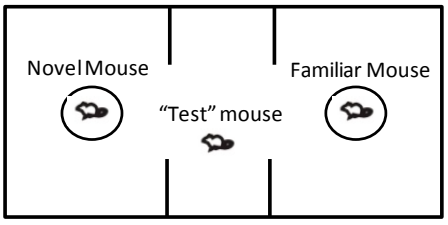

(**e**) Dimensions of the social behavior apparatus

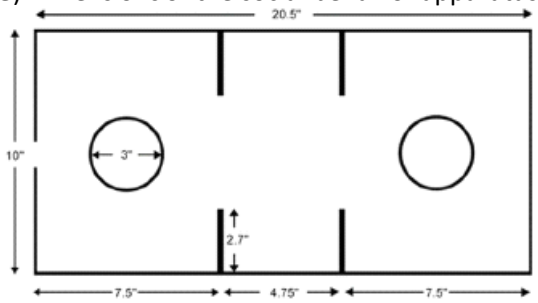

Figure 6

Figure 6. Tests of social behaviors and social learning / memory. To measure social behavior and social learning / memory, a three-chambered rectangular apparatus was utilized consisting of black Plexiglas (Sankoorikal et al, 2006). Two wire cages were placed at opposite ends of the apparatus to house “stimulus” mice. The behavioral testing apparatus is viewed from above. Four ten minute sessions were sequentially conducted to measure preference for social interaction and short-term and long-term social learning. (**a**) During the acclimation period, the “test” mouse was presented with two empty cages. (**b**) During the preference for social interaction session, the “test” mouse was presented with an empty cage and a cage that housed a novel mouse. (**c**) During the short-term social learning session, the “test” mouse was presented with a cage containing the same mouse from the previous session (i.e., now-familiar mouse) and a cage containing a novel mouse. (**d**) During the long-term social learning session, the “test” mouse was presented with a cage containing the “familiar” mouse from 24 hour earlier and a cage containing a novel mouse. The amount of time the “test” mice spent sniffing (i.e., nose pointed toward cage and within one inch of cage) each respective cage was determined for each session. (**e**) Dimensions of the behavioral testing apparatus.

experiments, the wire cylinders were placed in the center of each chamber at opposite ends of the apparatus. The diameter and height of the wire cylinders were sufficient for the “stimulus” mouse to move comfortably, and the openings in the wire cylinders were evenly spaced allowing for auditory, visual, and olfactory investigation as well as some tactile contact. The flooring of the apparatus consisted of a blue diaper mat. This diaper mat was replaced with a clean mat, and the entire apparatus was cleaned with 90% ethanol following the series of tests on each mouse.

Four 10 minute sessions were conducted that included (1) acclimation (two empty cages), (2) preference for social interaction (novel mouse, empty cage), (3) short-term learning of social cues (familiar mouse, novel mouse), and (4) long-term learning of social cues (familiar mouse - 24 hr later, novel mouse). Other than the test of long-term social learning (performed on the following day), each of the test sessions were conducted in sequential order and directly followed the previous test session.

a. Acclimation period: At the start of the “acclimation” period, the “test” mouse was placed in the center chamber of the apparatus with a new diaper mat and both wire cylinders. The “test” mouse was allowed to freely explore the entire apparatus for ten minutes. Following the acclimation period, the “test” mouse was removed from the apparatus and placed in its home cage.

b. Preference for social interaction (Sankoorikal et al, 2006; Nadler et al, 2004; Crawely et al, 2007): At the beginning of the “preference for

social interaction" session, a novel mouse was placed in one wire cylinder, while the other wire cylinder was left empty. The "test" mouse was then reintroduced into the center chamber of the apparatus and allowed to freely explore the entire apparatus for ten minutes. Following the preference for social interaction test, the "test" mouse was removed from the apparatus and placed in its home cage.

c. Short-term social learning / memory (refer to Nadler et al, 2004; Crawely et al, 2007): A second novel mouse was then placed in the second cylinder located on the opposite side of the apparatus from the cylinder containing the now-familiar mouse. The "test" mouse was then reintroduced into the center chamber of the apparatus and allowed to freely explore the entire apparatus for ten minutes. Following the short-term social learning / memory test, the "test" mouse was removed from the apparatus and placed in its home cage. The second novel mouse then was removed from the apparatus and placed in its home cage.

d. Acclimation to now-familiar mouse: The "test" mouse was then reintroduced into the center chamber of the apparatus containing the first "now-familiar" mouse and allowed to freely explore the entire apparatus for an additional forty-five minutes. After the forty-five minute session, both mice were removed from the apparatus and placed in their home cages.

e. Long-term social learning / memory (refer to Nadler et al, 2004; Crawely et al, 2007): On the second day (24 hours later), the "familiar" mouse from the previous day was randomly placed under one of the wire

cylinders, and another novel mouse was placed under the second wire cylinder. The “test” mouse was then reintroduced into the center chamber of the apparatus and allowed to freely explore the entire apparatus for a ten minute period. Following the long-term social learning / memory test, the “test” mouse was removed from the apparatus and placed in its home cage.

All testing sessions were recorded by a video camera that was fixed above the social interaction box and independently scored at a later time by two individuals who were unaware of the animals’ genotype. Because the majority of social interaction occurs during the first five minutes of a testing session (Nadler et al, 2004), the time the “test” mouse spent sniffing the wire cage was measured during this time frame. For the acclimation period, three dependent variables were measured to control for potential effects of the testing environment, and included (1) the time the “test” mouse spent sniffing (i.e., nose pointed toward cage and within one inch of cage) each respective wire cylinder, (2) the time spent in each of the side chambers on opposite ends of the apparatus, and (3) the number of entries the “test” mouse made into the chambers on opposite ends of the apparatus. For all other sessions, the time the “test” mouse spent sniffing each respective wire cylinder was scored.

2. Tests of anxiety-like behavior

The elevated plus maze (EPM) was employed to measure anxiety-like behavior (refer to Hogg, 1996) and one-trial learning as defined by the classic

reduction in open arm exploration on day 2 (refer to Roy et al, 2009) in mice. The EPM apparatus consists of two open and two closed arms, and each arm of the EPM measures 2 inches wide and 14 inches long. These arms emanate from a central platform that is square (2 x 2 inches) to form a plus shape. The arms and central platform of the apparatus are elevated to a height of 24.5 inches above the floor. The closed arms are surrounded by a 6 inch high enclosure constructed of black Plexiglas. Following each experiment, the entire apparatus was cleaned with 90% ethanol.

Anxiety-like behavior in mice was measured using a five minute trial. At the start of each EPM session, the “test” mouse was placed on the center platform of the EPM apparatus with its head facing the open arm. The “test” mouse was allowed to freely explore the entire apparatus for a period of five minutes. The “test” mouse was then removed from the EPM apparatus and placed in its home cage. For the one-trial learning test, the “test” mouse is re-tested in the EPM apparatus for an additional five minute session separated by twenty-four hours. For each testing session, two dependent variables were measured including (1) the time spent in the open arms and (2) the number of entries into the open arms. An open arm entry was defined as having all four paws into the arm of the EPM. All testing sessions were recorded by a video camera that was fixed above the EPM apparatus and scored at a later time.

3. Measurement of locomotor activity

The “test” mouse was placed in an open field to measure locomotor activity and to screen for anxiety-like behavior (Grentsch et al, 1987). The open field was a rectangular opaque Plexiglas enclosure (beige in color) that measured 19.75 x 19.75 inches wide, and the height of the walls was 15.25 inches. The flooring was constructed of the same beige Plexiglass, and the top of the open field apparatus was open to the environment. To measure locomotor activity and anxiety, the “test” mouse was placed in a corner of the open field arena, and its movements were recorded under florescent light during a ten minute session. A SMART II Video Tracker system (San Diego Instruments, San Diego, CA) was used to track movements of the “test” mice. Each enclosure was divided into nine pre-defined areas including the center area, four corner areas, and four wall areas. The dependent variables to measure anxiety included (1) the total time spent in the center region, (2) the total number of entries into the center region, and (3) the total distance traveled in the center region. The dependent variables to measure exploratory activity included (1) the total distance traveled and (2) the total entries within and between each of the nine regions of the enclosures. Following each experiment, the entire apparatus was cleaned with 90% ethanol.

4. Tests of behavioral despair and learned helplessness

The forced swim test is utilized to measure aspects of behavioral despair and learned helplessness in rodents (Porsolt et al, 1977). The forced swim

apparatus consisted of a cylindrical chamber constructed of clear Plexiglas with a diameter of 8.5 inches and height of 10 inches. The top of the cylinder was left open to the environment throughout the experiment. For each trial, the chamber was filled with 25 ± 1˚C water to a depth of 5.75 inches. The "test" mouse was then gently placed into the cylinder for 15 minutes. Twenty-four hours later, the mice were re-exposed to the same conditions for an additional six minute trial. The dependent variable scored for the forced swim test was 'immobility' or the cessation of limb movements except minor involuntary hind limb movements during the 2 - 6 minute interval. Following each trial, the water was discarded and replaced with clean water adjusted to the aforementioned height and temperature. All testing sessions were recorded by a video camera and scored at a later time.

5. Measurement of olfactory sensory habituation

In rodents, dyadic social interactions are largely mediated by olfactory response. The olfactory sensory habituation test provides an important indicator for differences in the response to olfactory cues (Crawley et al, 2007). For this experiment, the "test" mouse was placed in a clean mouse cage constructed of clear Plexiglas and containing fresh litter. Before testing began, the "test" mouse was acclimated to its new cage for at least thirty minutes. The "test" mouse was then presented with nine cotton applicators that were dipped in either water or almond extract (1:100 dilution), or wiped in a zig-zag pattern across the bottom surface of a cage that contained an "unfamiliar" mouse. The "unfamiliar" mouse

was a singly housed male mouse (C57BL/6J) that had lived in the cage for at least 3 days. For each trial the cotton applicators were suspended from the cage lid and were presented in the following sequence: (1) water, (2) water, (3) water, (4) almond, (5) almond, (6) almond, (7) unfamiliar cage, (8) unfamiliar cage, (9) unfamiliar cage. Each swab was presented for 2 minutes for a total session lasting 18 minutes per mouse. The amount of time that the "test" mouse spent sniffing each cotton swab was scored. All testing sessions were recorded by a video camera and scored at a later time.

C. Isolation and culture of neuronal cells from murine strains

Mouse neurons were aseptically dissected from the frontal cortex and cultured from each respective genotype (WT, *Nf1*$^{+/-}$, *Nf1*$^{+/-}$ / *Pak1*$^{-/-}$, *Pak1*$^{-/-}$). Following microdissection by Dr. Rajesh Khanna, neuronal cells were isolated by dissociation both enzymatically and mechanically (via trituration through a flame-polished Pasteur pipette) in a Papain solution (12 units/ml; Worthington) as described previously (Brittain et al, 2009). The Papain solution contained Leibovitz's L-15 medium (Invitrogen), 0.42 mg/ml cysteine (Sigma), 250 units/ml DNase I (type IV; Sigma), 25 mm NaHCO3, penicillin (50 units/ml)/streptomycin (50 µg/ml), 1 mm sodium pyruvate, and 1 mg/ml glucose (Invitrogen). After dissociation, the cells were gently washed by centrifugation in Neurobasal medium containing 20 mg/ml bovine serum albumin and penicillin/streptomycin, glucose, pyruvate, and DNase I (as above) and then plated on poly-d-lysine-coated acid-washed glass coverslips at high density (~4000 cells/mm2). Growth

media (1 ml/well) consisted of Neurobasal medium containing 2% NuSerum, 2% B27, supplemented with penicillin/streptomycin (100 units/ml; 50 µg/ml), 0.1 mm l-glutamine, and 0.4 mm l-Glutamax (Invitrogen). Cytosine β-d-arabinofuranoside (5 µm; Sigma) was added 24 hours after plating to reduce the number of non-neuronal cells. After four days in culture and two times each week thereafter, half of the growth medium was replaced with medium without cytosine β-d-arabinofuranoside.

For this experiment, the neuronal cultures were assigned to one of two experimental conditions: (i) at basal levels and (ii) following the application of recombinant murine stem cell factor (rmSCF; PreproTech) at 10 ng/ml. rmSCF was applied to the neuronal cultures for 2 minutes. The cells were then washed with ice-cold PBS and lysed in buffer containing Laemmle dye with 10% β-mercaptoethanol, boiled for five minutes at 95˚C, and then frozen at -80˚C until further analysis.

D. Immunoblotting ERK / p-ERK in mouse cortical neurons

Whole cell protein extracts were obtained from cultured prefrontal cortical neurons in lysis buffer (50mM Tris pH 7.4, 150mM NaCl, 2mM EDTA pH 8.0, 1% Triton X-100, 1mM PMSF, 1mM NaF, 1mM Na3VO4,10% glycerol and complete protease inhibitor). The samples were sonicated and cellular debris was removed by centrifugation at 13,000g for 30 min at 4˚C. Protein concentrations were determined using a BCA assay (Thermo Scientific). Equivalent amounts of protein was electrophoresed on 10% SDS-PAGE gels, transferred to PVDF

membranes (GE Healthcare, Little Chalfont, United Kingdom), and detected by Western blotting using the ECL Plus system (Amersham Biosciences). Antibodies used were Phospho-ERK Antibody (Cell Signaling Technology), ERK1 Antibody (Cell Signaling Technology), and GAPDH (MIllipore). Protein isolation and Western blotting was conducted in collaboration with Dr. Rajesh Kanna.

E. Electrophysiological measurement of IPSCs in the BLA

Using the whole-cell patch-clamp, inhibitory synaptic currents were measured by Dr. Andrei Molosh from glutamatergic projection neurons in the basolateral amygdala (**Figure 7**). Adult male mice were decapitated using a guillotine. The brains were then rapidly removed and placed in oxygenated artificial cerebrospinal fluid (ACSF) [130 mM NaCl; 3.5 mM KCl; 1.1 mM KH_2PO_4; 1.3 mM $MgCl_2$; 2.5 mM $CaCl_2$; 30 mM $NaHCO_3$; 10 mM glucose]. Coronal slices (350 μM) were then prepared containing the BLA. Prior to recording, these slices were incubated at room temperature for 1 hour in oxygenated ACSF [95% O_2 / 5% CO_2 mixture]. The coronal slices were then transferred to a submersion-type slice chamber that was mounted on the stage of a Nikon E600FN Eclipse (Nikon Instruments, Melville, NY) microscope and perfused with ACSF [1-2 ml per minute] heated to 32˚C.

Projection neurons were identified according to their characteristic size and shape (Pickel et al, 2008). Prior to recording utilizing the whole-cell patch

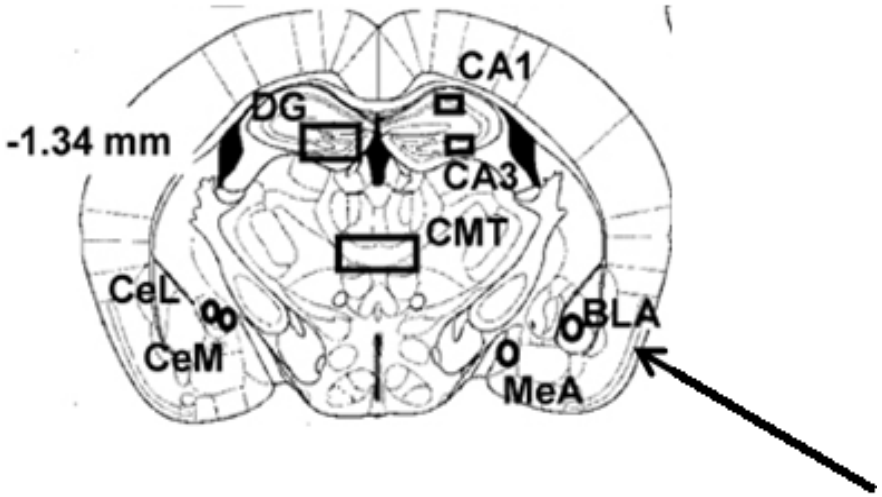

Figure 7. The basolateral amygdala (BLA) in the mouse brain. The figure above illustrates a representative coronal slice from the mouse brain that contains the BLA (adapted from Paxinos and Watson). Coronal slices (350 μM) were prepared containing the BLA for electrophysiological and protein expression studies. BLA - basolateral amygdala; CA1 and CA3 - Cornu ammonis areas in hippocampus; CeL - central amygdala, lateral division; CeM - central amygdala; CMT - central medial thalamic nucleus; DG - Dentate Gyrus; MeA - medial amygdala

clamp, borosilicate glass electrodes (WPI, Sarasota, FL) (resistance 3-6 MΩ) were prepared that contained a potassium gluconate based solution [130 mM K-Gluconate, 3 mM KCl, 3 mM $MgCl_2$, 5 mM phosphocreatine, 2 mM K-ATP, 0.2 mM NaGTP, 10 mM HEPES]. While maintaining a holding potential of -60 mV, whole-cell access resistances were monitored throughout each experiment. These resistances ranged from 5-20 MΩ, and a change of 15% was deemed acceptable.

At the start of each experiment, a series of standardized current clamp protocols were performed to confirm that the BLA neuron that was patched was, in fact, a BLA projection neuron. Pharmacological agents were administered to BLA projection neurons by adding the specified concentration directly to the ACSF prior to perfusion. First, spontaneous inhibitory synaptic currents (sIPSC) were recorded in the presence of 6,7-Dinitroquinoxaline-2,3-dione (DNQX; 20 μM) and 3-(2-carboxypiperazin-4-yl)propyl-1-phosphonic acid (CPP; 10 μM) at a holding potential of -55 mV. DNQX and CPP function as AMPA and NMDA antagonists. Miniature IPSC (mIPSC) were then recorded following the administration of 1 μM tetrodotoxin (TTX), a potent neurotoxin that selectively blocks sodium channels. Both sIPSC and miniature IPSC (mIPSC) were captured continuously for 30 seconds at a sampling frequency of 20 kHz. Spontaneous currents were later analyzed using the pClamp 10.2 (Molecular Devices, Sunnyvale, CA). To determine whether the increases in IPSCs detected in the BLA were GABA- or glycine-mediated, 1 μM CGP 52432 ($GABA_B$ antagonist) and 5 μM SR 95531 hydrobromide ($GABA_A$ antagonist) were added

at the specified concentration directly to the ACSF following the administration of DNQX / CPP and then TTX.

F. Quantification of protein in the BLA and PFC

Tissue slices were prepared following decapitation and transferred to centrifuge tubes placed in dry ice for rapid freezing and stored at −80˚C. The resulting tissues were first homogenized in a solution containing 400 µl of 50 mM ammonium bicarbonate for five minutes. Whole cell protein extracts were obtained from brain slices in lysis buffer (30mM Tris, pH7.4, 150mM NaCl, 1% Triton X-100, 0.1% SDS, 1mM PMSF, 10mM EDTA, 1mM Na2CO3, 160mM NaF, complete protease inhibitor) with ProteoSpin total protein detergent clean up micro kit (Norgen, Canada). Then protein concentrations of the lysates were determined using a BCA Protein Assay Kit (Pierce, Rockford, IL).

Protein samples were then subjected to tryptic digestion. After thermal denaturation at 95˚C for five minutes, protein samples were reduced through the addition of dithiothreitol (DTT) to a final concentration of 5mM and incubated at 60˚C for 45 minutes. Alkylation was achieved by adding iodoacetamide (IAA) to a final concentration of 20 mM prior to incubation at room temperature for 45 minutes in the dark. A second aliquot of DTT was then added, increasing the final concentration of DTT to 10 mM. The samples were then incubated at room temperature for 30 minutes to quench the alkylation reaction. Next, trypsin was added (1:30 w/w) and microwave-assisted enzymatic digestion was carried out at

45˚C for 15 minutes at the power of 50 W, and enzymatic digestion was quenched through the addition of neat formic acid.

LC-MS/MS analyses of the tryptic digests were performed by Dr. Zaneer Segu using a Dionex 3000 Ultimate nano-LC system (Dionex, Sunnyvale, CA) interfaced to LTQ Orbitrap hybrid mass spectrometer (Thermo Scientific, San Jose, CA). Prior to separation, a 2-µl aliquot of trypsin digestion (1.5 µg protein equivalent) was loaded on PepMap300 C18 cartridge (5 µm, 300 Å, Dionex) and eluted through the analytical column (150 mm x 100 µm i.d, 200 Å pores) packed with C18 magic (Michrom Bioresources, Auburn, CA). Peptides originating from protein tryptic digests were separated using a reversed-phase gradient from 3-55% B, 97% acetonitrile with 0.1% formic at 500 nl/min flow rate and passed through an ADVANCE ionization source (Michrom Bioresources, Auburn, CA).

The mass spectrometer was operated in an automated data-dependent mode that was switching between MS scan and CID-MS. In this mode, eluted LC products undergo an initial full-spectrum MS scan from *m*/*z* 300 to 2000 in the Orbitrap at 15,000 mass resolutions. Subsequently CID-MS (at 35% normalized collision energy) was performed in the ion trap. The precursor ion was isolated using the data-dependent acquisition mode with a 2 *m*/*z* isolation width to select automatically and sequentially five most intense ions (starting with the most intense) from the survey scan. The total cycle (6 scans) is continuously repeated for the entire LC-MS run under data-dependent conditions with dynamic exclusion set to 60 seconds. Performing MS scanning in the Orbitrap offers high

mass accuracy and accurate charge state assignment of the selected precursor ions.

G. Bioinformatics and analyses of proteomic data

Mascot version 2.1.3 was used for all search results obtained in this work. The data were searched against Swiss-Prot database for house mouse. Trypsin was selected as the enzyme and one missed cleavage was allowed. A carbomidomethyl was selected as a fixed modification of all cysteine residues. The mass tolerance of both MS and MS/MS data were set to 0.8 Da. Peptides with mass accuracy better than 2 ppm and Mascot ion score of 30 and above were considered as positive identification. The quantitative analysis of proteins was carried out using ProteinQuant Suit developed at Indiana University (Mann et al, 2008). Briefly, the raw data obtained from LTQ-Orbitrap XL mass spectrometer are converted to MASCOT generic file (MGF). MGF files were then parsed with ProtParser subject to specific parsing criteria. Minimum MOWSE score was set to 30 and proteins with two peptides match or above were considered as a confident match. Then all parsed files were combined into a master file that contains the list of all proteins and peptides identified in the span of all the processed LC-MS/MS analyses. Then the combined master files were incorporated with their corresponding mzXML files, and were submitted to ProteinQuant as described previously (Mann et al, 2008).

Bioinformatics and statistical analysis of protein data were conducted using Partek®Genomics Suite (©Partek Incorporated, St. Louis, MI) in

collaboration with Dr. Chirayu Goswami. To analyze the data for each protein, the log base 2 was first determined for each data point in order to correct for non-uniform residuals and to generate absolute values [http://www.sportsci.org]. A one-way analyses of variance (ANOVA) analysis was then performed comparing protein expression for each respective genotype (i.e., WT, *Nf1*$^{+/-}$, *Nf1*$^{+/-}$ / *Pak1*$^{-/-}$, and *Pak1*$^{-/-}$). When significant differences were obtained, Fisher's protected least significant difference (PLSD) *post hoc* test was applied to conduct individual comparisons between groups. Significance was determined at $P < 0.05$ for all analyses.

H. Statistical Analyses

Data were analyzed using one-way or two-way analyses of variance (ANOVAs) or repeated measures ANOVAs. To measure of short-term and long-term social learning in the *social behavior tests*, preference for social novelty was evaluated using within-genotype repeated measures ANOVAs performed on time spent sniffing cages (i.e., nose pointed toward cage and within one inch) using cage occupancy (e.g., novel mouse or “familiar” mouse) as the factor. To assess *anxiety-* and *depression-like* behaviors, two factor (mouse genotype x day) mixed ANOVAs were performed on time spent in and entries into the open arm of the EPM and percent time spent immobile in the FST, respectively. The data from the *open field test* were analyzed using a student’s *t*-test (WT vs. *Nf1*$^{+/-}$) or one-way ANOVAs (*Nf1*$^{+/-}$ vs. *Nf1*$^{+/-}$ / *Pak1*$^{-/-}$ vs. Pak1$^{-/-}$). For the *olfactory habituation test*, two factor (mouse genotype x scent) mixed ANOVAs were performed on the

amount of time spent sniffing the cotton applicator suspended from the cage lid for each respective scent. To analyze relative *ERK activation* (basal levels vs. SCF), a two factor (genotype x SCF application) mixed ANOVA was performed on ERK1/2 / p-ERK1/2 levels quantified using Western blotting. When significant effects were obtained using ANOVAs, the data were further analyzed using *post hoc* Fisher's protected least significant difference (PLSD) tests. For electrophysiology, statistical analyses included paired *t*-test and one-way ANOVAs using a Dunnet's *post-hoc*. For all comparisons the confidence level for significance was set at $P < 0.05$.

RESULTS

A. Experiment 1: Behavioral effects associated with the heterozygous gene deletion of *Nf1* (*Nf1*$^{+/-}$) in mice

1. Effects on sociability / social learning

During the acclimation period, the WT and *Nf1*$^{+/-}$ mice were presented with two empty cages that were placed on opposite ends of the three chambered apparatus to control for effects of the testing room environment. Statistical analyses consisted of a two factor (mouse genotype x cage occupancy) mixed ANOVA performed on three dependent variables including time spent sniffing each respective cage, time spent in each of the side chambers, and entries into each of the side chambers. No differences were observed between genotypes [$F(1,22)=0.691$; $P=0.69$] or within each genotype [$F(1,22)=0.149$; $P=0.703$ for empty cage verses empty cage] for the time spent sniffing each respective empty cage, and no genotype x cage interaction [$F(1,22)=0.125$; $P=0.13$] was detected (**Figure 8a**). Additionally, WT and *Nf1*$^{+/-}$ strains showed no differences between genotypes [$F(1,22)=0.073$; $P=0.79$] in time spent in each of the side chambers, and exhibited no left-right side preference [$F(1,22)=0.327$; $P=0.573$] nor was there a genotype x side interaction [$F(1,22)=3.831$; $P=0.063$] in the three chambered apparatus (**Figure 8b**). Additionally, no significant effects of between genotypes [$F(1,22)=0.077$; $P=0.79$] or within each genotype [$F(1,22)=2.390$; $P=0.136$] were detected on numbers of entries into the side chambers

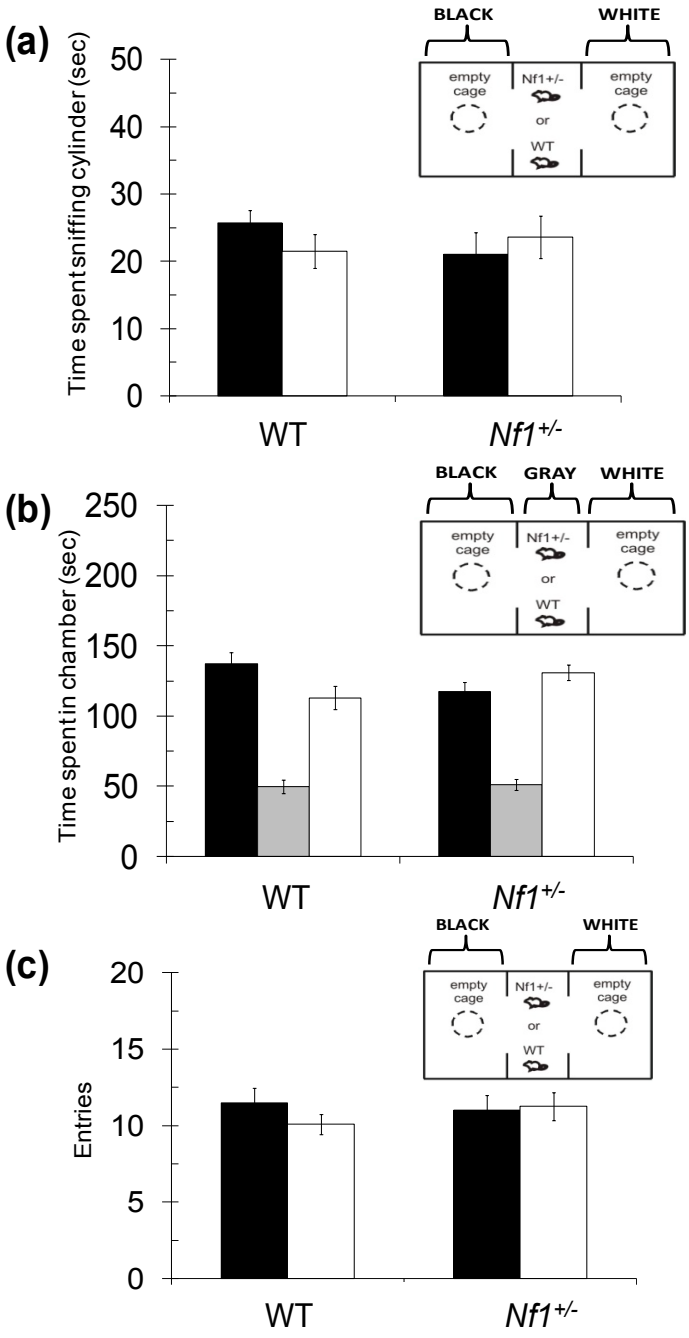
(a)
Time spent sniffing cylinder (sec)
50
40
30
20
10
0
BLACK
WHITE
empty cage
Nf1+/-
or
WT
empty cage
WT
Nf1+/-
(b)
Time spent in chamber (sec)
250
200
150
100
50
0
BLACK
GRAY
WHITE
empty cage
Nf1+/-
or
WT
empty cage
WT
Nf1+/-
(c)
Entries
20
15
10
5
0
BLACK
WHITE
empty cage
Nf1+/-
or
WT
empty cage
WT
Nf1+/-

Figure 8

Figure 8. The testing room environment has no effect(s) on time spent sniffing cylinders, side preference or entries into the side chambers. During the acclimation session, the WT and *Nf1*$^{+/-}$ mice were presented with two empty cages that were placed on opposite ends of the three chambered apparatus. The graphs depict (**a**) the amount of time spent sniffing each cylinder, (**b**) time spent in the chambers on opposite sides of the apparatus, or (**c**) the total entries into each respective chamber. Data were collected for the first five minutes of the ten minute session and represent the mean ± SEM for each group. Because the time spent in each of the chambers are mutually exclusive rather than independent measures, statistical analyses were only performed between the two side chambers, and the time spent in the center chamber was presented solely for visual comparisons.

(**Figure 8c**). Therefore, these results confirm the absence of an innate side preference in the testing room environment.

a. Preference for social interaction

Following the acclimation period, the WT and *Nf1*$^{+/-}$ mice were presented with a cage containing a novel mouse and an empty cage that were placed on opposite ends of the three chambered apparatus in order to assess their preference for social interaction. The amount of time the "test" mouse spent sniffing a cage containing a novel mouse was measured, as compared to an empty cage. Statistical analyses consisted of a two factor (mouse genotype x cage occupancy) mixed ANOVA performed on time spent sniffing each respective cage. Statistical analysis revealed that both WT and *Nf1*$^{+/-}$ strains spent significantly more time sniffing the cage with a novel mouse over the empty cage [$F(1,22)=105.8$; $P=0.0001$ for cage with novel mouse verses empty cage]. No significant effects were detected between genotypes [$F(1,22)=1.544$; $P=0.227$] in amount of time spent sniffing the cage, nor was there a genotype x cage interaction [$F(1,22)=0.881$; $P=0.358$]. Fisher's PLSD post hoc analysis detected significantly more time sniffing the cage containing the novel mouse than the empty wire cage for both WT and *Nf1*$^{+/-}$ genotypes ($P < 0.001$; **Figure 9**). These findings demonstrate that both genotypes show similar levels of sociability.

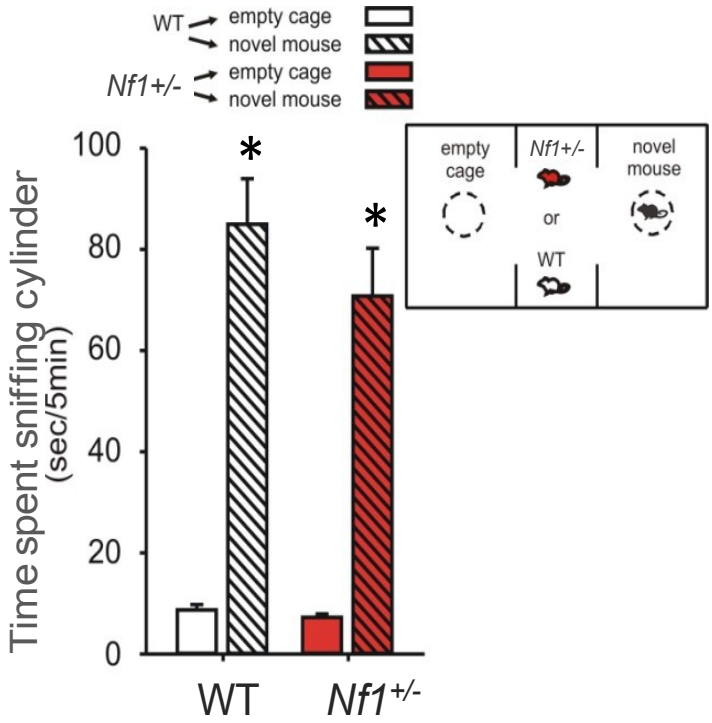

Figure 9. *Nf1*$^{+/-}$ mice show normal preference for social interaction, as compared to WT (n=12/group). During the "preference for social interaction" session, the WT and *Nf1*$^{+/-}$ mice were presented with a cage containing a novel mouse and an empty cage that were placed on opposite ends of the three chambered apparatus. The graph illustrates the amount of time "test" mouse spent sniffing each respective cage. Data were collected for the first five minutes of the ten minute session and represent the mean ± SEM for each group. *P < 0.05 for a within-group comparison between the cage containing the novel mouse verses the empty cage.

b. Short-term social learning / memory

Short-term social learning / memory was quantified as a measure of "preference for social novelty", and was defined by the following cage occupancy (i.e., novel mouse or "familiar" mouse) as the within-genotype factor. Statistical analyses consisted of a two factor (mouse genotype x cage occupancy) mixed ANOVA performed on time spent sniffing each respective cage. When presented with a cage containing a novel mouse and a cage containing a now-familiar mouse (3 min. following exposure to "test" mouse), both WT and *Nf1*$^{+/-}$ genotypes spent significantly more time sniffing the cage containing the novel mouse over the cage containing the now-familiar mouse [$F(1,22)=15.1$; $P=0.001$ for cage with novel mouse verses cage with the familiar mouse]. No differences were observed between genotypes [$F(1,22)=0.899$; $P=0.353$] in amount of time spent sniffing the cages, and genotype x cage interaction [$F(1,22)=0.361$; $P=0.554$] was detected. Fisher's PLSD post hoc analysis detected significantly more time sniffing the cage containing the novel mouse over the cage containing the familiar mouse for both WT and *Nf1*$^{+/-}$ genotypes ($P < 0.05$), and demonstrate that *Nf1*$^{+/-}$ mice show intact short-term social learning (**Figure 10a**).

c. Long-term social learning / memory

Similar to the short-term learning / memory test, long-term social learning / memory was assessed as a measure of "preference for social novelty". The WT and *Nf1*$^{+/-}$ mice were presented with a cage containing a novel mouse and cage

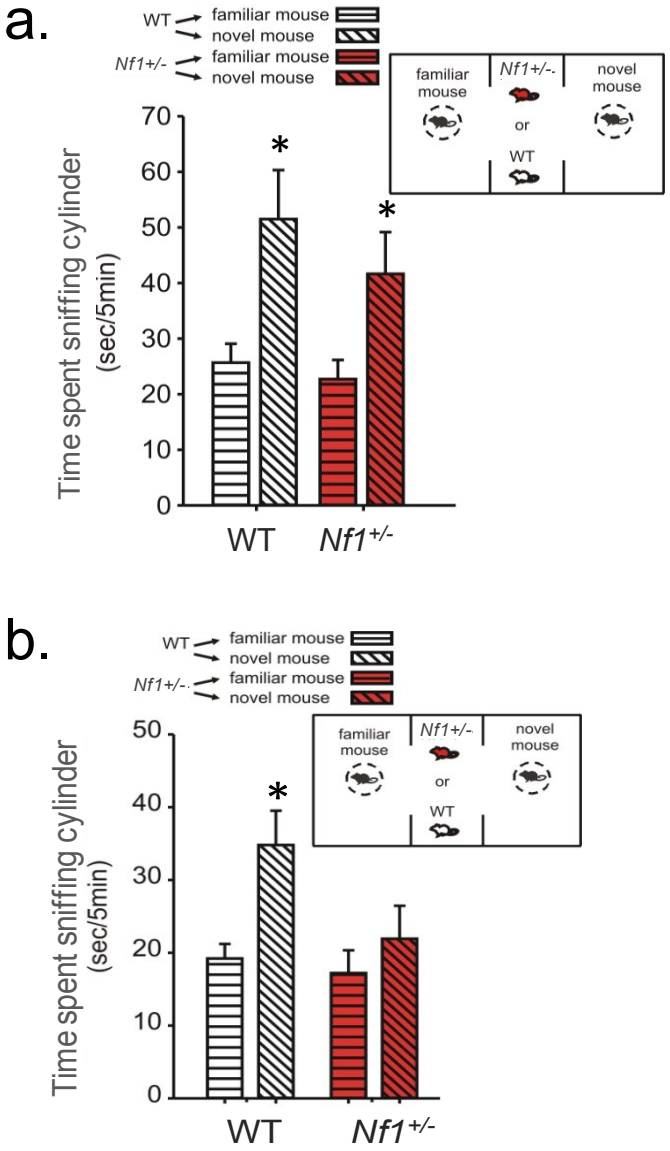
a.
WT
familiar mouse
novel mouse
Nf1+/-
familiar mouse
novel mouse
familiar mouse
Nf1+/-
novel mouse
or
WT
Time spent sniffing cylinder (sec/5min)
70
60
50
40
30
20
10
0
*
*
WT
Nf1+/-
b.
WT
familiar mouse
novel mouse
Nf1+/-
familiar mouse
novel mouse
familiar mouse
Nf1+/-
novel mouse
or
WT
Time spent sniffing cylinder (sec/5min)
50
40
30
20
10
0
*
WT
Nf1+/-

Figure 10

Figure 10. *Nf1*$^{+/-}$ mice show intact short-term social learning, but display deficits in long-term social learning, as compared to WT (n=12/group). The graphs depict the effects of the *Nf1* gene deletion on short-term and long-term social learning, as measured by their "preference for social novelty". (**a**) During the "short-term social learning" session, the WT and *Nf1*$^{+/-}$ mice were presented with a cage containing the now-familiar mouse from the previous session and one containing a novel mouse that were placed on opposite ends of the three chambered apparatus. (**b**) During the "long-term social learning" session, the WT and *Nf1*$^{+/-}$ mice were presented with a cage containing the same familiar mouse from the previous day and a cage containing a novel mouse. The graphs illustrate the amount of time "test" mouse spent sniffing each respective cage. Data were collected for the first five minutes of the ten minute session and represent the mean ± SEM for each group. *$P < 0.05$ for a within-group comparison between the cage containing the now-familiar mouse and the cage containing the novel mouse.

containing the same familiar mouse from 24 hours earlier. Similar to the short-term social learning test, statistical analyses consisted of a two factor (mouse genotype x cage occupancy) mixed ANOVA performed on time spent sniffing each respective cage. No differences were observed between genotypes [$F(1,22)=2.843$; $P=0.106$] in amount of time spent sniffing the cages and no significant genotype x cage interaction was seen [$F(1,22)=3.4$; $P=0.08$]. However, a significant effect was detected in the amount of time the "test" mice spent sniffing each respective cage [$F(1,22)=11.7$; $P=0.002$ for cage with novel mouse verses cage with the familiar mouse]. Fisher's PLSD post hoc analysis detected significantly more time sniffing the cage containing the novel mouse over the cage containing the familiar mouse for WT ($P < 0.005$), but no significant difference for *Nf1*$^{+/-}$ genotype ($P = 0.25$; **Figure 10b**). Therefore, unlike WT mice, these results suggest that *Nf1*$^{+/-}$ mice are unable to retain and discriminate between social cues following a 24 hour delay.

2. Effects on anxiety-like behavior

Two behavioral tests were employed to test for differences in anxiety-like behavior between WT and *Nf1*$^{+/-}$ mice, including the elevated plus maze (Hogg, 1996) and the open field test (Grentsch et al, 1987). The elevated plus maze was also used to measure one-trial learning to assess whether *Nf1*$^{+/-}$ show the classic reduction in open arm duration and open arm entries seen on day 2 that are associated with learning / memory (Roy et al, 2009).

a. Elevated plus maze

For the EPM, statistical analyses consisted of a two factor (mouse genotype x time) mixed ANOVA performed on time spent in the open arms and entries into the open arms of the EPM. No significant effects were detected between genotypes in amount of time spent in the open arm [$F(1,22)=0.369$; $P=0.550$] or entries into the open arm [$F(1,22)=0.527$; $P=0.476$] of the EPM, nor were there a genotype x time interactions for either open arm time [$F(1,22)=0.004$; $P=0.950$] or open arm entries [$F(1,22)=0.215$; $P=0.648$]. However, statistical analyses revealed a significant effect of time (i.e., 24 hours) on both open arm duration [$F(1,22)=10.9$; $P=0.003$ for day 2 verses day 1] and open arm entries [$F(1,22)=11.5$; $P=0.003$ for day 2 verses day 1]. Fisher's PLSD *post hoc* analysis detected significant decreases in open arm duration and open arm entries on day 2 relative to day 1 for both WT and *Nf1*$^{+/-}$ genotypes ($P < 0.05$; **Figure 11a-b**). Therefore, these results indicate that WT and *Nf1*$^{+/-}$ mice exhibit no significant differences in anxiety or deficits in one-trial learning, as measured by the EPM.

b. Open field test

The time spent in the center region and entries into the center region of a novel open field are inversely correlated with anxiety-like behavior in rodents (Grentsch et al, 1987). A student's *t*-test was performed to analyze time spent in the center region, entries into the center region, distance traveled in the center

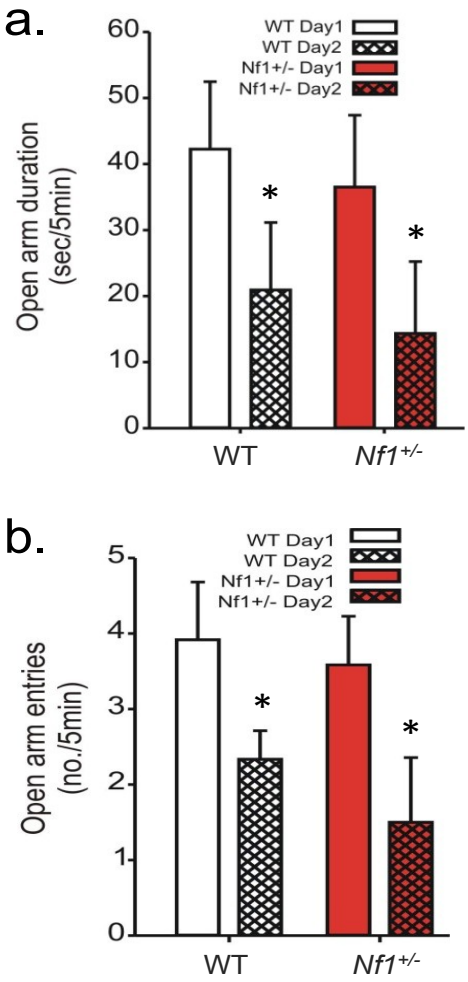
a.
WT Day1
WT Day2
Nf1+/- Day1
Nf1+/- Day2
Open arm duration (sec/5min)
60
50
40
30
20
10
0
*
*
WT
Nf1+/-
b.
WT Day1
WT Day2
Nf1+/- Day1
Nf1+/- Day2
Open arm entries (no./5min)
5
4
3
2
1
0
*
*
WT
Nf1+/-

Figure 11

Figure 11. *Nf1*$^{+/-}$ mice exhibit no differences in anxiety-like behavior or one-trial learning, as compared to WT (n=12/group). Open arm duration and open arm entries were measured in WT and *Nf1*$^{+/-}$ mice during a five minute test using the elevated plus maze. Additionally, mice re-tested in the elevated plus maze 24 hours later to assess one-trial learning. The graphs illustrate (**a**) the time spent in the open arm and (**b**) entries into the open arm. Data were collected during two five minute trials separated by 24 hours and represent the mean ± SEM for each group. *$P < 0.05$ for a within-group comparison between day 1 verses day 2 for each respective genotype.

region, total entries, and total distance traveled during a ten minute session in *Nf1*$^{+/-}$ mice, as compared to WT. No differences were detected between in time spent in the center region (t=0.193, P=0.849), entries into the center region (t=-0.760, P=0.455), or distance traveled in the center region (t=-0.909, P=0.373; see **Figure 12a-c**). Additionally, no differences were detected between *Nf1*$^{+/-}$ and WT strains in total entries (t=0.-956, P=0.349) or total distance traveled (t=0.-1.354, P=0.189) during the ten minute session (see **Figure 12d-e**). These findings suggest that *Nf1*$^{+/-}$ genotype does not impact anxiety-like behaviors, nor does *Nf1*$^{+/-}$ genotype influence locomotor or exploratory activity in mice.

3. Effects on behavioral despair / learned helplessness

Previous studies have found an increased risk for development of mood disorders in patients diagnosed with NF1 (Samuelsson and Riccardi, 1989; Zoller and Rembeck, 1999; Johnson et al, 1999). Swimming “immobility” is thought to be positively correlated with depression-like response in rodents (Porsolt et al, 1977). Percent of time immobile was measured in WT and *Nf1*$^{+/-}$ during two trials that were separated by 24 hours. Statistical analyses for the forced swim test consisted of a two factor (mouse genotype x time) mixed ANOVA performed percent time spent immobile in the Plexiglas cylinder containing water. No significant differences were detected between WT and *Nf1*$^{+/-}$ genotypes in their percent of time immobile [$F(1,22)=0.511$; $P=0.482$], nor a genotype x time interaction [$F(1,22)=0.684$; $P=0.417$]. While a significant effect of day (i.e., 24

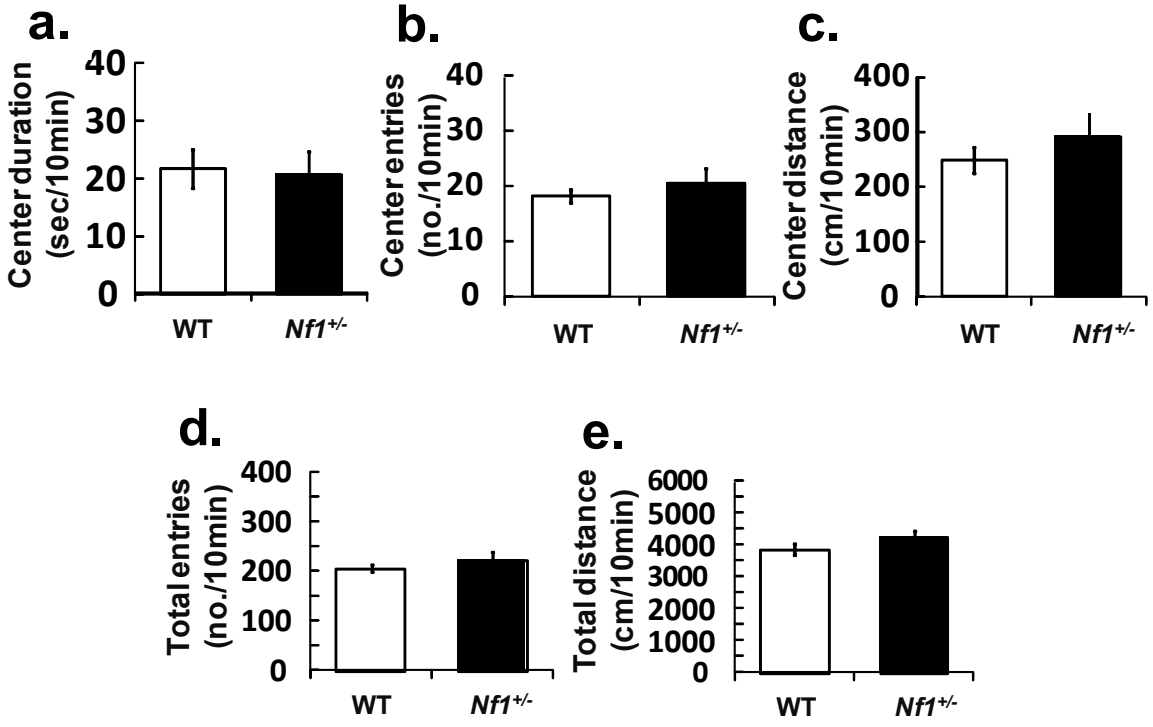
a.
Center duration (sec/10min)
40
30
20
10
0
WT
Nf1+/-
b.
Center entries (no./10min)
40
30
20
10
0
WT
Nf1+/-
c.
Center distance (cm/10min)
400
300
200
100
0
WT
Nf1+/-
d.
Total entries (no./10min)
400
300
200
100
0
WT
Nf1+/-
e.
Total distance (cm/10min)
6000
5000
4000
3000
2000
1000
0
WT
Nf1+/-

Figure 12

Figure 12. No differences were detected between *Nf1*$^{+/-}$ and WT strains (n=12/group) in novel open field exploration. A SMART II Video Tracker (VT) system was used to track movement of the *Nf1*$^{+/-}$ and WT mice in a square enclosure that was divided into nine pre-defined areas (i.e., center area, four corner areas, and four wall areas). The graphs depict (**a**) time spent in the center region, (**b**) entries into the center region, (**c**) distance traveled in the center region, (**d**) total entries, and (**e**) total distance traveled during the ten minute session. Data shown represent the mean ± SEM for each group.

hours) on their percent of time immobile [F(1,22)=5.087; P=0.034 for day 2 verses day 1] was detected, *post hoc* analyses revealed no significant differences (**Figure 13**). Therefore, these results indicate that the *Nf1*$^{+/-}$ genotype does not affect behavioral despair and learned helplessness in mice.

4. Effects on olfactory sensory habituation

Olfaction is the primary sensory input for social behavior in mice. To assess their ability to smell and their habituation to social and non-social odors, *Nf1*$^{+/-}$ and WT mice were presented with cotton applicators dipped in water, almond extract and the scent of a novel mouse (Crawley et al, 2007). To obtain the scent of a novel mouse, a cotton applicator wiped in a zig-zag pattern across the bottom surface of a cage that contained an unfamiliar mouse that lived in the cage for at least three days. Two factor (mouse genotype x scent) mixed ANOVAs were performed on the amount of time spent sniffing the cotton applicator suspended from the cage lid. The scents that were presented included (1) water, (2) diluted almond extract, (3) novel mouse. No significant differences were detected between *Nf1*$^{+/-}$ and WT genotypes for the time spent sniffing cotton applicators dipped in water [F(1,12)=1.692; P=0.218], almond extract [F(1,12)=0.682; P=0.425], or scent of a novel mouse [F(1,12)=0.005; P=0.945], nor was a genotype x scent interaction detected for water [F(1,12)=1.294; P=0.278], almond extract [F(1,12)=0.1.395; P=0.261], or scent of a novel mouse [F(1,12)=0.032; P=0.860]. **Figure 14** illustrates that both strains exhibited a

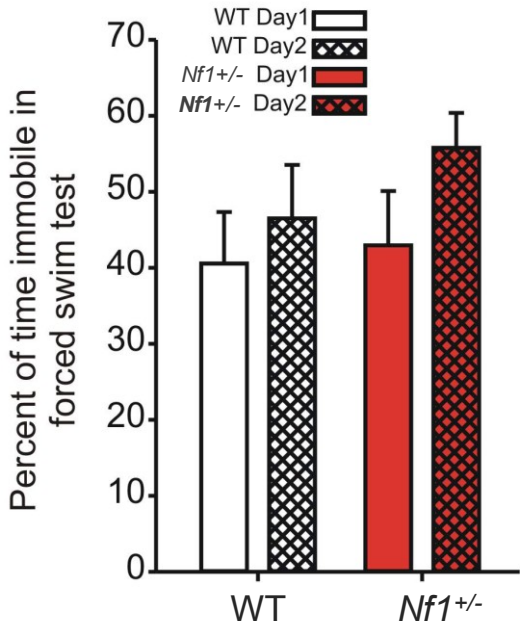

Figure 13. *Nf1*$^{+/-}$ and WT mice (n=12/group) show no differences in their percent of time immobile in the forced swim test (FST), a measure of behavioral despair and learned helplessness. Swimming "immobility" was assessed during the 2-6 minute interval on day 1 and day 2. Data shown represent the mean ± SEM of the percent of time immobile for each group.

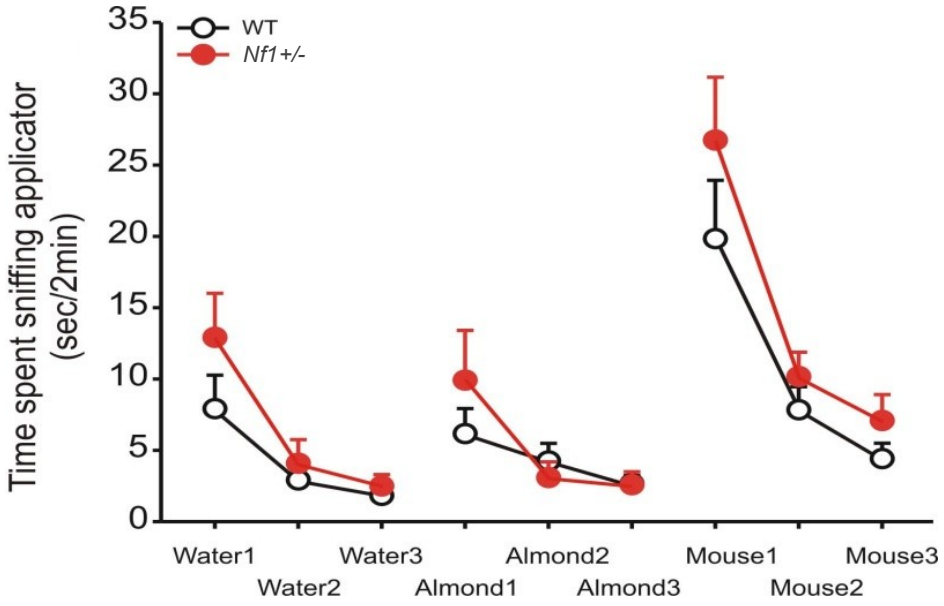

Figure 14. *Nf1*$^{+/-}$ and WT strains show normal olfaction in response to social and non-social odors (n=12/group). To assess non-social and social olfactory response, *Nf1*$^{+/-}$ and WT strains were presented with cotton applicators dipped in water, almond extract and the scent of a novel mouse (in triplicate). Data shown represent the mean ± SEM for each group.

significant habituation to the cotton applicator soaked with either water or almond extract, demonstrating moderate sniffing that was followed by a reduction in sniffing across the second and third exposures ($P < 0.05$). The most significant response was elicited from the social smell or the cotton applicator wiped across a cage containing a novel mouse that had no previous contact with the "test" mouse ($P < 0.01$). Therefore, both *Nf1*$^{+/-}$ and WT genotypes showed no differences in their ability to smell.

B. Experiment 2: Behavioral effects associated with the co-deletion of *Pak1* in *Nf1*$^{+/-}$ (*Nf1*$^{+/-}$/ *Pak1*$^{-/-}$) mice

1. Effects on sociability / social learning

Experiment 1 demonstrates normal preference for social interaction and intact short-term social learning / memory, but deficits in long-term social learning / memory seen in mice with the heterozygous gene deletion of *Nf1* (*Nf1*$^{+/-}$), as compared to WT. In addition, no differences were observed between *Nf1*$^{+/-}$ mice and WT in measures of anxiety-like behavior (EPM, open field test) or depression-associated response (forced swim test). The purpose of this experiment is to determine whether the genetic inactivation of *Pak1* in *Nf1*$^{+/-}$ (*Nf1*$^{+/-}$/ *Pak1*$^{-/-}$) mice would restore the deficits in long-term social learning / memory, as it does for *in vitro* and *in vivo* gain-in-function phenotypes (i.e., cellular proliferation, cellular migration) observed in *Nf1* haploinsufficient mast cells (McDaniel et al, 2008).

a. Preference for social interaction

For the preference for social interaction test, statistical analyses consisted of a two factor (mouse genotype x cage occupancy) mixed ANOVA performed on time spent sniffing each respective cage. When presented with a cage containing a novel mouse and an empty cage, statistical analysis revealed that *Nf1*$^{+/-}$, *Nf1*$^{+/-}$/ *Pak1*$^{-/-}$, and *Pak1*$^{-/-}$ mice all spent significantly more time sniffing the cage containing the novel mouse over the empty cage [$F(1,26)=100.45$; $P=0.001$ for cage with novel mouse verses cage with the familiar mouse]. No significant effects were detected between genotypes [$F(2,26)=0.713$; $P=0.500$] in amount of time spent sniffing the cage, nor was there a genotype x cage interaction [$F(2,26)=1.114$; $P=0.343$]. Fisher's PLSD post hoc analysis detected significantly more time sniffing the cage containing the novel mouse than the empty wire cage for *Nf1*$^{+/-}$, *Nf1*$^{+/-}$/ *Pak1*$^{-/-}$, and *Pak1*$^{-/-}$ genotypes ($P < 0.001$; **Figure 15**). These findings demonstrate that *Pak1* deletion in mice does not significantly affect levels of sociability, as compared to *Nf1*$^{+/-}$ mice.

b. Short-term social learning / memory

To analyze short-term social learning / memory, statistical analyses consisted of a two factor (mouse genotype x cage occupancy) mixed ANOVA performed on time spent sniffing each respective cage. When presented with a cage containing a novel mouse and a cage containing a now-familiar mouse, *Nf1*$^{+/-}$, *Nf1*$^{+/-}$/ *Pak1*$^{-/-}$, and *Pak1*$^{-/-}$ genotypes spent significantly more time sniffing

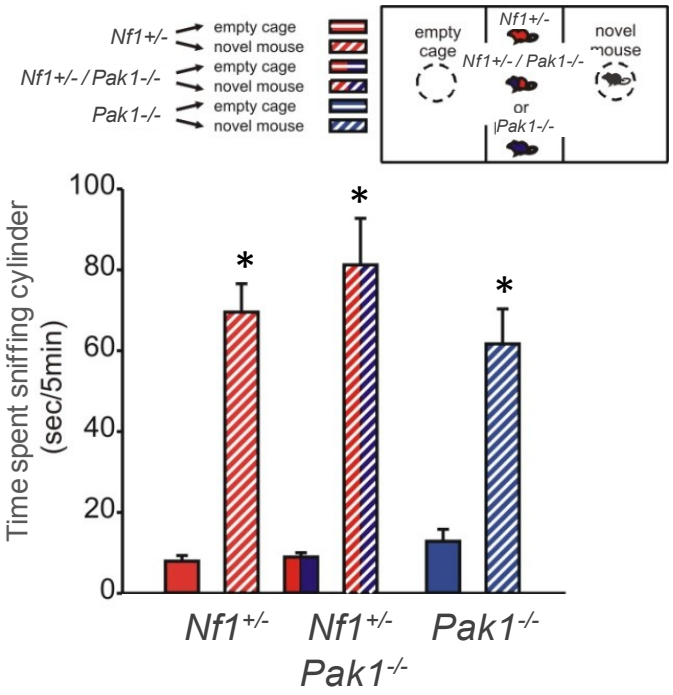

Figure 15. The deletion of *Pak1* (*Pak1*$^{-/-}$) in mice does not affect preference for social interaction, as compared to *Nf1*$^{+/-}$ mice. During the "preference for social interaction" session, *Nf1*$^{+/-}$ (n=12), *Nf1*$^{+/-}$ / *Pak1*$^{-/-}$ (n=11), *Pak1*$^{-/-}$ (n=6) mice were presented with a cage containing a novel mouse and an empty cage that were placed on opposite ends of the three chambered apparatus. The graph illustrates the amount of time "test" mouse spent sniffing each respective cage. Data were collected for the first five minutes of the ten minute session and represent the mean ± SEM for each group. *P < 0.05 for a within-group comparison between the cage containing the novel mouse verses the empty cage.

the cage containing the novel mouse over the cage containing the now-familiar mouse [F(1,26)=32.66; P=0.001 for cage with novel mouse verses cage with the familiar mouse]. No differences were observed between genotypes [F(2,26)=1.659; P=0.210] in amount of time spent sniffing the cages, and genotype x cage interaction [F(2,26)=1.537; P=0.234] was detected. Fisher's PLSD post hoc analysis detected significantly more time sniffing the cage containing the novel mouse over the cage containing the familiar mouse for *Nf1*$^{+/-}$, *Nf1*$^{+/-}$/ *Pak1*$^{-/-}$, and *Pak1*$^{-/-}$ mice ($P < 0.05$), and demonstrate that all three strains demonstrate intact short-term social learning (**Figure 16a**).

c. Long-term social learning / memory

Similar to the short-term social learning / memory test, statistically analyses for the long-term social learning / memory consisted of a two factor (mouse genotype x cage occupancy) mixed ANOVA performed on time spent sniffing each respective cage. When *Nf1*$^{+/-}$, *Nf1*$^{+/-}$/ *Pak1*$^{-/-}$, and *Pak1*$^{-/-}$ mice were presented with a cage containing a novel mouse and a cage containing the same familiar mouse from 24 hours earlier, no differences were observed between genotypes [F(2,26)=0.117; P=0.890] in amount of time spent sniffing the cages and no significant genotype x cage interaction was seen [F(2,26)=3.04; P=0.065]. However, a significant effect was detected in the amount of time the "test" mice spent sniffing each respective cage [F(1,26)=7.325; P=0.012 for cage with novel mouse verses cage with the familiar mouse]. Similar to the findings from

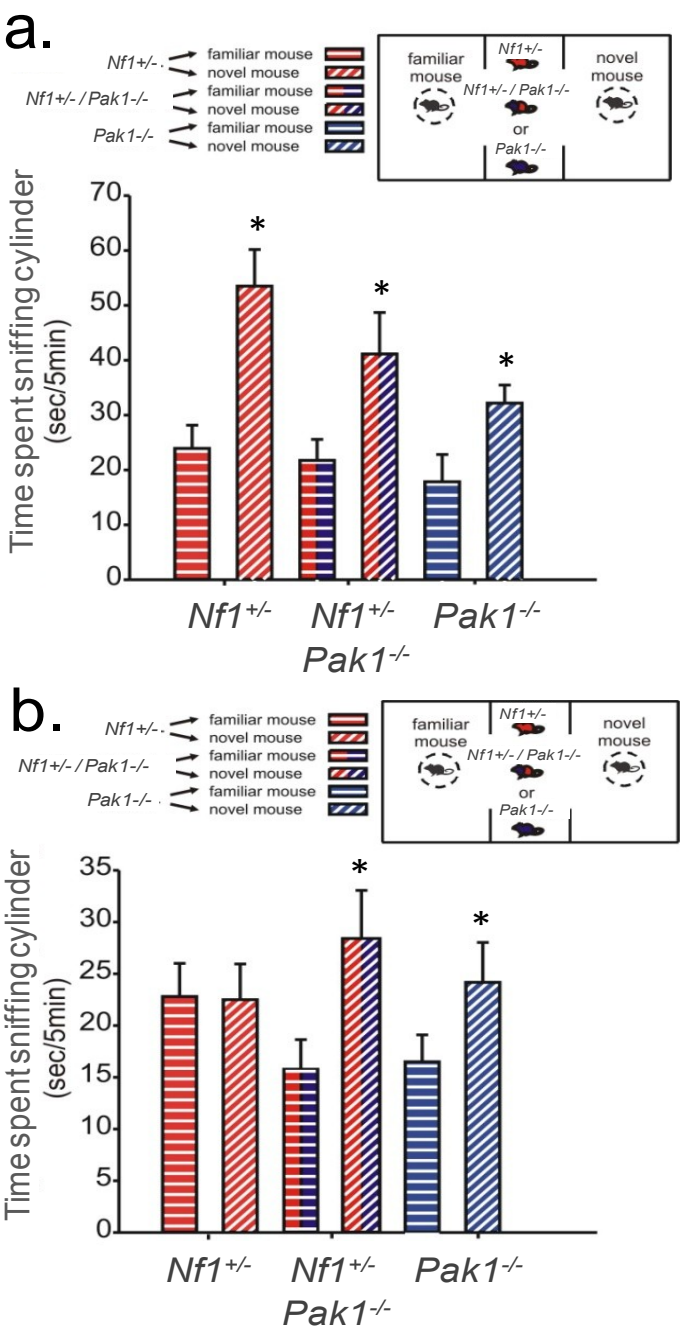
a.
Nf1+/-
familiar mouse
novel mouse
Nf1+/- / Pak1-/-
familiar mouse
novel mouse
Pak1-/-
familiar mouse
novel mouse
familiar mouse
Nf1+/-
novel mouse
Nf1+/- / Pak1-/-
or
Pak1-/-
Time spent sniffing cylinder (sec/5min)
70
60
50
40
30
20
10
0
*
*
*
Nf1+/-
Nf1+/- Pak1-/-
Pak1-/-
b.
Nf1+/-
familiar mouse
novel mouse
Nf1+/- / Pak1-/-
familiar mouse
novel mouse
Pak1-/-
familiar mouse
novel mouse
familiar mouse
Nf1+/-
novel mouse
Nf1+/- / Pak1-/-
or
Pak1-/-
Time spent sniffing cylinder (sec/5min)
35
30
25
20
15
10
5
0
*
*
Nf1+/-
Nf1+/- Pak1-/-
Pak1-/-

Figure 16

Figure 16. The co-deletion of *Pak1* (*Pak1*$^{-/-}$) in *Nf1*$^{+/-}$ mice does not affect short-term social learning, but restores the deficits in long-term social learning seen in *Nf1*$^{+/-}$ mice. The graphs depict the effects of the *Pak1* gene deletion on short-term and long-term social learning, as measured by their "preference for social novelty". (**a**) During the "short-term social learning" session, the *Nf1*$^{+/-}$ (n=12), *Nf1*$^{+/-}$ / *Pak1*$^{-/-}$ (n=11), *Pak1*$^{-/-}$ (n=6) mice were presented with a cage containing the now-familiar mouse from the previous session and one containing a novel mouse that were placed on opposite ends of the three chambered apparatus. (**b**) During the "long-term social learning" session, the *Nf1*$^{+/-}$, *Nf1*$^{+/-}$ / *Pak1*$^{-/-}$, *Pak1*$^{-/-}$ mice were presented with a cage containing the same familiar mouse from the previous day and a cage containing a novel mouse. The graphs illustrate the amount of time "test" mouse spent sniffing each respective cage. Data were collected for the first five minutes of the ten minute session and represent the mean ± SEM for each group. *$P < 0.05$ for a within-group comparison between the cage containing the now-familiar mouse and the cage containing the novel mouse.

experiment 1, Fisher's PLSD post hoc analysis detected no significant difference in the amount of time *Nf1*$^{+/-}$ genotype spent sniffing the cage containing the novel mouse over the cage containing the familiar mouse, but both *Nf1*$^{+/-}$/ *Pak1*$^{-/-}$ and *Pak1*$^{-/-}$ genotypes spent significantly more time sniffing the cage containing the novel mouse over the cage containing the familiar mouse ($P < 0.05$; **Figure 16b**). Therefore, unlike *Nf1*$^{+/-}$ mice, *Nf1*$^{+/-}$ / *Pak1*$^{-/-}$ mice are able to retain and discriminate between social cues following a 24 hour delay indicating that the genetic inactivation of *Pak1* restores the deficits in long-term social learning seen in *Nf1*$^{+/-}$ mice.

2. Effects on anxiety-like behavior

In experiment 1, no significant differences were detected in anxiety-like behavior or one-trial learning comparing WT and *Nf1*$^{+/-}$ genotypes, as measured by the elevated plus maze. In experiment 2 the EPM was used to assess anxiety-like behavior and one-trial learning associated with the homozygous *Pak1* gene deletion in *Nf1*$^{+/-}$ mice. For the EPM, statistical analyses consisted of a two factor (mouse genotype x day) mixed ANOVA performed on time spent in the open arms and entries into the open arms of the EPM. No differences were detected between genotypes in amount of time spent in the open arm [$F(2,22)=1.797$; $P=0.186$], and no genotype x cage interaction was seen [$F(2,26)=1.293$; $P=0.292$]. Similar to experiment 1, statistical analyses revealed a significantly effect of time on open arm duration [$F(2,26)=36.61$; $P=0.001$ for day 2 verses day 1]. Fisher's PLSD post hoc analysis detected significant decreases in open arm duration on day 2 relative to day 1 for *Nf1*$^{+/-}$, *Nf1*$^{+/-}$/ *Pak1*$^{-/-}$, and *Pak1*$^{-/-}$ genotypes

(P < 0.05; **Figure 17a**). Additionally, no differences were observed between genotypes in entries into the open arm [F(2,26)=1.923; P=0.166] of the elevated plus maze, nor was there a genotype x time interaction for open arm entries [F(2,26)=0.633; P=0.539]. Statistical analyses did reveal a significant effect of time on open arm entries [F(1,26)=47.39; P=0.001 for day 2 verses day 1]. Fisher's PLSD *post hoc* analysis detected significant decreases in open arm duration and open arm entries on day 2 relative to day 1 for *Nf1*$^{+/-}$, *Nf1*$^{+/-}$/ *Pak1*$^{-/-}$, and *Pak1*$^{-/-}$ genotypes (P < 0.05; **Figure 17b**). Therefore, the findings indicate *Nf1*$^{+/-}$, *Nf1*$^{+/-}$/ *Pak1*$^{-/-}$, and *Pak1*$^{-/-}$ genotypes show no significant differences in anxiety-like behaviors, as measured by the EPM on day 1. In addition, all three genotypes showed the classic reduction in open arm time and open arm entries observed on day 2 consistent with normal one-trial learning in the EPM.

3. Effects on behavioral despair / learned helplessness

In experiment 1, no significant differences were detected in depression-associated immobility comparing WT and *Nf1*$^{+/-}$ genotypes, as measured by the forced swim test. In experiment 2, the forced swim test was again employed to assess swimming immobility in *Nf1*$^{+/-}$, *Nf1*$^{+/-}$/ *Pak1*$^{-/-}$, and *Pak1*$^{-/-}$ genotypes. Statistical analyses for the forced swim test consisted of a two factor (mouse genotype x time) mixed ANOVA performed percent time spent immobile in the Plexiglas cylinder containing water. Significant differences were detected between *Nf1*$^{+/-}$, *Nf1*$^{+/-}$/ *Pak1*$^{-/-}$, and *Pak1*$^{-/-}$ genotypes in their percent of time

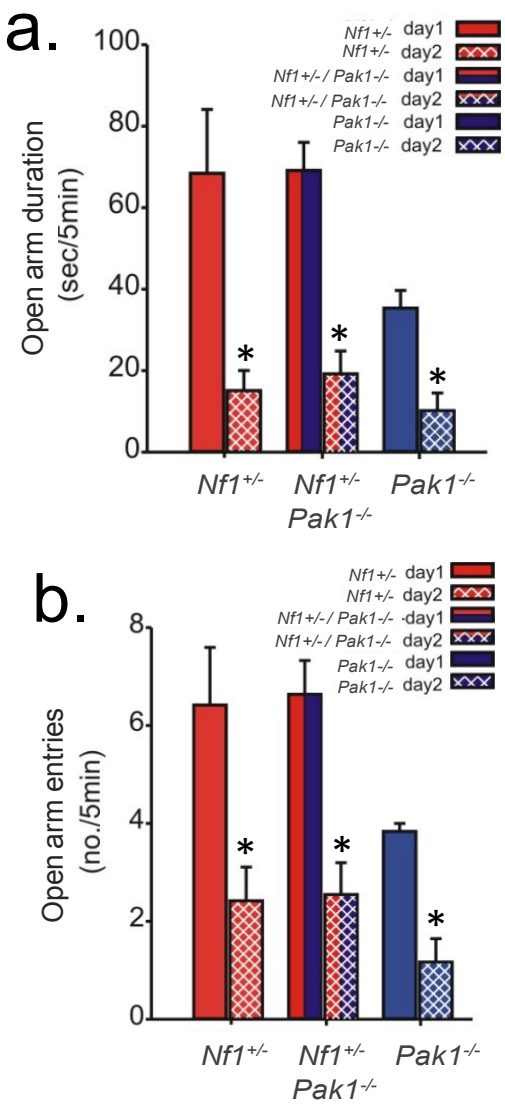
a.
Open arm duration (sec/5min)
100
80
60
40
20
0
Nf1+/- day1
Nf1+/- day2
Nf1+/-/ Pak1-/- day1
Nf1+/-/ Pak1-/- day2
Pak1-/- day1
Pak1-/- day2
*
*
*
Nf1+/-
Nf1+/- Pak1-/-
Pak1-/-
b.
Open arm entries (no./5min)
8
6
4
2
0
Nf1+/- day1
Nf1+/- day2
Nf1+/-/ Pak1-/- day1
Nf1+/-/ Pak1-/- day2
Pak1-/- day1
Pak1-/- day2
*
*
*
Nf1+/-
Nf1+/- Pak1-/-
Pak1-/-

Figure 17

Figure 17. *Nf1*$^{+/-}$ / *Pak1*$^{-/-}$ and *Pak1*$^{-/-}$ mice exhibit no differences in anxiety-like behavior or one-trial learning, as compared to *Nf1*$^{+/-}$ mice. Open arm duration and open arm entries were measured in *Nf1*$^{+/-}$ (n=12), *Nf1*$^{+/-}$ / *Pak1*$^{-/-}$ (n=11), *Pak1*$^{-/-}$ (n=6) mice during a five minute test using the elevated plus maze. Additionally, mice were re-tested in the elevated plus maze 24 hours later to assess one-trial learning. The graphs illustrate (**a**) the time spent in the open arm and (**b**) entries into the open arm entries. Data were collected during two five minute trials separated by 24 hours and represent the mean ± SEM for each group. *$P < 0.05$ for a within-group comparison between day 1 verses day 2 for each respective genotype.

immobile [F(2,26)=6.905; P=0.004], but no significant genotype x time interaction was observed [F(2,26)=0.496; P=0.615]. Additionally, a significant effect of day on their percent of time immobile was detected [F(1,26)=9.237; P=0.005 for day 2 verses day 1]. *Post hoc* analyses revealed significant decreases in the percent of time immobile *Nf1*$^{+/-}$/ *Pak1*$^{-/-}$, and *Pak1*$^{-/-}$ genotypes, as compared to *Nf1*$^{+/-}$ mice ($P < 0.05$; **Figure 18**). Therefore, these results indicate that the *Pak1* deletion is associated with decreases in depression-associated immobility in mice.

4. Effects on olfactory sensory habituation

In experiment 1, no differences were detected in olfaction or olfactory habituation between *Nf1*$^{+/-}$ and WT genotypes, as measured by the olfactory sensory habituation test. To measure the ability of the *Nf1*$^{+/-}$, *Nf1*$^{+/-}$ / *Pak1*$^{-/-}$, and *Pak1*$^{-/-}$ mice to smell and their habituation to social and non-social odors, *Nf1*$^{+/-}$ and WT mice were presented with cotton applicators dipped in water, almond extract and the scent of a novel mouse (Crawley et al, 2007). Two factor (mouse genotype x scent) mixed ANOVAs were performed on the amount of time spent sniffing the cotton applicator suspended from the cage lid. The scents that were presented included (1) water, (2) diluted almond extract, (3) novel mouse. No significant differences were detected between *Nf1*$^{+/-}$, *Nf1*$^{+/-}$/ *Pak1*$^{-/-}$, and *Pak1*$^{-/-}$ genotypes for the time spent sniffing cotton applicators dipped in water [F(2,15)=1.219; P=0.323], almond extract [F(2,15)=0.145; P=0.867], or scent of a

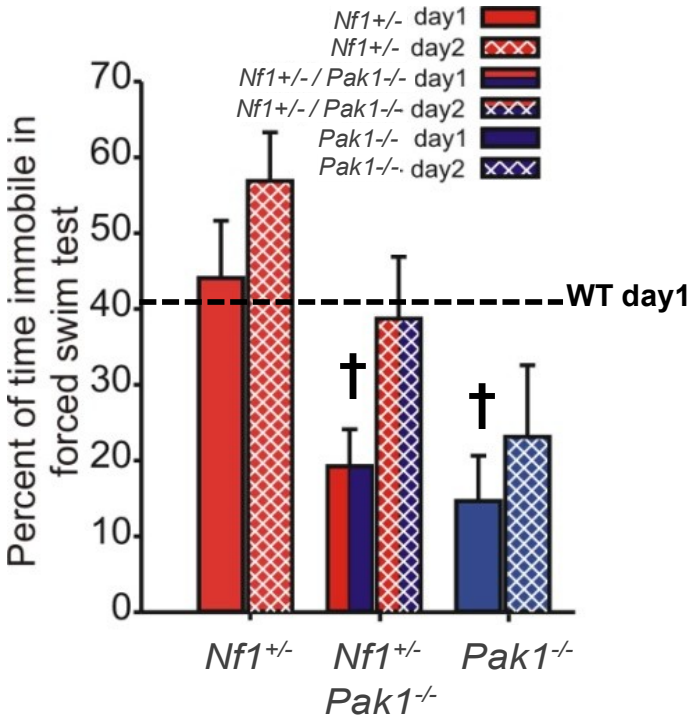

Figure 18. *Nf1*$^{+/-}$ / *Pak1*$^{-/-}$ and *Pak1*$^{-/-}$ mice show significant decreases in their percent of time immobile in the forced swim test (FST), as compared to *Nf1*$^{+/-}$ mice. Swimming "immobility" was assessed during the 2-6 minute interval on day 1 and day 2. Data shown represent the mean ± SEM of the percent of time immobile for each group. $^{\dagger}P < 0.05$ for a between-group comparison verses *Nf1*$^{+/-}$ genotype.

novel mouse [F(2,15)=0.774; P=0.479], nor was a genotype x scent interaction detected for water [F(2,15)=0.589; P=0.567], almond extract [F(2,15)=1.481; P=0.259], or scent of a novel mouse [F(2,15)=2.354; P=0.129]. Similar to the findings from experiment 1, all three strains exhibited a significant habituation to the cotton applicator soaked with either water or almond extract, demonstrating moderate sniffing that was followed by a reduction in sniffing across the second and third exposures ($P < 0.05$), and the most significant response was elicited from the scent of the novel mouse ($P < 0.01$; **Figure 19**).

C. Experiment 3: Role of *Nf1* and *Pak1* genes on ERK activation in murine cortical neurons

McDaniel et al (2008) demonstrates that the co-deletion of *Pak1* gene in $Nf1^{+/-}$ mast cells normalizes MAPK hyperactivation associated with the $Nf1^{+/-}$ gene deletion (McDaniel et al, 2008). To determine whether the co-deletion of *Pak1* gene would restore the $Nf1^{+/-}$-related MAPK hyperactivation in CNS neurons, mouse cortical neurons were cultured *in vitro* for 5 days and harvested from WT, $Nf1^{+/-}$, $Nf1^{+/-}$ / $Pak1^{-/-}$ and $Pak1^{-/-}$ mice. The resulting neurons were challenged with 10 ng/ml of stem cell factor (SCF) for approximately 2 minutes, and ERK1/2 / p-ERK1/2 levels were quantified using Western blotting. To assess ERK activation in mouse cortical neurons (basal levels vs. SCF), a two factor (genotype x SCF application) ANOVA was performed on ERK1/2 / p-ERK1/2

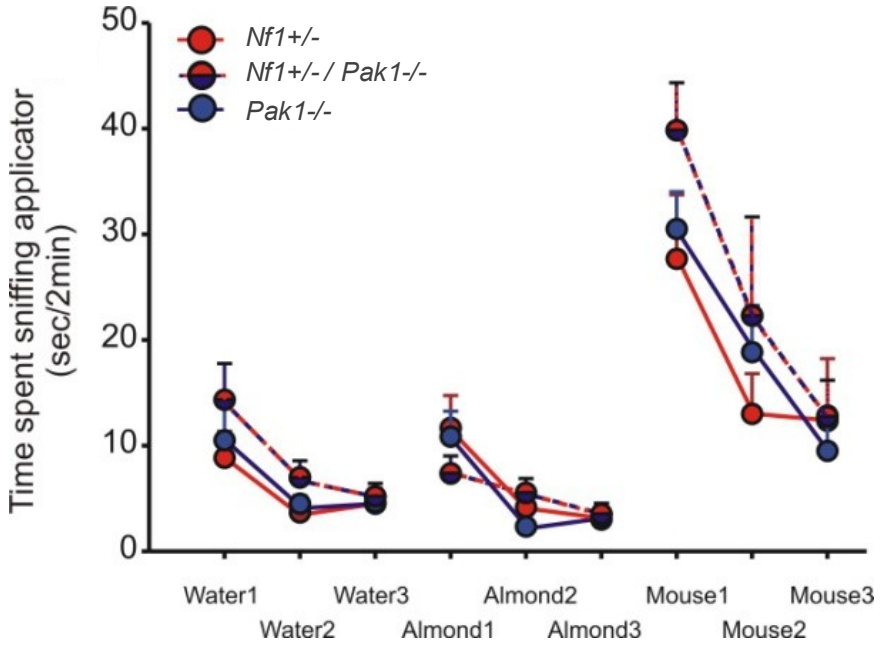

Figure 19. *Nf1*$^{+/-}$ and WT strains show normal olfaction in response to social and non-social odors (n=12/group). To assess non-social and social olfactory response, *Nf1*$^{+/-}$ (n=12), *Nf1*$^{+/-}$ / *Pak1*$^{-/-}$ (n=11), *Pak1*$^{-/-}$ (n=6) mice were presented with cotton applicators dipped in water, almond extract and the scent of a novel mouse (in triplicate). Data shown represent the mean ± SEM for each group.

content characterized using Western blotting, a semi-quantitative measure. Significant differences were detected between genotypes WT, *Nf1*$^{+/-}$, *Nf1*$^{+/-}$ / *Pak1*$^{-/-}$ and *Pak1*$^{-/-}$ in ERK1/2 / p-ERK1/2 levels [F(3,8)=11.01; P=0.003], and genotype x SCF interaction was detected [F(3,8)=41.64; P=0.0001]. In addition, statistical analyses revealed a highly significant effect of SCF on ERK activation [F(1,8)=247.37; P=0.0001 for SCF verses basal]. Fisher's PLSD *post hoc* tests were applied to conduct individual comparisons within and between groups. Consistent with the findings from McDaniel et al (2008), no differences were detected in ERK1/2 activation between cultures at basal levels (**Figure 20**). Stimulation with SCF for 2 minutes resulted in a significant increase in p-ERK1/2 relative to ERK1/2 in WT, *Nf1*$^{+/-}$, *Nf1*$^{+/-}$ / *Pak1*$^{-/-}$ genotypes. As compared to WT, *Nf1*$^{+/-}$ genotype showed significantly greater ERK1/2 activation, and the co-deletion of *Pak1* in *Nf1*$^{+/-}$ neuronal cultures (i.e., *Nf1*$^{+/-}$ / *Pak1*$^{-/-}$) decreased the hyperactivation of p-ERK1/2 to levels consistent with WT ($P < 0.05$). The administration of SCF to *Pak1*$^{-/-}$ cultured neurons yielded no effect on ERK1/2 activation. Therefore, these findings indicate that the *Nf1*$^{+/-}$ genotype leads to MAPK hyperactivation following SCF stimulation, and this hyperactivation is restored by the co-deletion of *Pak1* in cultured cortical neurons in mice. Significance was determined at $P < 0.05$ for all analyses.

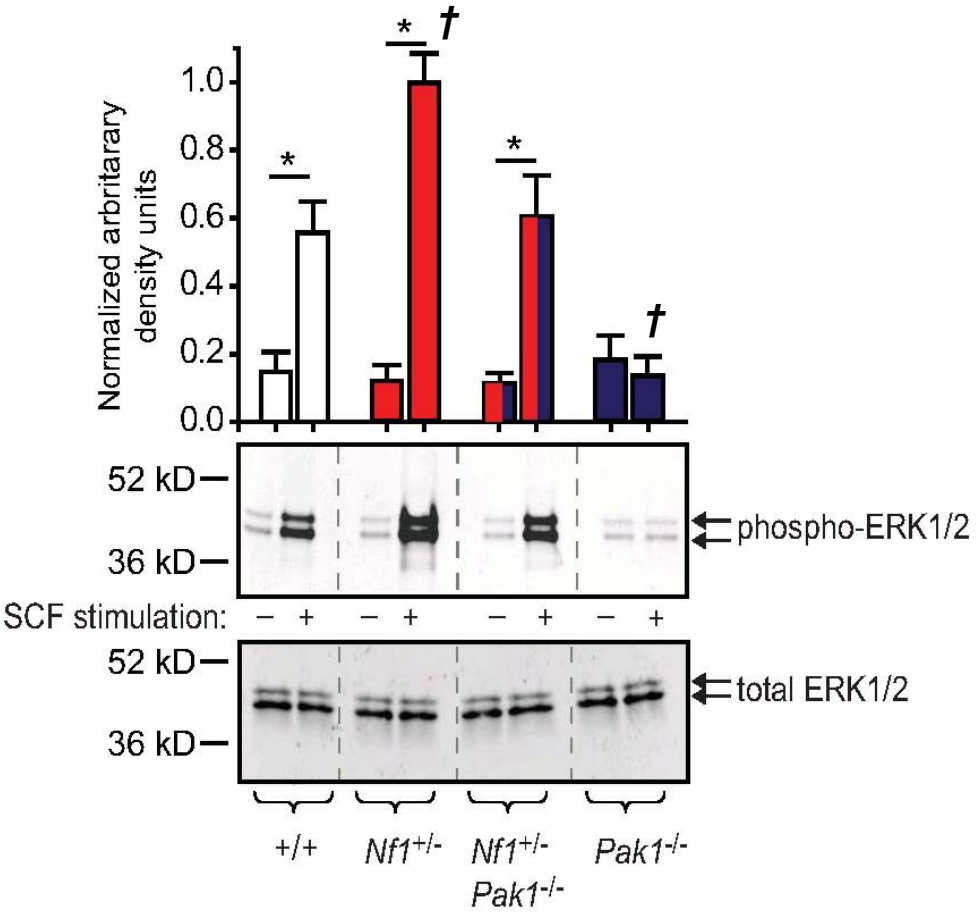
Normalized arbitrary density units
1.0
0.8
0.6
0.4
0.2
0.0
*
*
†
*
†
52 kD
36 kD
phospho-ERK1/2
SCF stimulation:
– + – + – + – +
52 kD
36 kD
total ERK1/2
+/+
Nf1+/-
Nf1+/- Pak1-/-
Pak1-/-

Figure 20

Figure 20. The co-deletion of *Pak1* (*Nf1*$^{+/-}$ / *Pak1*$^{-/-}$) restores MAPK hyperactivation associated with *Nf1*$^{+/-}$ in neuronal cultures. Western blotting was used to quantify p-ERK1/2 in cultured cortical neurons at basal levels and 2 minutes following stimulation with SCF (10 ng/ml). Phospho-ERK1/2 was quantified by immunoblotting using phospho-specific antibodies, and total ERK1/2 was used as loading controls. Each value represents the mean and the error bars represent the standard error of the mean of three independent experiments (*$P < 0.05$ vs basal levels; $^{\dagger}P < 0.05$ vs. WT).

D. Experiment 4: Role of *Nf1* and *Pak1* in the regulation of inhibitory synaptic currents in the BLA in mice

1. Effects of *Nf1*$^{+/-}$ genotype on IPSCs in the BLA

Utilizing the whole-cell patch clamp, isolated spontaneous inhibitory synaptic currents (sIPSC) and miniature IPSC (mIPSC) were recorded at a standardized holding potential of -55 mV in WT (n=11) and *Nf1*$^{+/-}$ (n=11) mice. To assess inhibitory IPSCs in the BLA, statistical analyses using a paired *t*-test were performed to compare WT and *Nf1*$^{+/-}$ genotypes. In the presence of AMPA and NMDA antagonists (DNQX, CPP), *Nf1*$^{+/-}$ mice showed no differences in sIPSC amplitude [t10=0.23, P=0.823] or mIPSC [t10=0.057, P=0.956] in the presence of tetrodotoxin (TTX), as compared to WT (**Figure 21a**). However, *Nf1*$^{+/-}$ mice exhibited significant increases in sIPSC [t10=2.518, P=0.02] and mIPSC [t10=2.368, P=0.028] frequency in BLA projection neurons, as compared to WT (**Figure 21b**). In the presence of $GABA_A$ antagonist (SR 95531 hydrobromide) and $GABA_B$ antagonist (CGP 52432), the mIPSCs observed in glutamatergic projection neurons in the BLA were entirely blocked, an effect consistent with GABA inhibition.

2. Effects of *Pak1* co-deletion in *Nf1*$^{+/-}$ mice on IPSCs in BLA

As before, the whole-cell patch clamp was used to measure sIPSC and mIPSC recorded at -55 mV in *Nf1*$^{+/-}$ (n=11), *Nf1*$^{+/-}$ / *Pak1*$^{-/-}$ (n=11), and *Pak1*$^{-/-}$

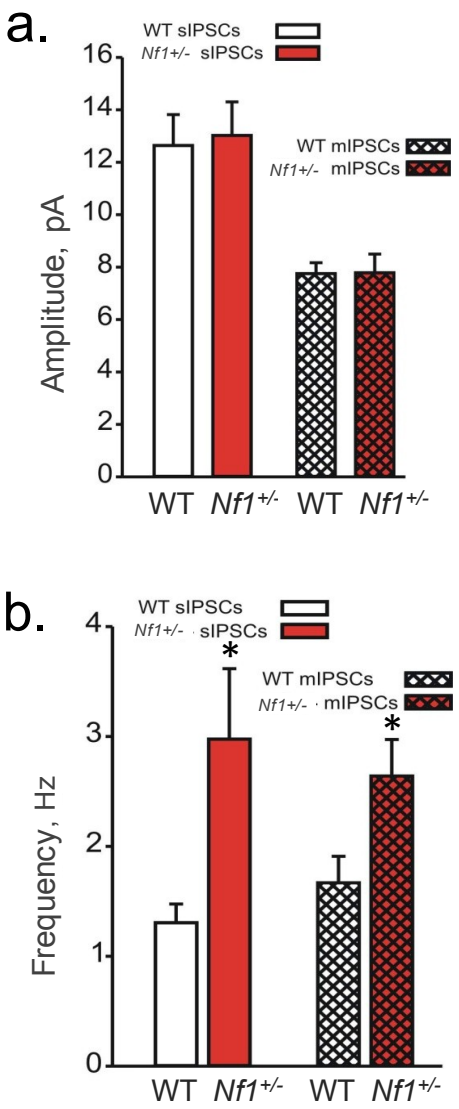
a.
WT sIPSCs
Nf1+/- sIPSCs
WT mIPSCs
Nf1+/- mIPSCs
Amplitude, pA
16
14
12
10
8
6
4
2
0
WT
Nf1+/-
WT
Nf1+/-
b.
WT sIPSCs
Nf1+/- sIPSCs
WT mIPSCs
Nf1+/- mIPSCs
Frequency, Hz
4
3
2
1
0
*
*
WT
Nf1+/-
WT
Nf1+/-

Figure 21

Figure 21. *Nf1*$^{+/-}$ mice exhibit no differences in sIPSC and mIPSC amplitude, but increases in sIPSC and mIPSC frequency in BLA, as compared to WT (n=11/group). Isolated spontaneous inhibitory synaptic currents (sIPSC) and miniature IPSC (mIPSC) were recorded from BLA glutamatergic projection neurons at a standardized holding potential of -55 mV in WT and *Nf1*$^{+/-}$ mice. The graphs illustrate the (**a**) sIPSC and mIPSC amplitude and (**b**) sIPSC and mIPSC frequency. Data represent the mean ± SEM for each group. **P* < 0.05 for comparison between genotypes [Calibration: 1s, 40 pA.].

(n=11) mice. Statistical analyses included one-way ANOVAs comparing each respective genotype. When significance was obtained, Dunnets' *post-hoc* tests were applied to conduct individual comparisons between genotypes on IPSC amplitude and frequency. In the presence of AMPA and NMDA antagonists, *Nf1*$^{+/-}$, *Nf1*$^{+/-}$ */ Pak1*$^{-/-}$, and *Pak1*$^{-/-}$ mice showed no differences in sIPSC amplitude [F(2,36)=0.5, P=0.61 for *Nf1*$^{+/-}$ */ Pak1*$^{-/-}$, and *Pak1*$^{-/-}$ versus *Nf1*$^{+/-}$] or mIPSC [F(2,36)=0.527, P=0.595 for *Nf1*$^{+/-}$ */ Pak1*$^{-/-}$, and *Pak1*$^{-/-}$ versus *Nf1*$^{+/-}$] in the presence of TTX, as compared to WT (**Figure 22a**). However, *Nf1*$^{+/-}$ */ Pak1*$^{-/-}$, and *Pak1*$^{-/-}$ mice showed significant decreases in sIPSC [F(2,26)=4.606, P=0.016 for *Nf1*$^{+/-}$ */ Pak1*$^{-/-}$ and *Pak1*$^{-/-}$ versus *Nf1*$^{+/-}$] and mIPSC [F(2,26)=14.54, P<0.0001 for *Nf1*$^{+/-}$ */ Pak1*$^{-/-}$, and *Pak1*$^{-/-}$ versus *Nf1*$^{+/-}$] frequency in BLA projection neurons, as compared to *Nf1*$^{+/-}$ mice (**Figure 22b**). Therefore, the co-deletion of *Pak1* in *Nf1*$^{+/-}$ mice normalizes the increases in spontaneous and minuture IPSCs observed in glutamatergic projection neurons in BLA of *Nf1*$^{+/-}$ mice.

E. Experiment 5: Role of *Nf1* and *Pak1* genes in the regulation of protein expression in the PFC and BLA in mice

Mass spectrometry was utilized to screen for differences in protein expression in the PFC and BLA associated with *Nf1*$^{+/-}$, *Nf1*$^{+/-}$ */ Pak1*$^{-/-}$ and *Pak1*$^{-/-}$ genotypes, as compared to WT (n=6 per group). Partek Genomics Suite (©Partek Incorporated, St. Louis, MO) was used to analyze these data. The log

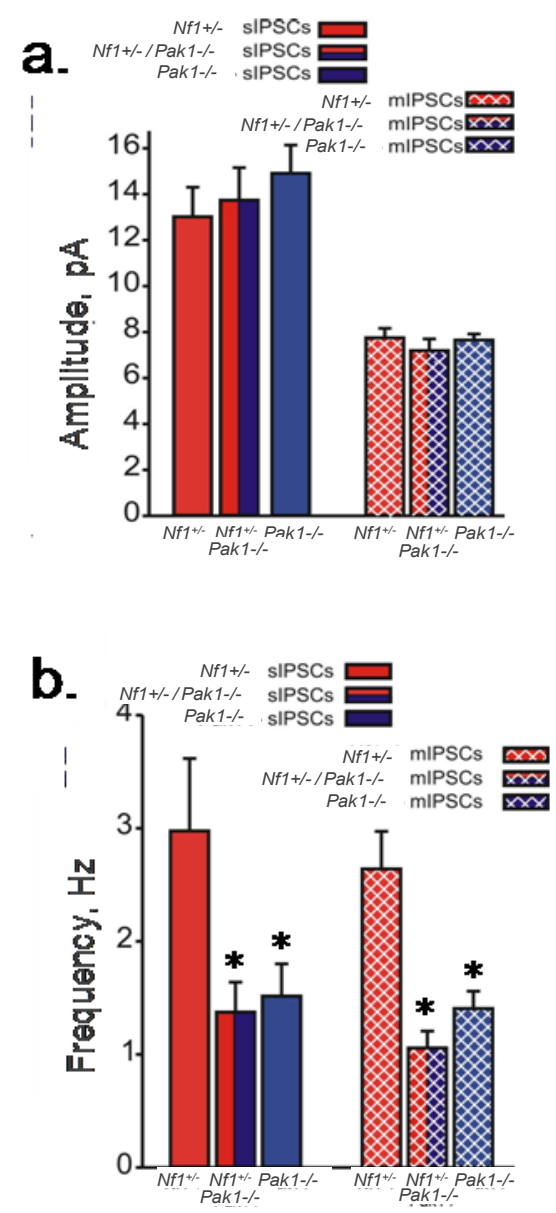
a.
Nf1+/- sIPSCs
Nf1+/-/Pak1-/- sIPSCs
Pak1-/- sIPSCs
Nf1+/- mIPSCs
Nf1+/-/Pak1-/- mIPSCs
Pak1-/- mIPSCs
Amplitude, pA
16
14
12
10
8
6
4
2
0
Nf1+/- Nf1+/- Pak1-/- Pak1-/-
Nf1+/- Nf1+/- Pak1-/- Pak1-/-
b.
Nf1+/- sIPSCs
Nf1+/-/Pak1-/- sIPSCs
Pak1-/- sIPSCs
Nf1+/- mIPSCs
Nf1+/-/Pak1-/- mIPSCs
Pak1-/- mIPSCs
Frequency, Hz
4
3
2
1
0
*
*
*
*
Nf1+/- Nf1+/- Pak1-/- Pak1-/-
Nf1+/- Nf1+/- Pak1-/- Pak1-/-

Figure 22

Figure 22. *Nf1*$^{+/-}$ / *Pak1*$^{-/-}$ and *Pak1*$^{-/-}$ mice show no differences in sIPSC and mIPSC amplitude, but decreases in sIPSC and mIPSC frequency in BLA, as compared to *Nf1*$^{+/-}$ mice (n=11/group). Isolated spontaneous inhibitory synaptic currents (sIPSC) and miniature IPSC (mIPSC) were recorded from BLA glutamatergic projection neurons at a standardized holding potential of -55 mV in *Nf1*$^{+/-}$, *Nf1*$^{+/-}$ / *Pak1*$^{-/-}$ and *Pak1*$^{-/-}$ mice. The graphs depict the (**a**) sIPSC and mIPSC amplitude and (**b**) sIPSC and mIPSC frequency. Data represent the mean ± SEM for each group. *P < 0.05 for comparison to *Nf1*$^{+/-}$ genotype [Calibration: 1s, 40 pA].

base2 was first determined for each data point associated with each protein identified using mass spectometry. A one-way ANOVA analysis was then performed comparing protein expression for each respective genotype (i.e., WT, *Nf1*$^{+/-}$, *Nf1*$^{+/-}$ / *Pak1*$^{-/-}$, and *Pak1*$^{-/-}$). Significance was determined at $P < 0.05$ for all analyses. When significant differences were obtained using the one-way ANOVA, Fisher's PLSD *post hoc* test was applied to conduct individual comparisons between groups. Proteins of interest were selected based on the following criteria: (1) significant differences between WT vs. *Nf1*$^{+/-}$ group, (2) significant differences between *Nf1*$^{+/-}$ vs. *Nf1*$^{+/-}$ / *Pak1*$^{-/-}$ group, and (3) were directionally consistent with a rescue.

In the PFC, the following twenty proteins were identified that showed significant differences in expression between WT vs. *Nf1*$^{+/-}$ group and (2) significant differences between *Nf1*$^{+/-}$ vs. *Nf1*$^{+/-}$ / *Pak1*$^{-/-}$ group, and were consistent with a rescue (see **Table 1** and **Table 2**). These proteins include the following: (1) **LSAMP** [F(3,20)=5.61; P=0.0058], (2) **CALB1** [F(3,20)=7.17; P=0.0019], (3) **ACTS** [F(3,20)=5.71; P=0.0054], (4) **HNRH1** [F(3,20=3.21; P=0.045], (5) **CAPRI** [F(3,20)=13.00; P=0.0001], (6) **H2A2B** [F(3,20)=4.11; P=0.0199], (7) **NUCL** [F(3,20)=6.02; P=0.0043], (8) **AP1B1** [F(3,20)=4.15; P=0.0194], (9) **MBP** [F(3,20)=4.53; P=0.0140], (10) **DREB** [F(3,20)=5.69; P=0.0055], (11) **CLCB** [F(3,20)=3.95; P=0.0232], (12) **THY1** [F(3,20)=4.21; P=0.0185], (13) **MAP1A** [F(3,20)=11.86; P=0.0001], (14) **ENOA** [F(3,20)=13.77; P=0.0001], (15) **STXB1** [F(3,20)=9.40; P=0.0001], (16) **DHE** [F(3,20)=8.09; P=0.0010], (17) **LDHA** [F(3,20)=8.65; P=0.0007], (18) **DYL2** [F(3,20)=3.44;

P=0.0365], (19) **DYN1** [F(3,20)=4.28; P=0.0173], (20) **NACAM** [F(3,20)=5.48; P=0.0065], and (21) **CAZA2** [F(3,20)=4.57; P=0.0135].

In the BLA, **ADAM22** [F(3,20)=12.13; P=0.0001] was identified displaying significant differences in expression between WT vs. *Nf1*$^{+/-}$ group and significant differences between *Nf1*$^{+/-}$ vs. *Nf1*$^{+/-}$ */ Pak1*$^{-/-}$ group consistent with a rescue (see **Table 1** and **Table 2**). Following protein identification, Pubmed and Protein search engines (www.ncbi.nlm.nih.gov) were used to further characterize proteins identified in the PFC and BLA based on their known biology and their relevance to NF1-related phenotypes. For a review of protein functions, see *Role of Nf1 and Pak1 in the regulation of protein expression in the BLA and PFC* section in Discussion.

Table 1: Protein expression differences seen in *Nf1*-deficient mice are restored by the co-deletion of *Pak1* gene in the PFC and BLA

Protein	Locus ID	Fold-change	Rescued by Pak1 deletion	Description
Prefrontal cortex:				
LSAMP	Q8BLK3	8.25	Full rescue	Limbic system-associated membrane protein
CALB1	P12658	6.21	Full rescue	Calbindin
ACTS	P68134	5.15	Full rescue	Alpha-actin-1
HNRH1	O35737	4.07	Full rescue	Heterogeneous nuclear ribonucleoprotein H
CAPRI	Q60865	3.53	Full rescue	Caprin-1
H2A2B	Q64522	3.44	Full rescue	Histone H2A type 2-B
NUCL	P09405	3.21	Full rescue	Nucleolin
AP1B1	O35643	2.87	Full rescue	AP-1 complex subunit beta-1
MBP	P04370	2.47	Full rescue	Myelin basic protein
DREB	Q9QXS6	2.03	Full rescue	Drebrin
CLCB	Q6IRU5	1.86	Full rescue	Clathrin light chain B
THY1	P01831	1.57	Full rescue	Thy-1 membrane glycoprotein
MAP1A	Q9QYR6	1.49	Full rescue	Microtubule-associated protein 1A
ENOA	P17182	-1.37	Full rescue	Alpha-enolase
STXB1	O08599	-1.63	Full rescue	Syntaxin-binding protein 1
DHE	P26443	-1.88	Full rescue	Glutamate dehydrogenase 1
LDHA	P06151	-2.02	Full rescue	L-lactate dehydrogenase A chain
DYL2	Q9D0M5	-2.27	Full rescue	Dynein light chain 2
DYN1	P39053	-2.56	Full rescue	Dynamin-1
NACAM	P70670	-3.12	Full rescue	Nascent-associated complex subunit alpha
CAZA2	P47754	-3.57	Full rescue	F-actin-capping protein subunit alpha-2
Basolateral amygdala:				
ADAM22	Q9R1V6	-6.17	Partial rescue	ADAM metallopeptidase domain 22

*$P < 0.05$ vs. WT^-; One-way ANOVA [performed on log transformed protein expression data]

Table 2: Summary of protein expression differences seen in *Nf1*-deficient mice that are restored by the co-deletion of *Pak1* gene in the PFC and BLA in mice

Protein	Locus ID	*Nf1*$^{+/-}$ vs. WT		*Nf1*$^{+/-}$ / *Pak1*$^{-/-}$ vs. WT		*Pak1*$^{-/-}$ vs. WT		*Nf1*$^{+/-}$ / *Pak1*$^{-/-}$ vs. *Nf1*$^{+/-}$	
Prefrontal cortex:		**Fold-change**	***P*-value**	**Fold-change**	***P*-value**	**Fold-change**	***P*-value**	**Fold-change**	***P*-value**
LSAMP	Q8BLK3	8.25	0.001	1.18	0.780	2.64	0.107	-7.01	0.003
CALB1	P12658	6.21	0.001	2.32	0.051	1.72	0.193	-2.68	0.024
ACTS	P01831	5.15	0.006	1.61	0.386	6.55	0.002	-3.20	0.041
HNRH1	O35737	4.07	0.041	-1.38	0.619	-1.31	0.677	-5.64	0.014
CAPRI	Q60865	3.53	0.001	-1.19	0.563	-1.46	0.205	-4.19	0.001
H2A2B	Q64522	3.44	0.008	1.23	0.627	-1.05	0.902	-2.80	0.024
NUCL	P09405	3.21	0.030	-2.14	0.144	-1.77	0.266	-6.85	0.001
AP1B1	O35643	2.87	0.016	-1.31	0.510	1.08	0.847	-3.76	0.004
MBP	P04370	2.47	0.020	-1.38	0.378	-1.09	0.804	-3.42	0.003
DREB	Q9QXS6	2.03	0.020	-1.20	0.526	-1.46	0.192	-2.44	0.005
CLCB	Q6IRU5	1.86	0.045	-1.38	0.279	-1.14	0.657	-2.57	0.004
THY1	P01831	1.57	0.049	-1.15	0.528	1.61	0.040	-1.81	0.013
MAP1A	Q9QYR6	1.49	0.049	-2.04	0.001	-1.26	0.234	-3.04	0.001
ENOA	P17182	-1.37	0.032	1.63	0.002	1.39	0.025	2.23	0.001
STXB1	O08599	-1.63	0.049	2.04	0.006	1.35	0.213	3.32	0.001
DHE	P26443	-1.88	0.007	1.14	0.526	1.42	0.110	2.16	0.002
LDHA	P06151	-2.02	0.004	1.43	0.107	-1.18	0.433	2.89	0.001
DYL2	Q9D0M5	-2.27	0.015	-1.06	0.858	1.00	0.994	2.15	0.021
DYN1	P39053	-2.56	0.046	1.12	0.801	1.84	0.182	2.87	0.027
NACAM	P70670	-3.12	0.044	1.66	0.349	2.38	0.116	5.18	0.005
CAZA2	P47754	-3.57	0.034	2.18	0.179	-1.26	0.687	7.79	0.002
Basolateral amygdala:									
ADAM22	Q9R1V6	-6.17	0.001	-2.24	0.034	1.05	0.900	2.75	0.010

Results from one-way ANOVA [performed on log transformed protein expression data]; Fisher's PLSD *post hoc* test

DISCUSSION

Neurofibromatosis type 1 is one of the most common single gene disorders in humans. While NF1 is diagnosed by the presentation of physical features, a higher incidence of developmental behavioral disorders is seen including learning disabilities, attention problems, social deficits and psychiatric disorders. Silva et al (1997) was the first to find that *Nf1*$^{+/-}$ mice display spatial learning deficits comparable to those observed in NF1 patients. Subsequent studies in the hippocampus have implicated the hyperactivation of RAS-dependent signaling, increased GABA-mediated inhibition, and deficits in LTP as potential mechanisms underlying these spatial learning deficits (Costa et al, 2002; Li et al, 2005; Cui et al, 2008). However, neurofibromin is not isolated to the hippocampus, but is expressed throughout the CNS, including the prefrontal cortex and the amygdala. Therefore, a primary objective for the present dissertation was to characterize the *Nf1*$^{+/-}$ mouse model for abnormalities in processes associated with social and emotional learning.

For this purpose, *Nf1*$^{+/-}$ mice were first screened for deficits in behaviors including social interaction and social learning, anxiety-like behavior, one-trial learning (EPM), and depression-associated response. This series of experiments revealed that *Nf1*$^{+/-}$ mice show selective deficits in long-term social learning / memory. Next, utilizing a genetic intercross, it was further demonstrated that the co-deletion of *Pak1* restores these deficits in long-term social learning / memory. The heterozygous *Nf1* gene deletion (*Nf1*$^{+/-}$) is associated with hyperactivation of the MAPK signaling pathway (see Le and Parada, 2007 for review). Similar to

previous findings in mast cells (McDaniel et al, 2008), the immediate effects of the co-deletion of *Pak1* on stem cell factor (SCF)-mediated MAPK hyperactivation were also demonstrated in *Nf1*$^{+/-}$ neurons cultured from the PFC. Consistent with previous findings in CA1 pyramidal cells of hippocampal slices (Costa et al, 2002; Cui et al, 2008), electrophysiological methods found increased inhibitory synaptic currents (IPSCs) in glutamatergic projection neurons in the BLA, a brain region that is critical for learning social cues. These increases in IPSC frequency seen in *Nf1*$^{+/-}$ mice were restored by the co-deletion of *Pak1* gene. Utilizing the same genetic intercross method, mass spectrometry was employed to identify novel protein candidates that may contribute to these abnormalities associated with the *Nf1*$^{+/-}$ genotype.

A. *Nf1*$^{+/-}$ mutation leads to sustained deficits in social learning

The *Nf1*$^{+/-}$ strain provides a unique model to study genetic, molecular, and cellular mechanisms that are responsible for the learning disabilities, attention deficits, social and emotional problems associated with NF1 (see Shilyansky et al, 2010 for review). Previous studies indicate that NF1 children display social problems including with social withdrawal, poor interpersonal skills, and problems with social perception (Barton and North, 2004; Kayl and Moore, 2000; Eliason, 1986). Such deficits could also be the result from the inability to learn and retain appropriate social cues. *Nf1*$^{+/-}$ mice show normal preference for social interaction (see **Figure 9**), and display intact short-term social learning (see **Figure 10a**). However, when presented with a novel mouse

and the same "familiar" mouse 24 hours later, *Nf1*$^{+/-}$ mice are unable to differentiate between the novel mouse and the "familiar" mouse, while WT mice continue to show robust long-term social learning (see **Figure 10b**). Therefore, these findings suggest that the social profile of the *Nf1*$^{+/-}$ mouse model is largely consistent with the social abnormalities seen in NF1 patients. Therefore, the identification of the mechanism(s) responsible for these social learning deficits seen in *Nf1*$^{+/-}$ mice may provide important information to improve the treatment options for these NF1-related social learning problems.

While human studies have found a moderately increased risk for the development of anxiety and depression in patients diagnosed with NF1 (Samuelsson and Riccardi, 1989; Zoller and Rembeck, 1999; Johnson et al, 1999), *Nf1*$^{+/-}$ mice displayed no differences in anxiety-like behavior, as measured using the elevated plus maze and in the open field test (see **Figures 11-12**). Furthermore, WT and *Nf1*$^{+/-}$ mice displayed no differences in their percent time immobile during two trials that were separated by 24 hours in the forced swim test (see **Figure 13**). Therefore, these experiments were unable to capture effects of the *Nf1*$^{+/-}$ genotype on rodent behavioral measures that are associated with anxiety and depression in humans. However, anxiety and depression are complex psychiatric disorders influenced by multiple factors including the genetics, the environment, and gene x environment interactions (Nandi et al, 2009).

In addition to anxiety-like behavior, the EPM was utilized to test one-trial learning as defined by the classic reduction in open arm time and open arm

entries commonly observed when rodents are re-tested in the EPM on day 2 (Roy et al, 2009). *Nf1*$^{+/-}$ mice displayed no differences in one-trial learning (see **Figure 11**). These findings suggest that the *Nf1*$^{+/-}$ genotype does not globally affect learning / memory, but leaves some forms of learning / memory intact. However, the motivations that underlie one-trial learning in the EPM are not clearly defined in the literature, and may result from avoidance or fear-based learning or a reduction in open arm novelty. These motivations ultimately result in a shift in behavior from the open arms toward the closed arms of the EPM on day 2 (Roy et al, 2009).

B. Loss of *Pak1* rescues abnormalities in social learning and MAPK signal transduction seen in *Nf1*$^{+/-}$ mice

PAK1 has been identified as a critical RAS-mediated effector that has been shown to regulate the intracellular signal transduction of PI3K and MAPK, and has been implicated in numerous processes involved in CNS function, including synaptic plasticity (see Kreis and Barnier, 2009 for review). Previous studies demonstrate that the loss of *Pak1* normalizes the MAPK hyperactivation seen in haploinsufficient mast cells, and the co-deletion of *Pak1* in *Nf1*$^{+/-}$ mice restores gain-in-function phenotypes in mast cells (McDaniel et al, 2008). The same genetic intercross strategy was employed to determine whether the co-deletion of *Pak1* in *Nf1*$^{+/-}$ mice would restore the long-term social learning / memory deficits previously seen in *Nf1*$^{+/-}$ mice.

Similar to findings in experiment 1, no differences were observed between genotypes in preference for social interaction (see **Figure 15**) or short-term social learning (see **Figure 16a**). However, unlike the *Nf1*$^{+/-}$ genotype, both *Nf1*$^{+/-}$ / *Pak1*$^{-/-}$ and *Pak1*$^{-/-}$ mice showed significant preference for social novelty even after 24 hours, indicating that *Nf1*$^{+/-}$ / *Pak1*$^{-/-}$ mice are now able to retain and discriminate between familiar and unfamiliar social cues following a 24 hour delay (see **Figure 16b**). Therefore, the findings from experiment 2 demonstrate that the abnormalities in social learning seen in *Nf1*$^{+/-}$ mice can be rescued by the co-deletion of *Pak1* gene. Similar to the findings associated with the *Nf1*$^{+/-}$ genotype, the loss of *Pak1* had no effect on anxiety-like behavior (see **Figure 17**). Interestingly, the loss of *Pak1* was associated with decreased depression-associated immobility in mice (see **Figure 18**).

While the co-deletion of *Pak1* has been shown to restore the *Nf1*$^{+/-}$-related hyperactivation of MAPK in mast cells (McDaniel et al, 2008), the effects of *Nf1* and *Pak1* expression on MAPK activation were not yet characterized in neuronal cultures from the frontal cortex. We demonstrate that, in the presence of SCF, *Nf1*$^{+/-}$ neurons cultured from the frontal cortex show a significantly greater increase in active ERK1/2, as compared to WT, and the co-deletion of *Pak1* normalizes this hyperactivation of ERK1/2 to levels that are consistent with WT (see **Figure 20**). Therefore, the hyperactivation in MAPK signaling associated with *Nf1*$^{+/-}$ genotype is regulated in a PAK1-dependent manner in the CNS, and thereby, may contribute to the deficits in long-term social learning / memory seen in *Nf1*$^{+/-}$ mice (**Figure 23**).

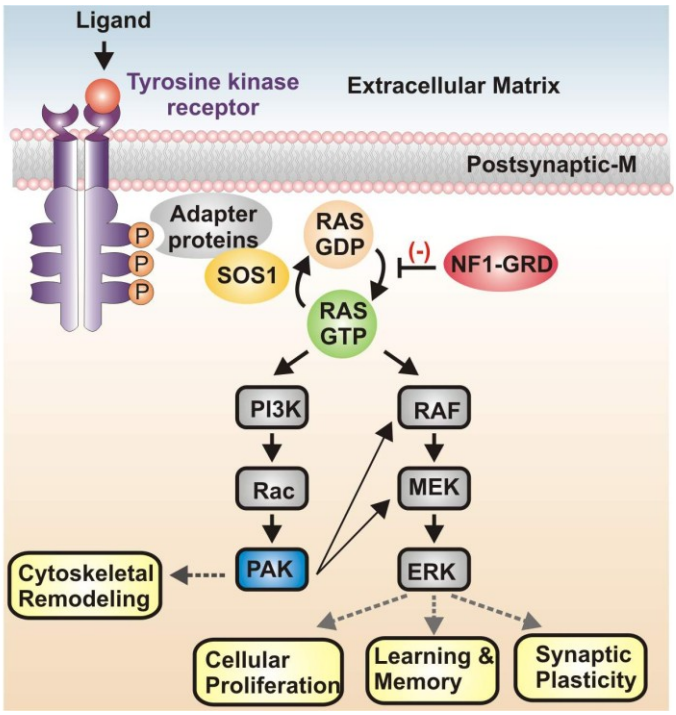

Figure 23. Illustration that depicts a hypothetical mechanism(s) explaining how PAK1 may interact with MAPK to restore abnormalities in learning and memory seen in *Nf1*$^{+/-}$ mice. Neurofibromin negatively regulates RAS GTPase activation, and is, in part, responsible for the propagation of the classical MAPK and PI3K signaling cascades. In addition to the *Nf1*$^{+/-}$-related hyperactivation of RAS-dependent pathways, *Nf1*$^{+/-}$ genotype affects cytoskeletal remodeling, cellular proliferation, synaptic plasticity and learning and memory. Our findings suggest that co-deletion of *Pak1* gene in *Nf1*$^{+/-}$ cells may restore these functions by normalizing the hyperactivation of MAPK.

The RAS/MAPK signaling cascade is mediated through the activation of receptor tyrosine kinase (RTK) by multiple growth factors including nerve growth factor (NGF), brain derived neurotophic factor (BDNF), stem cell factor (SCF), and many others (Campbell et al, 1998). In addition, SCF/c-kit are abundantly expressed in neurons and glia in the CNS of mice (Zhang and Fedoroff, 1997). *In vitro* studies show that the administration of recombinant SCF to astroglia leads to the up-regulation of other growth factors including NGF and BDNF (Zhang and Fedoroff, 1997). Because the *Pak1*$^{-/-}$ genotype did not display significant MAPK activation in response to SCF application, these results may indicate that MAPK activation associated with SCF/c-kit signaling is primarily mediated in a PAK1-dependent manner (see **Figure 20**). Due to its role in MAPK signaling in the PFC, SCF/c-kit and other growth factors likely play an integral role in the regulation of long-term social learning in mice and other processes in the CNS that are mediated in a PAK1-dependent manner.

C. *Nf1* and *Pak1* affect inhibitory synaptic currents (IPSCs) in BLA glutamatergic projection neurons in mice

Previous studies in *Nf1*$^{+/-}$-hippocampal neurons found increases in the frequency of inhibitory synaptic currents under periods of high-frequency stimulation (Cui et al, 2008). While no differences were observed in *Nf1*$^{+/-}$ mice in either sIPSC or mIPSC amplitude, *Nf1*$^{+/-}$ mice showed significant increases in both sIPSC and mIPSC frequency in glutamatergic projection neurons isolated from the BLA, as compared to WT (see **Figure 21**). The administration of a

$GABA_A$ antagonist (SR 95531 hydrobromide) and a $GABA_B$ antagonist (CGP 52432) block the mIPSCs, consistent with GABA-mediated inhibition. In the BLA, glutamatergic projection neurons are regulated by excitatory input that is largely sensory information and inhibitory input from local GABAergic interneurons (**see Figure 4**). Therefore, the increases in IPSCs frequency observed in glutamatergic projection neurons in the BLA seen *Nf1*$^{+/-}$ mice could potentially result from increased presynaptic GABA release from inhibitory interneurons localized to the BLA.

Next, we determined whether the genetic inactivation of *Pak1* in *Nf1*$^{+/-}$ (*Nf1*$^{+/-}$/ *Pak1*$^{-/-}$) mice would restore the increases in inhibitory synaptic currents seen in *Nf1*$^{+/-}$ mice. While no differences were detected in sIPSC or mIPSC amplitude, we found that the co-deletion of *Pak1* normalized the increases in sIPSC and mIPSC frequency, as compared to *Nf1*$^{+/-}$ mice (see **Figure 22**). These results demonstrate that increases in IPSCs in BLA glutamatergic projection neurons seen in *Nf1*$^{+/-}$ mice are corrected in the *Nf1*$^{+/-}$ / *Pak1*$^{-/-}$ mice. Abnormal tonic inhibition in the BLA can cause communication problems with PFC that can lead to inappropriate emotional assessment and assignment of saliency to social cues (see Bachevalier and Malkova 2006 for review). Ultimately, the balance of excitation and inhibition can have important effects on functions of the BLA, including social and emotion learning.

D. Role of *Nf1* and *Pak1* genes in the regulation of protein expression in the PFC and BLA

The prefrontal-amygdala circuit defines a primary processing center for emotional aspects of social response, and its dysregulation can have profound effects on social function in humans and rodents. Mass spectrometry was used to screen for differences in proteins expressed in the PFC and BLA associated with the *Nf1*$^{+/-}$ genotype and were restored by the co-deletion of *Pak1* gene in *Nf1*$^{+/-}$ mice. Proteins were selected based on the following criteria: (1) significant differences between WT vs. *Nf1*$^{+/-}$ group, (2) significant differences between *Nf1*$^{+/-}$ vs. *Nf1*$^{+/-}$ / *Pak1*$^{-/-}$ group, and (3) were consistent with a rescue (see **Tables 1-2**). The resulting proteins were then characterized based on their known biology and their relevance to NF1-related phenotypes utilizing resources from National Center for Biotechnology Information [www.ncbi.nlm.nih.gov].

1. Proteins identified in the PFC

In the PFC, the co-deletion of *Pak1* gene rescues differences in protein expression seen in *Nf1*$^{+/-}$ mice that perform multiple cellular functions including the regulation of RNA transcription, protein modification and packaging, cytoskeletal dynamics, vesicular fusion, and neurotransmission. Therefore, the proteomics findings in this dissertation indicate that the mechanism(s) involved in the PAK1-dependent rescue of the deficits in long-term social learning likely are complex, but affect a finite number of proteins that mediate specific cellular processes. Additionally, these proteomics findings reveal a more robust effect of

the *Pak1* gene co-deletion in the PFC identifying twenty one proteins, while only one protein exhibited an expression profile consistent with a rescue in the BLA.

a. Proteins involved in the regulation of DNA

Due to its role as a negative regulator of RAS activation, neurofibromin acts as a key regulator in signal transduction from the cell membrane to the nucleus (see Le and Parada, 2007 for review). DNA represents the cornerstone of the cellular function by providing the genomic code for RNAs and their respective proteins, and dysregulation in DNA structure and function can lead to important effects on the CNS. Histones play a central role in transcription regulation, DNA repair, DNA replication and chromosomal stability. In the PFC, both H2A2B and NUCL are expressed at higher levels in $Nf1^{+/-}$ mice. Histone H2A type 2-B or H2A2B is a core component of nucleosomes, proteins that wrap and compact DNA into chromatin, limiting DNA accessibility to the cellular machineries which require DNA as a template (Bergink et al, 2006). Nucleolin or NUCL is histone chaperone protein associated with intranucleolar chromatin and pre-ribosomal particles. NUCL induces chromatin decondensation by binding to histone H1, thereby, NUCL increases DNA accessibility needed for RNA transcriptional elongation (see Storck et al, 2007 for review). The upregulation of H2A2B and NUCL in $Nf1^{+/-}$ mice may alter the accessibility of DNA broadly affecting gene expression.

b. Proteins involved in the regulation of RNA

RNA transcription and its subsequent modification into mRNA represent core cellular processes. Both HNRH1 and CAPRI are expressed at higher levels in the PFC of *Nf1*$^{+/-}$ mice. Heterogeneous nuclear ribonucleoprotein H or HNRH1 is localized to the nucleoplasm in the nucleus, and is a component of the heterogeneous nuclear ribonucleoprotein (hnRNP) complexes which provide the substrate for the processing events that pre-mRNAs undergo before becoming functional, translatable mRNAs in the cytoplasm (Paul et al, 2006). Additionally, Caprin-1 or CAPRI regulates the transport and translation of mRNAs of proteins, and has been shown to mediate cellular proliferation (Wang et al, 2005). In neuronal cells, CAPRI directly binds to mRNAs associated with RNA granules, including BDNF, CAMK2A, CREB1, MAP2, NTRK2, GRIN1, KPNB1 mRNAs. Through processing and transport of mRNA, HNRH1 and CAPRI affect the expression of multiple proteins involved in the regulation of DNA transcription, cellular proliferation and cytoskeletal dynamics in the CNS.

c. Proteins involved in the regulation of protein translation

The endoplasmic reticulum (ER) is the site of protein synthesis, and the rough ER is responsible for transporting the newly synthesized proteins to the Golgi apparatus, the cellular site for protein modifications. Nascent polypeptide-associated complex subunit alpha or NACAM prevents inappropriate targeting of non-secretory polypeptides to the ER by binding to nascent polypeptide chains as they emerge from the ribosome and blocks their interaction with the signal

recognition particle (George et al, 2002). NACAM also reduces the inherent affinity of ribosomes for protein translocation sites in the ER membrane. Adapter-related protein complex 1 subunit beta-1 or AP1B1 plays a role in protein sorting in the Golgi apparatus by mediating both the recruitment of clathrin to membranes and the recognition of sorting signals within the cytosolic tails of transmembrane cargo molecules (Santambrogio et al, 2005). In the PFC, NACAM is expressed at lower levels in *Nf1*$^{+/-}$ mice, while AP1B1 is expressed at higher levels. Additionally, Clathrin light chain B or CLCB is expressed at higher levels in the PFC of *Nf1*$^{+/-}$ mice. CLCB is the major protein localized to the polyhedral coat of vesicles (Brodsky et al, 1987), and has been associated with schizophrenia in humans (Vercauteren et al, 2007). Thus, NACAM, AP1B1 and CLCB proteins are involved in the regulation of protein modification and secretion in the ER and Golgi apparatus.

d. Proteins involved in F-actin and microtubule dynamics

In the developing forebrain, cytoskeletal dynamics regulates cellular processes involved in neuronal polarization (i.e., neuronal migration, axon specification), dendritic spine morphology, and vesicular release (see Arimura and Kaibuchi for review). While the mechanisms that contribute to these cytoskeletal changes are still largely uncharacterized, the regulation of filamentous actin (F-actin) and microtubule dynamics are critical for these cellular processes associated with cytoskeletal dynamics. Consistent with disruption in cytoskeletal dynamics, Brown et al (2010) found that hippocampal neurons

cultured from *Nf1*$^{+/-}$ mouse embryos show reduced neurite lengths and growth cone areas. In addition, F-actin is abundantly expressed in the dendritic spine, the postsynaptic structure in neurons. F-actin dynamics is also involved in the enlargement of vesicular pool size and increases in vesicle-fusion probability (see Zucker, 1989 for review). Pharmacological experiments further demonstrate that interfering with F-actin inhibits long-term potentiation (LTP) in hippocampal neurons, a mechanism that is critical for synaptic plasticity and memory formation (Kim and Lisman, 1999).

In the PFC, three proteins were identified that are involved in the regulation of F-actin dynamics. Alpha-actin-1 or ACTS is expressed at higher levels in the PFC of *Nf1*$^{+/-}$ mice. ACTS is ubiquitously expressed in eukaryotic cells. The polymerization of globular actin (G-actin) leads to the formation of filamentous actin (F-actin) in the form of a two-stranded helix. F-actin-capping protein subunit alpha-2 or CAZA2 is expressed at lower levels in the PFC of *Nf1*$^{+/-}$ mice. F-actin-capping proteins bind in a Ca^{2+}-independent manner to the fast growing ends of actin filaments (barbed end), thereby blocking the exchange of subunits at these ends. Drebrin or DREB is expressed at higher levels in the PFC of *Nf1*$^{+/-}$ mice. DREB directly binds to F-actin. DREB is involved in organizing the dendritic pool of actin, and coordinates F-actin-microtubule interactions that mediate neuronal polarity and motility including neurite formation and the regulation of growth cones (Geraldo et al, 2008). Thereby, DREB regulates both cell shape and plasticity, and has been associated with

Alzheimer's disease and Down syndrome (Harigaya et al, 1996; Dun and Chilton, 2010).

In the CNS, PAK1 is essential for cytoskeletal dynamics by acting in a kinase-dependent manner to regulate F-actin formation and microtubule stabilization (see Jacobs et al, 2007 for review; **Figure 24**). PAK1 has been shown to regulate LIM kinase activity, leading to the destabilization cofilin and the inactivation and aggregation of F-actin fibers (Ishibashi, 2008). The overexpression of PAK1 leads to increases in cellular motility and actin polymerization, while the expression of dominant negative PAK1 results in decreases in migration and organized actin structures (Sells et al, 1999). Through its interaction of LIMK and cofilin, PAK1, thereby, mediates cytoskeletal dynamics including F-actin assembly and vesicular transport (Vadlamudi et al, 2002). It has been shown that disruption of cortical F-actin can evoke vesicle translocation, thereby liberating large dense core vessicles bound to F-actin (Rose et al, 2001; Neco et al, 2003). In addition, MAPK signaling regulates F-actin disassembly, thereby modulating vesicular release. For example, the inhibition of MAPK signaling blocks the effect of activity dependent potentials suppressing the vesicular release (Park et al, 2006). In neurons, MAPK activation in a calcium dependent manner leads to phosphorylation of synapsin I, which causes F-actin disassembly and subsequent translocation of vesicles (Yamagata et al, 2002).

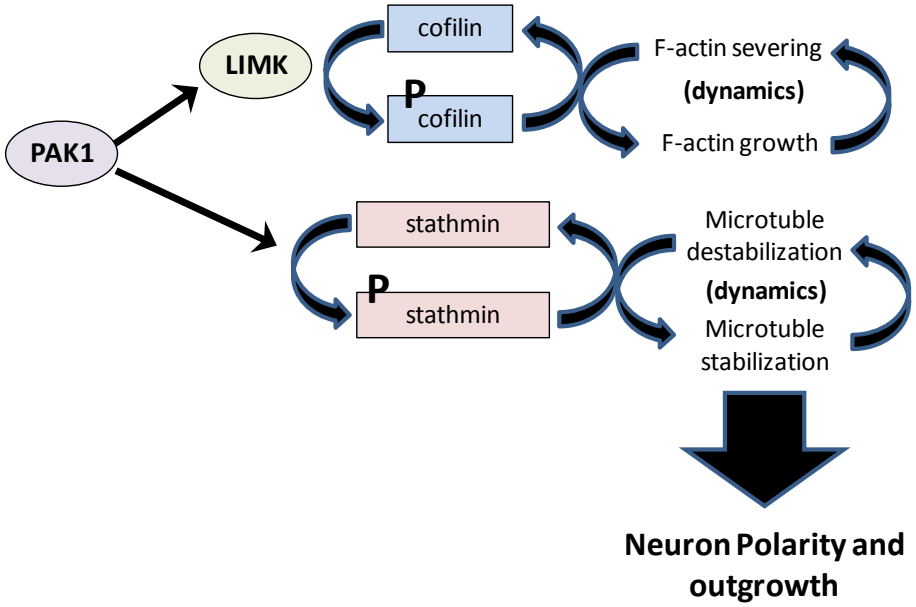

Adapted from Jacobs et al, 2007

Figure 24. Model illustrating the role of Pak1 in the regulation of F-actin and microtubules. The specification of an axon and subsequent outgrowth of axons and dendrites require the dynamic turnover of F-actin and microtubules. PAK1 and its downstream targets, in part, regulate F-actin growth / severing and microtubule stabilization / destabilization. Pak1 activates LIMK-1, therby, inhibiting cofilin activation. Pak1 also mediates microtubule dynamics through the phosphorylation and inactivation of the microtubule-destabilizing protein stathmin.

In addition to the regulation of F-actin, PAK1 also mediates microtubule dynamics through the phosphorylation and inactivation of the microtubule-destabilizing protein stathmin (Daub et al, 2001; see **Figure 24**). Three proteins were identified that are associated with dysregulation in microtubule dynamics. For instance, microtubule-associated protein 1A or MAP1A is expressed at higher levels in the PFC of *Nf1*$^{+/-}$ mice. MAP1A is a structural protein involved in the filamentous cross-bridging between microtubules and other skeletal elements (Pedrotti et al, 1994). Dynein light chain 2 (DYL2) is expressed at lower levels in the PFC of *Nf1*$^{+/-}$ mice. DYL2 is involved in some aspects of dynein-related intracellular transport and motility, and may play a role in changing or maintaining the spatial distribution of cytoskeletal structures localized to cytoplasm. Dynamin-1 or DYN1 is expressed at lower levels in the PFC of *Nf1*$^{+/-}$ mice. DYN1 is a microtubule-associated force-producing protein that is involved in producing microtubule bundles. DYN1 is able to bind and hydrolyze GTP, and interacts with soluble N-ethylmaleimide-sensitive factor attachment protein receptors (Gorini et al, 2010). DYN1 regulates receptor-mediated endocytosis associated with vesicular trafficking, has been associated with schizophrenia and bipolar disorder (Martins-de-Souza et al, 2009; Gray et al, 2010).

e. Proteins associated with vesicular fusion

Following protein modification, finished protein products, or glycoproteins, are transported in vesicles (i.e., vesicular trafficking) to the cellular membrane. Synaptic vesicles then bind to receptors on the surface of the membrane, and the

glycoproteins are excreted from the neuron through vesicular translocation (Südhof et al, 1993). Membrane fusion in neurons is Ca^{2+} dependent process and involves the interaction of synaptic vesicle proteins, plasma membrane proteins, and cytoplasmic proteins (Söllner et al, 1993). Neurons contain large dense-core vesicles and small synaptic vesicles that are responsible for secretion of neuropeptides or hormones and classical neurotransmitters, respectively. Both large dense-core vesicles and small synaptic vesicles show activity dependent release (Shakiryanova et al, 2005).

Thy-1 membrane glycoprotein or THY1 is expressed at higher levels in the PFC of *Nf1*$^{+/-}$ mice. THY1 is a component of both large dense-core and small clear vesicles in the CNS, and plays an important role in the regulation of vesicular release of neurotransmitter and neuromodulators at the synapse. THY1 is expressed by neuronal cells in culture (Wilkerson and Touster, 1993). THY1 mediates signal transduction by increasing intracellular Ca^{2+} levels (Barboni et al, 1991) and stimulating tyrosine phosphorylation (Hsi et al, 1989). *Thy-1* null mice show selective social learning deficits in the social transmission of food preference test (Mayeux-Portas et al, 2000). Additionally, *Thy-1*$^{-/-}$ mice exhibit excessive GABAergic inhibition and deficits in LTP in the dentate gyrus (Hollrigel et al, 1998; Nosten-Bertrand et al, 1996). These deficits in social learning can be restored by the administration of a $GABA_A$ receptor antagonist (Mayeux-Portas et al, 2000).

Syntaxin binding protein 1 or STXBP1 is detected at lower levels in the PFC of *Nf1*$^{+/-}$ mice. STXBP1 is involved in the regulation of SNARE-dependent

membrane fusion necessary for membrane expansion during neurite formation (Steiner et al, 2002). STXBP1 is a presynaptic protein that binds to the closed conformation of syntaxin, and thus inhibits its assembly into the SNARE complex (Yang et al, 2000) Release from STXBP1 and activation of the open conformation of syntaxin is key to synaptic membrane fusion and the release of neurotransmitters into the synaptic gap (Mitchell et al, 2005). Additionally, syntaxin has been shown to promote neurite outgrowth in cell culture (Steiner et al, 2002). Through its interaction with syntaxin, STXB1 participates in the regulation of synaptic vesicle docking and fusion, possibly through interaction with GTP-binding proteins (Mitchell et al, 2005), and has been associated with increased risk for schizophrenia and bipolar disorder (Vercauteren et al, 2007; Behan et al, 2009).

Detected at higher levels in the PFC, limbic system-associated membrane protein or LSAMP is a glycoprotein that mediates selective neuronal growth and axon targeting by through the guidance of developing axons and the remodeling of mature circuits in the limbic system. LSAMP is expressed on the surface of somata and dendrites of neurons in cortical and subcortical regions (Horton and Levitt, 1988; Zacco et al, 1990). LSAMP can enhance or inhibit neurite outgrowth depending on the neuronal population (Pimenta and Levitt, 2004). While basic neuroanatomical organization and sensory and motor development appear to be normal, Lsamp$^{-/-}$ mice display a heightened reactivity to novelty and hyperactivity in a novel arena indicating a possibly maladaptive response to novel environmental stressors (Catania et al, 2008). Additionally, LSAMP has been

implicated in schizophrenia, mood disorders, and an increased risk for suicide (Behan et al, 2009; Must et al, 2008).

f. Proteins associated with myelination

In the central nervous system, PAK1 is enriched in oligodendrocytes or glial cells that provide a supporting role for neurons and produce the myelin sheath insulating axons (Dharmawardhane et al, 1997). Myelin allows for the efficient conduction of action potentials down the axon by reducing ion leakage and decreasing the capacitance of the cell membrane. *Nf1*$^{+/-}$ mice show increases in the expression of MBPs in the PFC. Myelin basic proteins or MBP isoforms (isoform 4-isoform 13) are the most abundant protein components of the myelin membrane in the CNS. MBPs play an essential role in both the formation and stabilization of the myelin sheath. Human studies have found decreased expression of MBPs in temporal lobe of schizophrenics (Martins-de-Souza et al, 2009)

g. Proteins involved in neurotransmission

Two proteins were identified in the PFC that may modulate neurotransmission. Glutamate dehydrogenase 1 or DHE is expressed at lower levels in the PFC of *Nf1*$^{+/-}$ mice. DHE is localized to the mitochondrial matrix and may be involved in learning and memory by increasing the turnover of the excitatory neurotransmitter glutamate. DHE3 is subject to allosteric regulation in that it is activated by ADP by occupying the NADH binding site, and inhibited by

GTP. Bao et al (2009) generated a transgenic mouse model with increased expression of DHE that exhibits a life-long excess of synaptic glutamate release in the CNS. These transgenic mice display neuronal losses in select brain regions (e.g., the CA1 of the hippocampus) and decreases in LTP and in spine density in dendrites of CA1 neurons. These findings demonstrate that DHE dysregulation can lead to synaptic changes in cellular processes associated with learning and memory. Calbindin 1 or CALB1 is expressed at higher levels in the PFC of *Nf1*$^{+/-}$ mice. CALB1 buffers cytosolic Ca^{2+} levels, and may stimulate membrane Ca^{2+}-ATPase. It has been proposed that dysregulation of calcium homeostasis may be an important factor in the pathogenesis of Parkinson's disease and that calcium buffers such as CALB1 may be neuroprotective (Chan et al, 2009; Mattson, 2007). Therefore, dysregulation in DHE and CALB1 seen in *Nf1*$^{+/-}$ mice may lead to changes in glutamatergic neurotransmission and cytosolic Ca^{2+} levels in the CNS, respectively.

h. Other proteins involved in cellular function

Alpha-enolase or ENOA is expressed at lower levels in the PFC of *Nf1*$^{+/-}$ mice. ENOA is a multifunctional enzyme that regulates multiple cellular processes including glycolysis, cell growth, hypoxia tolerance and allergic responses. L-lactate dehydrogenase A chain or LDHA is expressed at lower levels in the PFC of *Nf1*$^{+/-}$ mice. LDHA is involved in the fermentation of pyruvate to lactate. These proteins mediate pathways involved in energy production that are associated with the metabolism of glucose.

2. Protein identified in the BLA

In the basolateral amygdala, disintegrin and metalloproteinase domain-containing protein 22 or ADAM22 is expressed at lower levels in *Nf1*$^{+/-}$ mice. ADAM22 is a ligand for integrin that regulates cell adhesion and spreading and inhibits cellular proliferation. ADAM22 (a receptor) and its ligand LGI1 are widely involved in the regulation of neuronal development and synaptic functions (see Han and Kim, 2008 for review). The LGI1/ADAM22 complex is thought to interact with and stabilize the AMPAR/stargazing complex on the PSD-95 scaffolding platform anchoring the AMPAR/stargazin complex at postsynaptic sites (Fukata et al, 2010). PSD-95 expression mediates synaptogenesis, and the development of excitatory verses inhibitory synapses (see Cline, 2005 for review). Furthermore, LGI1 has been shown to bind to Kv1.1, a presynaptic voltage-gated potassium channel subunit (Schulte et al, 2006). Mice lacking ADAM22 display reduced body weight, hypomyelination of peripheral nerves, and ataxia, and die before postnatal day 20 as a result of multiple seizures (Sagane et al, 2005). Thereby, ADAM22 plays an integral role in the regulation of neurotransmission and protein trafficking, and has been implicated in the development of epilepsy in humans (Diani et al, 2008).

D. The NF1 mouse model: the genetics, biochemistry, cell biology and behavior

The impact of scientific research using animal models is largely dependent on the relevance of the animal model to the human condition. By utilizing

homologous recombination strategies to selectively knock-out the *Nf1* gene in mice (Jacks et al, 1994), the *Nf1*$^{+/-}$ mouse model closely mimics the genetic determinant that underlies the development of NF1 in humans. Likewise, the biochemical and cellular processes mediated by neurofibromin (i.e., RAS, MAPK, PAK1, etc.) are conserved in the *Nf1*$^{+/-}$ mouse model. Because the NF1 condition is a simple autosomal dominant disorder, the *Nf1*$^{+/-}$ mouse closely resembles the biological dysfunctions that are seen in the NF1 condition in humans. Therefore, the construct validity associated with the *Nf1*$^{+/-}$ mouse model and its relationship to NF1 in humans is well-defined. To date, many of the features associated with the NF1 condition in humans have been detected in the *Nf1*$^{+/-}$ mouse model including learning and memory deficits (Silva et al, 1997). Consistent with the social problems seen in NF1 patients, this dissertation is the first to provide evidence that the *Nf1*$^{+/-}$ mouse model displays significant disruption in social learning. Therefore, these novel findings strengthen the face validity of the *Nf1*$^{+/-}$ mouse model.

The *NF1* gene functions as a classic tumor suppressor gene in humans (Colman et al, 1995). Similar to humans, the complete loss of the *Nf1* gene leads to tumorigenesis in chimeric mice partially composed of *Nf1*$^{-/-}$ cells providing further face validity for the *Nf1*$^{+/-}$ mouse model (Chichowski et al, 1999). However, the disruptions in cognition, learning and memory, and social function associated with the *NF1* gene deletion are independent of tumor disposition in humans (Moore et al, 1994) and mice (Silva et al, 1997). Therefore, the genetic mechanism that underlies disruption in CNS function is *Nf1* haploinsufficiency or

a gene dosing effect leading to incomplete or partial dominance. In the periphery, *Nf1* haploinsufficiency has been associated with enhanced MAPK activity and increases in SCF-mediated mast cell proliferation, survival, and colony formation (Ingram et al, 2000).

In the CNS, *Nf1* haploinsufficiency would be consistent with the high level of variability that is associated with NF1-related learning disabilities, attention and social function (Hofman et al, 1994; North et al, 1997; Dilts et al, 1996; Brewer et al, 1997; Johnson et al, 1999; Kayl and Moore 2000; Noll et al, 2007). In addition to previous studies in the CNS, this dissertation identifies disruptions in SCF-mediated hyperactivation of MAPK in $Nf1^{+/-}$ neurons cultured from the PFC and observed increases in IPSCs in glutamatergic projection neurons in BLA. Thereby, these findings are consistent with *Nf1* haploinsufficiency in CNS neurons. Similar to the biologic and cellular interactions in the tumor microenvironment (Staser et al, 2010), *Nf1* haploinsufficiency may redefine the tripartite synapse in multiple brain regions resulting in disruption in CNS function, and ultimately abnormalities in CNS processes (e.g., learning and memory). However, the $Nf1^{+/-}$ microenvironment in the CNS defined by interactions between pre-synaptic neurons, post-synaptic neurons, and glia remains to be elucidated.

While much progress has been made to identify the mechanism(s) that underlie the learning disabilities observed in $Nf1^{+/-}$ mouse model, the mechanism(s) is not yet clearly established. Previous studies have focused on processes involved in hippocampal-based learning, and have implicated

increases in RAS activation and MAPK signaling, and have found increases in GABA-mediated inhibition and deficits in LTP in *Nf1*$^{+/-}$ mice (Silva et al, 1997; Costa et al, 2002; Li et al, 2005). Thereby, MAPK hyperactivation and increases in GABA-mediated inhibition have been proposed as potential mechanisms underlying hippocampal-based learning abnormalities (Shilyansky et al, 2010). To further characterize the mechanism(s) underlying the disruptions in social learning, this dissertation focused on the prefrontal-amygdala circuit. Similar to previous findings in the hippocampus, this dissertation demonstrates that the *Nf1*$^{+/-}$ mouse model displays MAPK hyperactivation in the PFC and increases in GABA-mediated inhibition in the BLA. This dissertation further demonstrates these disruptions in social learning, MAPK signaling and IPSCs are mediated in a *Pak1*-dependent manner. Due to its activation of PAK1 and MAPK, SCF/c-kit signaling represents a potential mechanism of interest to learning abnormalities seen in *Nf1*-deficient mice.

Expression profiling strategies have been implemented to identify candidate genes and/or candidate proteins that contribute to endophenotypes associated with disease. For this purpose, mass spectrometry was conducted to identify protein expression differences associated with the *Nf1*$^{+/-}$ genotype in mice that were rescued by the co-deletion of *Pak1*. Because the disruption in long-term social learning/memory is mediated in a *Pak1*-dependent manner, this dissertation identified proteins with expression profiles that are consistent with a *Pak1*-dependent rescue. In the PFC, proteins involved in the regulation of F-actin and microtubule dynamics represent targets of interest due to their close

association with PAK1 and MAPK signaling in the regulation of cytoskeletal dynamics and vesicular release (see Kreis and Barnier, 2009 for review). Consistent with disruption in cytoskeletal dynamics (i.e., F-actin growth, microtubule stabilization), a reduction in neurite lengths and growth cone areas have been documented in hippocampal neurons cultured from *Nf1*$^{+/-}$ mouse embryos (Brown et al, 2010). LSAMP and STXB1, and DREB have been implicated in neurite formation (Pimenta and Levitt, 2004; Steiner et al, 2002; Geraldo et al, 2008). In the BLA, ADAM22 provides an interesting protein candidate due to its role in the regulation of AMPA receptors by stabilizing the AMPAR/stargazing complex on the PSD-95 scaffolding platform and anchoring the AMPAR/stargazin complex at postsynaptic sites (Fukata et al, 2010). Therefore, disruption in the amygdala-prefrontal circuit may contribute to abnormalities in social learning seen in the *Nf1*$^{+/-}$ mouse model.

E. NF1, the amygdala, and autism

Autism spectrum disorders comprise a heterogeneous group of conditions characterized by developmental abnormalities in cognition, communication, and social function (see Pardo and Eberhart, 2007 for review). NF1 shows a dramatically increased frequency in autistic patients with an estimated prevalence of 1.2% (Martin et al, 2007). Furthermore, the chromosomal region harboring the *NF1* locus has been linked to autism (IMGSAC, 2001; Yonan et al, 2003), and several studies have detected a significant association between the *NF1* locus and autism in humans (Mbarek et al, 1999; Mouridsen et al, 1992;

Marui et al, 2004). While the relationship between autism and NF1 is not yet well-established, the *NF1* gene deletion may represent an important etiological variable for autistic development.

NF1 children often show problems with social interaction and social perception in that they inappropriately perceive and interpret social cues, including facial expressions, body gestures, and tone of voice (Eliason, 1986). The present dissertation demonstrates that *Nf1*$^{+/-}$ mice show deficits in social learning that are associated with disruption in the prefrontal-amygdala circuit. Likewise, subjects with autism and Asperger's syndrome display symptoms of prosopagnosia or marked impairments in the processing of facial expressions (Davies et al, 1994; Schultz et al, 2000). Interestingly, human subjects with amygdala damage also have difficulty with facial recognition tasks (Adolphs et al, 1994; Young et al, 1995; Adolphs et al, 1998). In autistic patients, disruption in face processing is associated with abnormalities in structure and functional activation of the amygdala (Pierce et al, 2001). In addition, a postmortem study found abnormalities in neuronal structure (i.e., neuronal size, cell packing density) in various sub-nuclei of the amygdala (Kemper and Bauman, 1998). Therefore, "social learning" may be an important variable to consider in examining the relationship between the *NF1* gene deletion, NF1-related social deficits, and autism.

Several brain regions have been implicated in autistic development such as the cerebellum, amygdala, hippocampus, and PFC (Courchesne et al, 1988; Sweeten et al, 2002). In particular, the amygdala represents a region of interest

due to its role in the mediation of social and aggressive behaviors (see Aggleton, 1992 for review). For instance, the bilateral removal of the amygdala, hippocampus and cortical regions in monkeys that are six months of age present autistic-like features, including unexpressive faces, very little eye contact, stereotypic behaviors, and self-directed activity (see Bachevalier, 1994 for review; Bachevalier, 1996). Additionally, several structural neuroimaging studies have shown abnormalities in the sizes of the amygdala, hippocampus and other limbic areas in patients with autism, as compared to controls (Kates et al, 1998; Aylward et al, 1999; Abell et al, 1999). Other imaging studies using MRI techniques found an enlargement in cortical regions in autistic patients relative to controls (Piven et al, 1995; Piven et al, 1996). Because the *Nf1*$^{+/-}$ mouse model displays social learning abnormalities, the genetic, molecular, electrophysiological and behavioral findings presented in this dissertation may help identify novel targets for the treatment for social deficits in NF1 patients and potentially NF1-related autism.

F. Summary and future directions

The present dissertation first screened the *Nf1*$^{+/-}$ mouse model in order to assess aspects of social and emotional learning. We found selective deficits in long-term social learning in *Nf1*$^{+/-}$ mice, while we detected no differences in their preference for social interaction, short-term social learning, anxiety, one-trial learning (EPM) or depression-associated response. The deficits in social learning seen in the *Nf1*$^{+/-}$ mouse model are consistent with social problems seen in NF1 patients. Given that patients with autism have an increased incidence of NF1, the

NF1 gene has been identified as a potential risk factor for some forms of autism (see Zafeiriou et al, 2007 for review). In the *Nf1*$^{+/-}$ mouse model, behavioral studies could be conducted to further characterize social learning and social communication including the social transmission of food preference test and ultrasonic vocalization test, respectively.

The social transmission of food preference test measures the ability of mice to obtain meaningful information associated with food preference (non-social cues) through social interactions with a cage-mate (Wrenn, 2004). To assess the development of social communication in rodents, ultrasonic vocalizations induced by their separation from their dam are measured in mouse pups (Scattoni et al, 2009). Low levels of separation-induced of infant vocalization (50-80 kHz) and low levels of retrieval by the dam would be indicative of a failure to respond appropriately to socially meaningful stimuli. Likewise, disruption in ultrasonic vocalization (e.g., fewer ultrasonic vocalization calls or less quieting by mouse pups; failure to respond by dam) would be consistent with abnormal development of rodent communication.

This dissertation demonstrates a SCF-mediated hyperactivation of MAPK signaling in neurons cultured from the PFC of *Nf1*$^{+/-}$ mouse pups that are mediated in a *Pak1*-dependent manner. In addition to MAPK signaling (Beeser et al, 2005; Park et al, 2007), PAK1 regulates LIM kinase activity leading to the destabilization cofilin and the polymerization F-actin (Ishibashi, 2008). Future studies utilizing pharmacological manipulation strategies to selectively target MAPK and/or LIMK signaling could better characterize the signaling pathway(s)

that regulates social learning deficits seen in *Nf1*$^{+/-}$ mice. Additionally, electrophysiological studies could be conducted to characterize how pharmacological inhibition of MAPK and/or LIMK affect IPSCs observed in glutamatergic projection neurons in the BLA. Thereby, these future studies would determine the down-stream pathways that underlie the *Pak1*-dependent rescue of social learning and IPSCs seen in *Nf1*$^{+/-}$ mice.

Using the whole-cell patch clamp, this dissertation demonstrates increases in the frequency of IPSCs measured in glutamatergic projection neurons in the BLA of *Nf1*$^{+/-}$ mice. The administration of a $GABA_A$ antagonist (SR 95531 hydrobromide) and a $GABA_B$ antagonist (CGP 52432) block the IPSCs; therefore, these IPSCs are consistent with GABA-mediated inhibition. However, it is not known whether these increases in IPSC frequency are a product of increases in presynaptic GABA release from inhibitory interneurons localized to the BLA (see **Figure 4**). Utilizing microdialysis strategies, future studies could test how the *Nf1*$^{+/-}$ genotype affects the synaptic release of GABA in the BLA. Microdialysis could also be used to determine whether the co-deletion of *Pak1* restores GABA release in the BLA. Similarly, electrophysiological and microdialysis strategies could be further applied to these genetic intercrosses to analyze excitatory synaptic currents (EPSCs) in glutamatergic projection neurons in the BLA.

Utilizing mass spectrometry, protein expression was characterized in the PFC and BLA. These results were independently analyzed and confirmed using SPSS statistical software (SPSS Incorporated, Chicago, IL). In total, twenty-one

proteins were identified in the PFC, and one protein was identified in the BLA. In the PFC, multiple proteins were identified that are associated with F-actin and microtubule dynamics. Future studies using immunohistochemistry could be used to better characterize neuronal morphology including the distribution and content of F-actin and microtubules in neurons in the PFC in each genetic intercross. Due to the role of MAPK and synapsin I in F-actin disassembly and vesicular release (Yamagata et al, 2002), microdialysis strategies could be used to measure vesicular release in neurons localized to the PFC. In addition, individual proteins of interest were identified in the PFC and BLA. For instance, LSAMP, STXBP1, and DREB play important roles in neurite formation and outgrowth (Pimenta and Levitt, 2004; Steiner et al, 2002; Geraldo et al, 2008), and THY1 is associated with social learning abnormalities in mice (Mayeux-Portas et al, 2000). In the BLA, ADAM22 stabilizes the AMPAR/stargazing complex on the PSD-95 scaffolding platform, and thereby is involved in the regulation of AMPA receptors (Fukata et al, 2010). Following their confirmation using Western blotting, future studies could target each respective protein of interest using genetic and pharmacological manipulation in order to determine how each protein affects social learning in mice.

In conclusion, this dissertation demonstrates a selective disruption in long-term social learning / memory in *Nf1*$^{+/-}$ mice that is restored by the co-deletion of *Pak1*. The *Pak1* co-deletion also restores the *Nf1*$^{+/-}$-related hyperactivation in MAPK and increases in IPSCs in the prefrontal-amygdala circuit, brain regions that have been implicated in social and emotional processes. Additionally, the

Nf1$^{+/-}$ mouse models show dysregulation in protein expression in the PFC and BLA that are restored by the co-deletion of *Pak1* gene. This dissertation identifies dysfunction in F-actin and microtubule dynamics as well as several proteins of interest identified in the PFC (i.e., DREB, LSAMP, STXBP1, and THY1) and BLA (i.e, ADAM22). Together, these findings establish a role for *Nf1* and *Pak1* genes in the regulation of social learning in *Nf1*-deficient mice, and indicate that the pharmacological inhibition of PAK1 may represent a therapeutic target for the treatment of NF1-related social deficits in humans. However, future studies are necessary to clearly assess the predictive validity of *Pak1* gene as a viable candidate for the treatment of NF1-related social deficits.

REFERENCES

Abell F, Krams M, Ashburner J, Passingham R, Friston K, Frackowiak R, Happe F, Frith C, Frith U (1999) The neuroanatomy of autism: A voxel-based whole brain analysis of structural scans. NeuroReport 10:1647-51.

Adolphs R, Tranel D, Damasio H, Damasio A (1994) Impaired recognition of emotion in facial expressions following bilateral damage to the human amygdala. Nature 372:669-72.

Adolphs R, Tranel D, Damasio AR (1998) The human amygdala in social judgement. Nature 393:470-4.

Adolphs R (2002a) Neural systems for recognizing emotion. Curr Opin Neurobiol 12(2):169-77. Review.

Adolphs R (2002b). Recognizing emotion from facial expressions: psychological and neurological mechanisms. Behav Cogn Neurosci Rev 1(1):21-62. Review.

Adolphs R, Baron-Cohen S, Tranel D (2002) Impaired recognition of social emotions following amygdala damage. J Cogn Neurosci 14(8):1264-74.

Adolphs R (2009) The social brain: neural basis of social knowledge. Annu Rev Psychol 60:693-716. Review.

Aggleton JP (1992) The Amygdala: Neurobiological Aspects of Emotion, Memory, and Mental Dysfunction (Aggleton J, ed). New York: Wiley-Liss.

Amaral DG, Avendaño C, Benoit R (1989) Distribution of somatostatin-like immunoreactivity in the monkey amygdala. J Comp Neurol 284(2):294-313.

Amaral DG, Price JL, Pitkanen A, Carmichael ST (1992) Anatomical organization of the primate amygdaloid complex. In: The amygdala (Aggleton J, ed), pp 1-67. New York: Wiley-Liss.

Arias-Romero LE, Chernoff J (2008) A tale of two Paks. Biol Cell 100(2):97-108. Review.

Arimura N, Kaibuchi K (2007) Neuronal polarity: from extracellular signals to intracellular mechanisms. Nat Rev Neurosci 8(3):194-205. Review.

Atkins CM, Selcher JC, Petraitis JJ, Trzaskos JM, Sweatt JD (1998) The MAPK cascade is required for mammalian associative learning. Nat Neurosci 1(7):602-9.

Aylward EH, Minshew NJ, Goldstein G, Honeycutt NA, Augustine AM, Yates KO, Barta PE, Pearlson GD (1999) MRI volumes of amygdala and hippocampus in non-mentally retarded autistic adolescents and adults. Neurology 53(9):2145-50.

Bachevalier J (1994) Medial temporal lobe structures and autism: A review of clinical and experimental findings. Neuropsychologia 32(6):627-48.

Bachevalier J (1996) Medial temporal lobe and autism: A putative animal model in primates. J Autism Dev Disord 26(2):217-20.

Bachevalier J, Málková L (2006) The amygdala and development of social cognition: theoretical comment on Bauman, Toscano, Mason, Lavenex, and Amaral (2006). Behav Neurosci 120(4):989-91.

Bader JL (1986) Neurofibromatosis and cancer. Ann N Y Acad Sci 486:57-65.

Ballester R, Marchuk D, Boguski M, Saulino A, Letcher R, Wigler M, Collins F (1990) The NF1 locus encodes a protein functionally related to mammalian GAP and yeast IRA proteins. Cell 63(4):851-9.

Bao X, Pal R, Hascup KN, Wang Y, Wang WT, Xu W, Hui D, Agbas A, Wang X, Michaelis ML, Choi IY, Belousov AB, Gerhardt GA, Michaelis EK (2009) Transgenic expression of Glud1 (glutamate dehydrogenase 1) in neurons: in vivo model of enhanced glutamate release, altered synaptic plasticity, and selective neuronal vulnerability. J Neurosci 29(44):13929-44.

Barboni E, Gormley AM, Pliego Rivero FB, Vidal M, Morris RJ (1991) Activation of T lymphocytes by cross-linking of glycophospholipid-anchored Thy-1 mobilizes separate pools of intracellular second messengers to those induced by the antigen-receptor/CD3 complex. Immunology 72(4):457-63.

Barrash J, Tranel D, Anderson SW (2000) Acquired personality disturbances associated with bilateral damage to the ventromedial prefrontal region. Dev Neuropsychol 18(3):355-81.

Barton B, North K (2004) Social skills of children with neurofibromatosis type 1. Dev Med Child Neurol. 46(8):553-63.

Bausch B, Koschker AC, Fassnacht M, Stoevesandt J, Hoffmann MM, Eng C, Allolio B, Neumann HP (2006) Comprehensive mutation scanning of NF1 in apparently sporadic cases of pheochromocytoma. J Clin Endocrinol Metab 91(9):3478-81.

Beeser A, Jaffer ZM, Hofmann C, Chernoff J (2005) Role of group A p21-activated kinases in activation of extracellular-regulated kinase by growth factors. J Biol Chem 280(44):36609-15.

Behan AT, Byrne C, Dunn MJ, Cagney G, Cotter DR (2009) Proteomic analysis of membrane microdomain-associated proteins in the dorsolateral prefrontal cortex in schizophrenia and bipolar disorder reveals alterations in LAMP, STXBP1 and BASP1 protein expression. Mol Psychiatry 14(6):601-13.

Bekri S, Adélaïde J, Merscher S, Grosgeorge J, Caroli-Bosc F, Perucca-Lostanlen D, Kelley PM, Pébusque MJ, Theillet C, Birnbaum D, Gaudray P (1997) Detailed map of a region commonly amplified at 11q13-->q14 in human breast carcinoma. Cytogenet Cell Genet 79(1-2):125-31.

Belzeaux R, Lançon C (2006) Neurofibromatosis type 1: psychiatric disorders and quality of life impairment. Presse Med 35:277-80. Review.

Bergink S, Salomons FA, Hoogstraten D, Groothuis TA, de Waard H, Wu J, Yuan L, Citterio E, Houtsmuller AB, Neefjes J, Hoeijmakers JH, Vermeulen W, Dantuma NP (2006) DNA damage triggers nucleotide excision repair-dependent monoubiquitylation of histone H2A. Genes Dev 20(10):1343-52.

Bernards A, Snijders AJ, Hannigan GE, Murthy AE, Gusella JF (1993) Mouse neurofibromatosis type 1 cDNA sequence reveals high degree of conservation of both coding and non-coding mRNA segments. Hum Mol Genet 2(6):645-50.

Besmer P, Murphy JE, George PC, Qiu FH, Bergold PJ, Lederman L, Snyder HW Jr, Brodeur D, Zuckerman EE, Hardy WD (1986) A new acute transforming feline retrovirus and relationship of its oncogene v-kit with the protein kinase gene family. Nature 320(6061):415-21.

Bishop AL, Hall A (2000) Rho GTPases and their effector proteins. Biochem J 348 Pt 2:241-55. Review.

Blair RJ (2008) The amygdala and ventromedial prefrontal cortex: functional contributions and dysfunction in psychopathy. Philos Trans R Soc Lond B Biol Sci 363(1503):2557-65. Review.

Bliss TV, Collingridge GL (1993) A synaptic model of memory: long-term potentiation in the hippocampus. Nature 361:31-39.

Blum S, Moore AN, Adams F, Dash PK (1999) A mitogen-activated protein kinase cascade in the CA1/CA2 subfield of the dorsal hippocampus is essential for long-term spatial memory. J Neurosci 19(9):3535-44.

Bokoch GM, Wang Y, Bohl BP, Sells MA, Quilliam LA, Knaus UG (1996) Interaction of the Nck adapter protein with p21-activated kinase (PAK1). J Biol Chem 271(42):25746-9.

Bokoch GM, Reilly AM, Daniels RH, King CC, Olivera A, Spiegel S, Knaus UG (1998) A GTPase-independent mechanism of p21-activated kinase activation. Regulation by sphingosine and other biologically active lipids. J Biol Chem 273(14):8137-44.

Bozon B, Kelly A, Josselyn SA, Silva AJ, Davis S, Laroche S (2003) MAPK, CREB and zif268 are all required for the consolidation of recognition memory. Philos Trans R Soc Lond B Biol Sci 358(1432):805-14. Review.

Brannan CI, Perkins AS, Vogel KS, Ratner N, Nordlund ML, Reid SW, Buchberg AM, Jenkins NA, Parada LF, Copeland NG (1994) Targeted disruption of the neurofibromatosis type-1 gene leads to developmental abnormalities in heart and various neural crest-derived tissues. Genes Dev 8(9):1019-29.

Brewer VR, Moore BD 3rd, Hiscock M (1997) Learning disability subtypes in children with neurofibromatosis. J Learn Disabil 30(5):521-33.

Brodkin ES, Hagemann A, Nemetski SM, Silver LM (2004) Social approach-avoidance behavior of inbred mouse strains towards DBA/2 mice. Brain Res 1002(1-2):151-7.

Brodsky FM, Galloway CJ, Blank GS, Jackson AP, Seow HF, Drickamer K, Parham P (1987) Localization of clathrin light-chain sequences mediating heavy-chain binding and coated vesicle diversity. Nature 326(6109):203-205.

Brown JA, Gianino SM, Gutmann DH (2010) Defective cAMP generation underlies the sensitivity of CNS neurons to neurofibromatosis-1 heterozygosity. J Neurosci 30(16):5579-89.

Brown JL, Stowers L, Baer M, Trejo J, Coughlin S, Chant J (1996) Human Ste20 homologue hPAK1 links GTPases to the JNK MAP kinase pathway. Curr Biol 6(5):598-605.

Caffrey TM, Wade-Martins R (2007) Functional MAPT haplotypes: bridging the gap between genotype and neuropathology. Neurobiol Dis 27(1):1-10. Review.

Campbell SL, Khosravi-Far R, Rossman KL, Clark GJ, Der CJ (1998) Increasing complexity of Ras signaling. Oncogene. 17:1395-413.

Cassell MD, Gray TS (1989) Morphology of peptide-immunoreactive neurons in the rat central nucleus of the amygdala. J Comp Neurol 281(2):320-33.

Castle B, Baser ME, Huson SM, Cooper DN, Upadhyaya M (2003) Evaluation of genotype-phenotype correlations in neurofibromatosis type 1. J Med Genet 40(10):109.

Catania EH, Pimenta A, Levitt P. Genetic deletion of Lsamp causes exaggerated behavioral activation in novel environments (2008) Behav Brain Res 188(2):380-90.

Cawthon RM, O'Connell P, Buchberg AM, Viskochil D, Weiss RB, Culver M, Stevens J, Jenkins NA, Copeland NG, White R (1990) Identification and characterization of transcripts from the neurofibromatosis 1 region: the sequence and genomic structure of EVI2 and mapping of other transcripts. Genomics 7(4):555-65.

Chan CS, Gertler TS, Surmeier DJ (2009) Calcium homeostasis, selective vulnerability and Parkinson's disease. Trends Neurosci 32:249-256.

Chang TY, Chang CC, Ohgami N, Yamauchi Y (2006) Cholesterol sensing, trafficking, and esterification. Annu Rev Cell Dev Biol 22:129-57.

Chang TY, Chang CC, Bryleva E, Rogers MA, Murphy SR (2010) Neuronal cholesterol esterification by ACAT1 in Alzheimer's disease. IUBMB Life 62(4):261-7.

Cichowski K, Shih TS, Schmitt E, Santiago S, Reilly K, McLaughlin ME, Bronson RT, Jacks T (1999) Mouse models of tumor development in neurofibromatosis type 1. Science 286(5447):2172-6.

Cline H (2005) Synaptogenesis: a balancing act between excitation and inhibition. Curr Biol 15(6):R203-5. Review.

Cnossen MH, Moons KG, Garssen MP, Pasmans NM, de Goede-Bolder A, Niermeijer MF, Grobbee DE (1998) Minor disease features in neurofibromatosis type 1 (NF1) and their possible value in diagnosis of NF1 in children < or = 6 years and clinically suspected of having NF1. Neurofibromatosis team of Sophia Children's Hospital. J Med Genet 35(8):624-7.

Coles LC, Shaw PE (2002) PAK1 primes MEK1 for phosphorylation by Raf-1 kinase during cross-cascade activation of the ERK pathway. Oncogene 21(14):2236-44.

Colman SD, Williams CA, Wallace MR (1995) Benign neurofibromas in type 1 neurofibromatosis (NF1) show somatic deletions of the NF1 gene. Nat Genet 11(1):90-2.

Cooke SF, Bliss TV (2006) Plasticity in the human central nervous system. Brain 129(Pt 7):1659-73. Review.

Corkin S, Amaral DG, González RG, Johnson KA, Hyman BT (1997) H. M.'s medial temporal lobe lesion: findings from magnetic resonance imaging. J Neurosci 17(10):3964-79.

Costa RM, Yang T, Huynh DP, Pulst SM, Viskochil DH, Silva AJ, Brannan CI (2001) Learning deficits, but normal development and tumor predisposition, in mice lacking exon 23a of Nf1. Nat Genet 27(4):399-405.

Costa RM, Federov NB, Kogan JH, Murphy GG, Stern J, Ohno M, Kucherlapati R, Jacks T, Silva AJ (2002) Mechanism for the learning deficits in a mouse model of neurofibromatosis type 1. Nature 415(6871):526-30.

Costa RM, Silva AJ (2003) Mouse models of neurofibromatosis type I: bridging the GAP. Trends Mol Med 9(1):19-23. Review.

Coudé FX, Mignot C, Lyonnet S, Munnich A (2006) Academic impairment is the most frequent complication of neurofibromatosis type-1 (NF1) in children. Behav Genet 36(5):660-4.

Courchesne E, Yeung-Courchesne R, Press GA, Hesselink JR, Jernigan TL (1988) Hypoplasia of cerebellar vermal lobules VI and VII in autism. New Engl J Med 318(21):1349-54.

Crawford AH Jr, Bagamery N (1986) Osseous manifestations of neurofibromatosis in childhood. J Pediatr Orthop. 6(1):72-88.

Crawley JN, Chen T, Puri A, Washburn R, Sullivan TL, Hill JM, Young NB, Nadler JJ, Moy SS, Young LJ, Caldwell HK, Young WS (2007) Social approach behaviors in oxytocin knockout mice: comparison of two independent lines tested in different laboratory environments. Neuropeptides 41(3):145-63.

Créange A, Zeller J, Rostaing-Rigattieri S, Brugières P, Degos JD, Revuz J, Wolkenstein P (1999) Neurological complications of neurofibromatosis type 1 in adulthood. Brain 122:473-81.

Crews CM, Erikson RL (1993) Extracellular signals and reversible protein phosphorylation: what to Mek of it all. Cell 74(2):215-7. Review.

Cui Y, Costa RM, Murphy GG, Elgersma Y, Zhu Y, Gutmann DH, Parada LF, Mody I, Silva AJ (2008) Neurofibromin regulation of ERK signaling modulates GABA release and learning. Cell 135(3):549-60.

Cutting LE, Koth CW, Denckla MB (2000) How children with neurofibromatosis type 1 differ from "typical" learning disabled clinic attenders: nonverbal learning disabilities revisited. Dev Neuropsychol 17(1):29-47.

Damasio AR, Tranel D, Damasio H (1990) Individuals with sociopathic behavior caused by frontal damage fail to respond autonomically to social stimuli. Behav Brain Res 41(2):81-94.

Danglot G, Régnier V, Fauvet D, Vassal G, Kujas M, Bernheim A (1995) Neurofibromatosis 1 (NF1) mRNAs expressed in the central nervous system are differentially spliced in the 5' part of the gene. Hum Mol Genet 4(5):915-20.

Daston MM, Scrable H, Nordlund M, Sturbaum AK, Nissen LM, Ratner N (1992) The protein product of the neurofibromatosis type 1 gene is expressed at highest abundance in neurons, Schwann cells, and oligodendrocytes. Neuron 8(3):415-28.

Daub H, Gevaert K, Vandekerckhove J, Sobel A, Hall A (2001) Rac/Cdc42 and p65PAK regulate the microtubule-destabilizing protein stathmin through phosphorylation at serine 16. J Biol Chem 276(3):1677-80.

Davies S, Bishop D, Manstead AS, Tantam D (1994) Face perception in children with autism and Asperger's syndrome. J Child Psychol Psychiatry 35:1033-57.

DeBella K, Szudek J, Friedman JM (2000) Use of the national institutes of health criteria for diagnosis of neurofibromatosis 1 in children. Pediatrics 105:608-14.

DeClue JE, Papageorge AG, Fletcher JA, Diehl SR, Ratner N, Vass WC, Lowy DR (1992) Abnormal regulation of mammalian p21ras contributes to malignant tumor growth in von Recklinghausen (type 1) neurofibromatosis. Cell 69(2):265-73.

Dharmawardhane S, Sanders LC, Martin SS, Daniels RH, Bokoch GM (1997) Localization of p21-activated kinase 1 (PAK1) to pinocytic vesicles and cortical actin structures in stimulated cells. J Cell Biol 138(6):1265-78.

Diani E, Di Bonaventura C, Mecarelli O, Gambardella A, Elia M, Bovo G, Bisulli F, Pinardi F, Binelli S, Egeo G, Castellotti B, Striano P, Striano S, Bianchi A, Ferlazzo E, Vianello V, Coppola G, Aguglia U, Tinuper P, Giallonardo AT, Michelucci R, Nobile C (2008) Autosomal dominant lateral temporal epilepsy: absence of mutations in ADAM22 and Kv1 channel genes encoding LGI1-associated proteins. Epilepsy Res 80(1):1-8.

Dilts CV, Carey JC, Kircher JC, Hoffman RO, Creel D, Ward K, Clark E, Leonard CO (1996) Children and adolescents with neurofibromatosis 1: a behavioral phenotype. J Dev Behav Pediatr 17(4):229-39.

Downward J (1992) Regulation of p21ras by GTPase activating proteins and guanine nucleotide exchange proteins. Curr Opin Genet Dev 2:13-8.

Durand B, Migliaccio G, Yee NS, Eddleman K, Huima-Byron T, Migliaccio AR, Adamson JW (1994) Long-term generation of human mast cells in serum-free cultures of CD34+ cord blood cells stimulated with stem cell factor and interleukin-3. Blood 84(11):3667-74.

Duman RS, Winston SM, Clark JA, Nestler EJ (1990) Corticosterone regulates the expression of ADP-ribosylation factor messenger RNA and protein in rat cerebral cortex. J Neurochem 55(5):1813-6.

Dun XP, Chilton JK (2010) Control of cell shape and plasticity during development and disease by the actin-binding protein Drebrin. Histol Histopathol 25(4):533-40.

Eliason MJ (1986) Neurofibromatosis: implications for learning and behavior. J Dev Behav Pediatr 7(3):175-9.

Eliason MJ (1988) Neuropsychological patterns: neurofibromatosis compared to developmental learning disorders. Neurofibromatosis 1(1):17-25.

Fallon JH, Koziell DA, Moore RY (1978) Catecholamine innervation of the basal forebrain. II. Amygdala, suprarhinal cortex and entorhinal cortex. J Comp Neurol 180(3):509-32.

Feld M, Dimant B, Delorenzi A, Coso O, Romano A (2005) Phosphorylation of extra-nuclear ERK/MAPK is required for long-term memory consolidation in the crab Chasmagnathus. Behav Brain Res 158(2):251-61.

Ferner RE, Hughes RA, Weinman J (1996) Intellectual impairment in neurofibromatosis 1. J Neurol Sci 138(1-2):125-33.

Ferner RE (2007) Neurofibromatosis 1 and neurofibromatosis 2: a twenty first century perspective. Lancet Neurol 6(4):340-51.

Friedman JM, Birch PH (1997) Type 1 Neurofibromatosis: a descriptive analysis of the disorder in 1728 patients. Am J Med Genet 70:138-43.

Friedman JM (1999) Epidemiology of neurofibromatosis type 1. Am J Med Genet 89:1-6.

Friedman JM, Arbiser J, Epstein JA, Gutmann DH, Huot SJ, Lin AE, McManus B, Korf BR (2002) Cardiovascular disease in neurofibromatosis 1: report of the NF1 Cardiovascular Task Force. Genet Med 4(3):105-11.

Fukata Y, Lovero KL, Iwanaga T, Watanabe A, Yokoi N, Tabuchi K, Shigemoto R, Nicoll RA, Fukata M (2010) Disruption of LGI1-linked synaptic complex causes abnormal synaptic transmission and epilepsy. Proc Natl Acad Sci U S A 107(8):3799-804.

George R, Walsh P, Beddoe T, Lithgow T (2002) The nascent polypeptide-associated complex (NAC) promotes interaction of ribosomes with the mitochondrial surface in vivo. FEBS Lett 516(1-3):213-6.

Geraldo S, Khanzada UK, Parsons M, Chilton JK, Gordon-Weeks PR (2008) Targeting of the F-actin-binding protein drebrin by the microtubule plus-tip protein EB3 is required for neuritogenesis. Nat Cell Biol 10(10):1181-9.

Giovannini MG (2006) The role of the extracellular signal-regulated kinase pathway in memory encoding. Rev Neurosci 17(6):619-34. Review.

Goldgar DE, Green P, Parry DM, Mulvihill JJ (1989) Multipoint linkage analysis in neurofibromatosis type I: an international collaboration. Am J Hum Genet 44(1):6-12.

Gorini G, Ponomareva O, Shores KS, Person MD, Harris RA, Mayfield RD (2010) Dynamin-1 co-associates with native mouse brain BKCa channels: proteomics analysis of synaptic protein complexes. FEBS Lett 584(5):845-851.

Gray LJ, Dean B, Kronsbein HC, Robinson PJ, Scarr E (2010) Region and diagnosis-specific changes in synaptic proteins in schizophrenia and bipolar I disorder. Psychiatry Res 178(2):374-80.

Gustafson EL, Card JP, Moore RY (1986) Neuropeptide Y localization in the rat amygdaloid complex. J Comp Neurol 251(3):349-62.

Gutmann DH, Collins FS (1993) The neurofibromatosis type 1 gene and its protein product, neurofibromin. Neuron 10(3):335-43.

Han K, Kim E (2008) Synaptic adhesion molecules and PSD-95. Prog Neurobiol 84(3):263-83. Review.

Harigaya Y, Shoji M, Shirao T, Hirai S (1996) Disappearance of actin-binding protein, drebrin, from hippocampal synapses in Alzheimer's disease. J Neurosci Res 43(1):87-92.

Hecht F (1989) Recognition of neurofibromatosis before von Recklinghausen. Neurofibromatosis 2(3):180-4.

Hofman KJ, Harris EL, Bryan RN, Denckla MB (1994) Neurofibromatosis type 1: the cognitive phenotype. J Pediatr 124(4):S1-8.

Hogg S (1996) A review of the validity and variability of the elevated plus-maze as an animal model of anxiety. Pharmacol Biochem Behav 54(1):21-30. Review.

Hollrigel GS, Morris RJ, Soltesz I (1998) Enhanced bursts of IPSCs in dentate granule cells in mice with regionally inhibited long-term potentiation. Proc Biol Sci 265(1390):63-9.

Hornak J, Rolls ET, Wade D (1996) Face and voice expression identification in patients with emotional and behavioural changes following ventral frontal lobe damage. Neuropsychologia 34(4):247-61

Horton HL, Levitt P (1988) A unique membrane protein is expressed on early developing limbic system axons and cortical targets. J Neurosci 8:4653-4661.

Howard MA, Cowell PE, Boucher J, Broks P, Mayes A, Farrant A, Roberts N (2000) Convergent neuroanatomical and behavioral evidence of an amygdala hypothesis of autism. NeuroReport 11(13):2931-5.

Hsi ED, Siegel JN, Minami Y, Luong ET, Klausner RD, Samelson LE (1989) T cell activation induces rapid tyrosine phosphorylation of a limited number of cellular substrates. J Biol Chem 264(18):10836-42.

Iemura A, Tsai M, Ando A, Wershil BK, Galli SJ (1994) The c-kit ligand, stem cell factor, promotes mast cell survival by suppressing apoptosis. Am J Pathol 144(2):321-8.

IMGSAC (2001) A genomewide screen for autism: strong evidence for linkage to chromosomes 2q, 7q, and 16p. Am J Hum Genet 69:570-581.

Ingram DA, Yang FC, Travers JB, Wenning MJ, Hiatt K, New S, Hood A, Shannon K, Williams DA, Clapp DW (20001) Genetic and biochemical evidence that haploinsufficiency of the Nf1 tumor suppressor gene modulates melanocyte and mast cell fates in vivo. J Exp Med. 2000 Jan 3;191(1):181-8.

Ingram DA, Hiatt K, King AJ, Fisher L, Shivakumar R, Derstine C, Wenning MJ, Diaz B, Travers JB, Hood A, Marshall M, Williams DA, Clapp DW (2001) Hyperactivation of p21(ras) and the hematopoietic-specific Rho GTPase, Rac2, cooperate to alter the proliferation of neurofibromin-deficient mast cells in vivo and in vitro. J Exp Med 194(1):57-69.

Insel TR, Fernald RD (2004) How the brain processes social information: searching for the social brain. Annu Rev Neurosci 27:697-722. Review.

Ishibashi F (2008) High glucose increases phosphocofilin via phosphorylation of LIM kinase due to Rho/Rho kinase activation in cultured pig proximal tubular epithelial cells. Diabetes Res Clin Pract 80(1):24-33.

Jacks T, Shih TS, Schmitt EM, Bronson RT, Bernards A, Weinberg RA (1994) Tumour predisposition in mice heterozygous for a targeted mutation in Nf1. Nat Genet 7(3):353-61.

Jacobs T, Causeret F, Nishimura YV, Terao M, Norman A, Hoshino M, Nikolić M (2007) Localized activation of p21-activated kinase controls neuronal polarity and morphology. J Neurosci 27(32):8604-15.

Johannessen CM, Reczek EE, James MF, Brems H, Legius E, Cichowski K (2005) The NF1 tumor suppressor critically regulates TSC2 and mTOR. Proc Natl Acad Sci U S A 102(24):8573-8.

Johnson NS, Saal HM, Lovell AM, Schorry EK (1999) Social and emotional problems in children with neurofibromatosis type 1: evidence and proposed interventions. J Pediatr 134(6):767-72.

Kapp BS, Gallagher M, Underwood MD, McNall CL, Whitehorn D (1982) Cardiovascular responses elicited by electrical stimulation of the amygdala central nucleus in the rabbit. Brain Res 25;234(2):251-62.

Kates WR, Mostofsky SH, Zimmerman AW, Mazzocco MMM, Landa R, Warsofsky IS, Kaufmann WE, Reiss AL (1998) Neuroanatomical and neurocognitive differences in a pair of monozygous twins discordant for strictly defined autism. Ann Neurol 43:782-91.

Kavale KA, Forness SR (1996) Social skill deficits and learning disabilities: a meta-analysis. J Learn Disabil 29(3):226-37.

Kayl AE, Moore BD (2000) Behavioral phenotype of neurofibromatosis, type 1. Ment Retard Dev Disabil Res Rev 6(2):117-24.

Kemper TL, Bauman M (1998) Neuropathology of infantile autism. J Neuropathol and Exp Neurol 57(7):645-52.

Kennedy DP, Gläscher J, Tyszka JM, Adolphs R (2009) Personal space regulation by the human amygdala. Nat Neurosci 12(10):1226-7.

Keshet E, Lyman SD, Williams DE, Anderson DM, Jenkins NA, Copeland NG, Parada LF (1991) Embryonic RNA expression patterns of the c-kit receptor and its cognate ligand suggest multiple functional roles in mouse development. EMBO J 10(9):2425-35.

Keyhan N, Minden D, Ickowicz A (2006) Clinical case rounds in child and adolescent psychiatry: neurofibromatosis type 1, cognitive impairment, and attention deficit hyperactivity disorder. J Can Acad Child Adolesc Psychiatry 15(2):87-90.

Kim CH, Lisman JE (1999) A role of actin filament in synaptic transmission and long-term potentiation. J Neurosci 19(11):4314-24.

Knaus UG, Morris S, Dong HJ, Chernoff J, Bokoch GM (1995) Regulation of human leukocyte p21-activated kinases through G protein--coupled receptors. Science 269(5221):221-3.

Kodaki T, Woscholski R, Hallberg B, Rodriguez-Viciana P, Downward J, Parker PJ (1994) The activation of phosphatidylinositol 3-kinase by Ras. Curr Biol 4(9):798-806.

Köhler C, Hallman H, Melander T, Hökfelt T, Norheim E (1989) Autoradiographic mapping of galanin receptors in the monkey brain. J Chem Neuroanat 2(5):269-84.

Korf BR (1999) Plexiform neurofibromas. Am J Med Genet. 89(1):31-7.

Koth CW, Cutting LE, Denckla MB (2000) The association of neurofibromatosis type 1 and attention deficit hyperactivity disorder. Child Neuropsychol 6(3):185-94.

Kreis P, Barnier JV (2009) PAK signalling in neuronal physiology. Cell Signal 21(3):384-93.

Kritzer MF, Innis RB, Goldman-Rakic PS (1988) Regional distribution of cholecystokinin receptors in macaque medial temporal lobe determined by in vitro receptor autoradiography. J Comp Neurol 276(2):219-30.

Kyriakis JM, App H, Zhang XF, Banerjee P, Brautigan DL, Rapp UR, Avruch J (1992) Raf-1 activates MAP kinase-kinase. Nature 358(6385):417-21.

Le LQ, Parada LF (2007) Tumor microenvironment and neurofibromatosis type I: connecting the GAPs. Oncogene 26(32):4609-16. Review.

LeDoux JE (1993) Emotional memory systems in the brain. Behav Brain Res 58(1-2):69-79. Review.

LeDoux JE (1992) Brain mechanisms of emotion and emotional learning. Curr Opin Neurobiol 2(2):191-7. Review.

LeDoux J (2003) The emotional brain, fear, and the amygdala. Cell Mol Neurobiol 23(4-5):727-38. Review.

Lei M, Lu W, Meng W, Parrini MC, Eck MJ, Mayer BJ, Harrison SC (2000) Structure of PAK1 in an autoinhibited conformation reveals a multistage activation switch. Cell 102(3):387-97.

Li W, Cui Y, Kushner SA, Brown RA, Jentsch JD, Frankland PW, Cannon TD, Silva AJ (2005) The HMG-CoA reductase inhibitor lovastatin reverses the learning and attention deficits in a mouse model of neurofibromatosis type 1. Curr Biol 15(21):1961-7.

Listernick R, Ferner RE, Liu GT, Gutmann DH (2007) Optic pathway gliomas in neurofibromatosis-1: controversies and recommendations. Ann Neurol 61(3):189-98.

LoPresti ML, Schon K, Tricarico MD, Swisher JD, Celone KA, Stern CE (2008) Working memory for social cues recruits orbitofrontal cortex and amygdala: a functional magnetic resonance imaging study of delayed matching to sample for emotional expressions. J Neurosci 28(14):3718-28.

Luo Q, Holroyd T, Jones M, Hendler T, Blair J (2007) Neural dynamics for facial threat processing as revealed by gamma band synchronization using MEG. Neuroimage 34(2):839-47.

Mann B, Madera M, Sheng Q, Tang H, Mechref Y, Novotny MV (2008) ProteinQuant Suite: a bundle of automated software tools for label-free quantitative proteomics. Rapid Commun Mass Spectrom 22(23):3823-34.

Manser E, Chong C, Zhao ZS, Leung T, Michael G, Hall C, Lim L (1995) Molecular cloning of a new member of the p21-Cdc42/Rac-activated kinase (PAK) family. J Biol Chem 270(42):25070-8.

Marchuk DA, Saulino AM, Tavakkol R, Swaroop M, Wallace MR, Andersen LB, Mitchell AL, Gutmann DH, Boguski M, Collins FS (1991) cDNA cloning of the type 1 neurofibromatosis gene: complete sequence of the NF1 gene product. Genomics 11(4):931-40.

Margolis B, Skolnik EY (1994) Activation of Ras by receptor tyrosine kinases. J Am Soc Nephrol 5(6):1288-99. Review.

Martin GA, Viskochil D, Bollag G, McCabe PC, Crosier WJ, Haubruck H, Conroy L, Clark R, O'Connell P, Cawthon RM, et al (1990) The GAP-related domain of the neurofibromatosis type 1 gene product interacts with ras p21. Cell 63(4):843-9.

Martin I, Gauthier J, D'Amelio M, Védrine S, Vourc'h P, Rouleau GA, Persico AM, Andres CR (2007) Transmission disequilibrium study of an oligodendrocyte and myelin glycoprotein gene allele in 431 families with an autistic proband. Neurosci Res 59(4):426-30.

Martins-de-Souza D, Maccarrone G, Wobrock T, Zerr I, Gormanns P, Reckow S, Falkai P, Schmitt A, Turck CW (2010) Proteome analysis of the thalamus and cerebrospinal fluid reveals glycolysis dysfunction and potential biomarkers candidates for schizophrenia. J Psychiatr Res [Epub ahead of print]

Marui T, Hashimoto O, Nanba E, Kato C, Tochigi M, Umekage T, Ishijima M, Kohda K, Kato N, Sasaki T (2004) Association between the neurofibromatosis-1 (NF1) locus and autism in the Japanese population. Am J Med Genet 131B:43-47.

Maskati HA, Zbrozyna AW (1989) Stimulation in prefrontal cortex area inhibits cardiovascular and motor components of the defence reaction in rats. J Auton Nerv Syst 28(2):117-25.

Mattson MP (2007) Calcium and neurodegeneration. Aging Cell 6:337-350.

Mautner VF, Kluwe L, Thakker SD, Leark RA (2002) Treatment of ADHD in neurofibromatosis type 1. Dev Med Child Neurol 44(3):164-70.

Mayeux-Portas V, File SE, Stewart CL, Morris RJ (2000) Mice lacking the cell adhesion molecule Thy-1 fail to use socially transmitted cues to direct their choice of food. Curr Biol 10(2):68-75.

Mbarek O, Marouillat S, Martineau J, Barthélémy C, Müh JP, Andres C (1999) Association study of the NF1 gene and autistic disorder. Am J Med Genet 88:729-732.

McDaniel AS, Allen JD, Park SJ, Jaffer ZM, Michels EG, Burgin SJ, Chen S, Bessler WK, Hofmann C, Ingram DA, Chernoff J, Clapp DW (2008) Pak1 regulates multiple c-Kit mediated Ras-MAPK gain-in-function phenotypes in Nf1+/- mast cells. Blood 112(12):4646-54.

McDonald AJ (1984) Neuronal organization of the lateral and basolateral amygdaloid nuclei in the rat. J Comp Neurol 222(4):589-606.

McDonald AJ, Pearson JC (1989) Coexistence of GABA and peptide immunoreactivity in non-pyramidal neurons of the basolateral amygdala. Neurosci Lett 100(1-3):53-8.

McGaugh JL (2002) Memory consolidation and the amygdala: a systems perspective. Trends Neurosci 25(9):456. Review.

McLaughlin ME, Jacks T (2002) Thinking beyond the tumor cell: Nf1 haploinsufficiency in the tumor environment. Cancer Cell 1(5):408-10. Review.

Merino SM, Maren S (2006) Hitting Ras where it counts: Ras antagonism in the basolateral amygdala inhibits long-term fear memory. Eur J Neurosci. 2006 Jan;23(1):196-204.

Messiaen LM, Callens T, Mortier G, Beysen D, Vandenbroucke I, Van Roy N, Speleman F, Paepe AD (2000) Exhaustive mutation analysis of the NF1 gene allows identification of 95% of mutations and reveals a high frequency of unusual splicing defects. Hum Mutat 15(6):541-55.

Mitchell SJ, Ryan TA (2005) Munc18-dependent regulation of synaptic vesicle exocytosis by syntaxin-1A in hippocampal neurons. Neuropharmacology 48:372-380.

Moore BD, Ater JL, Needle MN, Slopis J, Copeland DR (1994) Neuropsychological profile of children with neurofibromatosis, brain tumor, or both. J Child Neurol 9(4):368-77.

Mouridsen SE, Andersen LB, Sorensen SA, Rich B, Isager T (1992) Neurofibromatosis in infantile autism and other types of childhood psychoses. Acta Paedopsychiatr 55:15-18.

Must A, Tasa G, Lang A, Vasar E, Kõks S, Maron E, Väli M (2008) Association of limbic system-associated membrane protein (LSAMP) to male completed suicide. BMC Med Genet 9:34.

Nadler JJ, Moy SS, Dold G, Trang D, Simmons N, Perez A, Young NB, Barbaro RP, Piven J, Magnuson TR, Crawley JN (2004) Automated apparatus for quantitation of social approach behaviors in mice. Genes Brain Behav 3(5):303-14.

Nandi A, Beard JR, Galea S (2009) Epidemiologic heterogeneity of common mood and anxiety disorders over the lifecourse in the general population: a systematic review. BMC Psychiatry 9:31.

National Institutes of Health Consensus Development Conference (1988) Neurofibromatosis: conference statement. Arch Neurol 45: 575-578.

Neco P, Rossetto O, Gil A, Montecucco C, Gutierrez LM (2003) Taipoxin induces F-actin fragmentation and enhances release of catecholamines in bovine chromaffin cells. J Neurochem 85:329-337.

Nikolić M (2008) The Pak1 kinase: an important regulator of neuronal morphology and function in the developing forebrain. Mol Neurobiol. 37(2-3):187-202. Review.

Noll RB, Reiter-Purtill J, Moore BD, Schorry EK, Lovell AM, Vannatta K, Gerhardt CA (2007) Social, emotional, and behavioral functioning of children with NF1. Am J Med Genet 143A(19):2261-73.

Nordlund M, Gu X, Shipley MT, Ratner N (1993) Neurofibromin is enriched in the endoplasmic reticulum of CNS neurons. J Neurosci 13(4):1588-600.

Norita M, Kawamura K (1980) Subcortical afferents to the monkey amygdala: an HRP study. Brain Res 190(1):225-30.

North K (1993) Neurofibromatosis type 1: Review of the first 200 patients in an Australian clinic. J Child Neurol 8:395-402.

North K, Joy P, Yuille D, Cocks N, Hutchins P (1995) Cognitive function and academic performance in children with neurofibromatosis type 1. Dev Med Child Neurol 37(5):427-36.

North KN, Riccardi V, Samango-Sprouse C, Ferner R, Moore B, Legius E, Ratner N, Denckla MB (1997) Cognitive function and academic performance in neurofibromatosis 1: consensus statement from the NF1 Cognitive Disorders Task Force. Neurology 48(4):1121-7.

Nosten-Bertrand M, Errington ML, Murphy KP, Tokugawa Y, Barboni E, Kozlova E, Michalovich D, Morris RG, Silver J, Stewart CL, Bliss TV, Morris RJ (1996) Normal spatial learning despite regional inhibition of LTP in mice lacking Thy-1. Nature 379(6568):826-9.

Ozonoff S (1999) Cognitive impairment in neurofibromatosis type 1. Am J Med Genet 89(1):45-52.

Pardo CA, Eberhart CG (2007) The neurobiology of autism. Brain Pathol 17(4):434-47.

Park YS, Jun DJ, Hur EM, Lee SK, Suh BS, Kim KT (2006) Activity-dependent potentiation of large dense-core vesicle release modulated by mitogen-activated protein kinase/extracellularly regulated kinase signaling. Endocrinology 147(3):1349-56.

Rose SD, Lejen T, Zhang L, Trifaro JM (2001) Chromaffin cell F-actin disassembly and potentiation of catecholamine release in response to protein kinase C activation by phorbol esters is mediated through myristoylated alanine-rich C kinase substrate phosphorylation. J Biol Chem 276:36757-36763.

Park ER, Eblen ST, Catling AD (2007) MEK1 activation by PAK: a novel mechanism. Cell Signal 19(7):1488-96.

Paul S, Dansithong W, Kim D, Rossi J, Webster NJ, Comai L, Reddy S (2006) Interaction of muscleblind, CUG-BP1 and hnRNP H proteins in DM1-associated aberrant IR splicing. EMBO J 25(18):4271-83.

Pedrotti B, Colombo R, Islam K (1994) Microtubule associated protein MAP1A is an actin-binding and crosslinking protein. Cell Motil 29(2)110-116.

Peng S, Zhang Y, Zhang J, Wang H, Ren B (2010) ERK in Learning and Memory: A Review of Recent Research. Int J Mol Sci 11(1):222-32.

Philippi CL, Mehta S, Grabowski T, Adolphs R, Rudrauf D (2009) Damage to association fiber tracts impairs recognition of the facial expression of emotion. J Neurosci 29(48):15089-99.

Pierce K, Müller RA, Ambrose J, Allen G, Courchesne E (2001) Face processing occurs outside the fusiform 'face area' in autism: evidence from functional MRI. Brain 124(10):2059-73.

Pimenta AF, Levitt P (2004) Characterization of the genomic structure of the mouse limbic system-associated membrane protein (Lsamp) gene. Genomics 83:790-801.

Piven J, Arndt S, Bailey J, Havercamp S, Andreasen NC, Palmer P (1995) An MRI study of brain size in autism. Am J Psychiatry 152(8):1145-9.

Piven J, Arndt S, Bailey J, Andreasen N (1996) Regional brain enlargement in autism: A magnetic resonance imaging study. J Am Acad Child Adolesc Psychiatry 35:530-6.

Porsolt RD, Bertin A, Jalfre M (1977) Behavioral despair in mice: a primary screening test for antidepressants. Arch Int Pharmacodyn Ther 229(2):327-36.

Purves D (2004) Neuroscience. Purves D, Augustine GJ, Fitzpatrick D, Hall WC, LaMantia AS, McNamara JO, Williams SM, Sunderland, MA: Sinauer Associates, Inc.

Quirion R, Welner S, Gauthier S, Bédard P(1987) Neurotensin receptor binding sites in monkey and human brain: autoradiographic distribution and effects of 1-methyl-4-phenyl-1,2,3,6-tetrahydropyridine treatment. Synapse 1(6):559-66.

Rainnie DG, Asprodini EK, Shinnick-Gallagher P (1991a) Excitatory transmission in the basolateral amygdala. J Neurophysiol 66(3):986-98.

Rainnie DG, Asprodini EK, Shinnick-Gallagher P (1991b) Inhibitory transmission in the basolateral amygdala. J Neurophysiol 66(3):999-1009.

Rasmussen SA, Yang Q, Friedman JM (2001) Mortality in neurofibromatosis 1: an analysis using U.S. death certificates. Am J Hum Genet 68(5):1110-8.

Reber L, Da Silva CA, Frossard N (2006) Stem cell factor and its receptor c-Kit as targets for inflammatory diseases. Eur J Pharmacol 533(1-3):327-40. Review.

Riccardi VM (1980) Pathophysiology of neurofibromatosis. IV. Dermatologic insights into heterogeneity and pathogenesis. J Am Acad Dermatol 3(2):157-66.

Richetta A, Giustini S, Recupero SM, Pezza M, Carlomagno V, Amoruso G, Calvieri S (2004) Lisch nodules of the iris in neurofibromatosis type 1. J Eur Acad Dermatol Venereol 18(3):342-4.

Rosser TL, Packer RJ (2003) Neurocognitive dysfunction in children with neurofibromatosis type 1. Curr Neurol Neurosci Rep 3(2):129-36.

Roy V, Chapillon P, Jeljeli M, Caston J, Belzung C (2009) Free versus forced exposure to an elevated plus-maze: evidence for new behavioral interpretations during test and retest. Psychopharmacology (Berl) 203(1):131-41.

Ruggieri M, Huson SM (1999) The neurofibromatoses. An overview. Ital J Neurol Sci 20(2):89-108.

Sagane K, Hayakawa K, Kai J, Hirohashi T, Takahashi E, Miyamoto N, Ino M, Oki T, Yamazaki K, Nagasu T (2005) Ataxia and peripheral nerve hypomyelination in ADAM22-deficient mice. BMC Neurosci. 6(33):1-12.

Saito H, Sakaguchi N, Matsumoto K, Tsubaki T, Numazaki T, Ebisawa M, Kobayashi M, Ozawa R, Yanagi H, Akasawa A (1994) Growth in methylcellulose of human mast cells in hematopoietic colonies stimulated by steel factor, a c-kit ligand. Int Arch Allergy Immunol. 1994;103(2):143-51.

Sajdyk TJ, Shekhar A (2000) Sodium lactate elicits anxiety in rats after repeated GABA receptor blockade in the basolateral amygdala. Eur J Pharmacol 394(2-3):265-73.

Sajdyk TJ, Johnson PL, Leitermann RJ, Fitz SD, Dietrich A, Morin M, Gehlert DR, Urban JH, Shekhar A (2008) Neuropeptide Y in the amygdala induces long-term resilience to stress-induced reductions in social responses but not hypothalamic-adrenal-pituitary axis activity or hyperthermia. J Neurosci 28(4):893-903.

Samuelsson B, Riccardi VM (1989) Neurofibromatosis in Gothenburg, Sweden. II. Intellectual compromise. Neurofibromatosis. 2(2):78-83.

Sánchez-Andrade G, James BM, Kendrick KM (2005) Neural encoding of olfactory recognition memory. J Reprod Dev 51(5):547-58. Review.

Sanders S, Shekhar A (1996) GABAA receptors in the basolateral amygdala of rats regulate "anxiety". Pharmacol Biochem Behav 52:701-705.

Sankoorikal GM, Kaercher KA, Boon CJ, Lee JK, Brodkin ES (2006) A mouse model system for genetic analysis of sociability: C57BL/6J versus BALB/cJ inbred mouse strains. Biol Psychiatry 59(5):415-23.

Santambrogio L, Potolicchio I, Fessler SP, Wong SH, Raposo G, Strominger JL (2005) Involvement of caspase-cleaved and intact adaptor protein 1 complex in endosomal remodeling in maturing dendritic cells. Nat Immunol 6(10):1020-8.

Scattoni ML, Crawley J, Ricceri L (2009) Ultrasonic vocalizations: a tool for behavioural phenotyping of mouse models of neurodevelopmental disorders. Neurosci Biobehav Rev 33(4):508-15. Review.

Schorry EK, Crawford AH, Egelhoff JC, Lovell AM, Saal HM (1997) Thoracic tumors in children with neurofibromatosis-1. Am J Med Genet 74(5):533-7.

Schulte U, Thumfart JO, Klöcker N, Sailer CA, Bildl W, Biniossek M, Dehn D, Deller T, Eble S, Abbass K, Wangler T, Knaus HG, Fakler B (2006) The epilepsy-linked Lgi1 protein assembles into presynaptic Kv1 channels and inhibits inactivation by Kvbeta1. Neuron 49(5):697-706.

Schultz RT, Gauthier I, Klin A, Fulbright RK, Anderson AW, Volkmar F, Skudlarski P, Lacadie C, Cohen DJ, Gore JC (2000) Abnormal ventral temporal cortical activity during face discrimination among individuals with autism and Asperger syndrome. Arch Gen Psychiatry 57:331-40.

Sells MA, Boyd JT, Chernoff J (1999) p21-activated kinase 1 (Pak1) regulates cell motility in mammalian fibroblasts. J Cell Biol 145(4):837-49.

Shakiryanova D, Tully A, Hewes RS, Deitcher DL, Levitan ES (2005) Activitydependent liberation of synaptic neuropeptide vesicles. Nat Neurosci 8:173-178.

Shekhar A, McCann UD, Meaney MJ, Blanchard DC, Davis M, Frey KA, Liberzon I, Overall KL, Shear MK, Tecott LH, Winsky L (2001) Summary of a National Institute of Mental Health workshop: developing animal models of anxiety disorders. Psychopharmacology (Berl) 157(4):327-39.

Shekhar A, Truitt W, Rainnie D, Sajdyk T (2005) Role of stress, corticotrophin releasing factor (CRF) and amygdala plasticity in chronic anxiety. Stress 8(4):209-19. Review.

Shilyansky C, Lee YS, Silva AJ (2010) Molecular and cellular mechanisms of learning disabilities: a focus on NF1. Annu Rev Neurosci 33:221-43.

Silva AJ, Frankland PW, Marowitz Z, Friedman E, Laszlo GS, Cioffi D, Jacks T, Bourtchuladze R (1997) A mouse model for the learning and memory deficits associated with neurofibromatosis type I. Nat Genet 15(3):281-4.

Silverman JL, Yang M, Lord C, Crawley JN (2010) Behavioural phenotyping assays for mouse models of autism. Nat Rev Neurosci11(7):490-502.

Snyder SH (2006) Neuroscience. Adam finds an exciting mate. Science 313(5794):1744-5.

Söllner T, Bennett MK, Whiteheart SW, Scheller RH, Rothman JE (1993) A protein assembly-disassembly pathway in vitro that may correspond to sequential steps of synaptic vesicle docking, activation, and fusion. Cell 75(3):409-18.

Südhof TC, De Camilli P, Niemann H, Jahn R (1993) Membrane fusion machinery: insights from synaptic proteins. Cell. 75(1):1-4. Review.

Staser K, Yang FC, Clapp DW (2010) Mast cells and the neurofibroma microenvironment. Blood 116(2):157-64. Review.

Steiner P, Sarria JC, Huni B, Marsault R, Catsicas S, Hirling H (2002) Overexpression of neuronal Sec1 enhances axonal branching in hippocampal neurons. Neuroscience 113:893-905.

Stephens L, Hawkins PT, Eguinoa A, Cooke F (1996) A heterotrimeric GTPase-regulated isoform of PI3K and the regulation of its potential effectors. Philos Trans R Soc Lond B Biol Sci 351(1336):211-5. Review.

Stokoe D, Macdonald SG, Cadwallader K, Symons M, Hancock JF (1994) Activation of Raf as a result of recruitment to the plasma membrane. Science 264(5164):1463-7.

Storck S, Shukla M, Dimitrov S, Bouvet P (2007) Functions of the histone chaperone nucleolin in diseases. Subcell Biochem 41:125-44. Review.

Sweeten TL, Posey DJ, Shekhar A, McDougle CJ (2002) The amygdala and related structures in the pathophysiology of autism. Pharmacol Biochem Behav 71(3):449-55.

Todd RM, Anderson AK (2009) Six degrees of separation: the amygdala regulates social behavior and perception. Nat Neurosci 12(10):1217-8.

Todd RM, Evans JW, Morris D, Lewis MD, Taylor MJ (2010) The changing face of emotion: age-related patterns of amygdala activation to salient faces. Soc Cogn Affect Neurosci [Epub ahead of print]

Tong J, Hannan F, Zhu Y, Bernards A, Zhong Y (2002) Neurofibromin regulates G protein-stimulated adenylyl cyclase activity. Nat Neurosci 5(2):95-6.

Tronson NC, Taylor JR (2007) Molecular mechanisms of memory reconsolidation. Nat Rev Neurosci 8(4):262-75. Review.

Truitt WA, Sajdyk TJ, Dietrich AD, Oberlin B, McDougle CJ, Shekhar A (2007) From anxiety to autism: spectrum of abnormal social behaviors modeled by progressive disruption of inhibitory neuronal function in the basolateral amygdala in Wistar rats. Psychopharmacology (Berl) 191(1):107-18.

Tucker T, Wolkenstein P, Revuz J, Zeller J, Friedman JM (2005) Association between benign and malignant peripheral nerve sheath tumors in NF1. Neurology 65(2):205-11.

Upadhyaya M, Osborn MJ, Maynard J, Kim MR, Tamanoi F, Cooper DN (1997) Mutational and functional analysis of the neurofibromatosis type 1 (NF1) gene. Hum Genet 99(1):88-92.

Vadlamudi RK, Li F, Adam L, Nguyen D, Ohta Y, Stossel TP, Kumar R (2002) Filamin is essential in actin cytoskeletal assembly mediated by p21-activated kinase 1. Nat Cell Biol 4(9):681-90.

Van Roy N, Vandesompele J, Berx G, Staes K, Van Gele M, De Smet E, De Paepe A, Laureys G, van der Drift P, Versteeg R, Van Roy F, Speleman F (2002) Localization of the 17q breakpoint of a constitutional 1;17 translocation in a patient with neuroblastoma within a 25-kb segment located between the ACCN1 and TLK2 genes and near the distal breakpoints of two microdeletions in neurofibromatosis type 1 patients. Genes Chromosomes Cancer 35(2):113-20.

Varnhagen CK, Lewin S, Das JP, Bowen P, Ma K, Klimek M (1988) Neurofibromatosis and psychological processes. J Dev Behav Pediatr 9(5):257-65.

Vercauteren FG, Flores G, Ma W, Chabot JG, Geenen L, Clerens S, Fazel A, Bergeron JJ, Srivastava LK, Arckens L, Quirion R (2007) An organelle proteomic method to study neurotransmission-related proteins, applied to a neurodevelopmental model of schizophrenia. Proteomics 7(19):3569-79.

Viskochil D (1999) In search of the Holy Grail: NF1 mutation analysis and genotype-phenotype correlation. Genet Med 1(6):245-7.

Vivarelli R, Grosso S, Calabrese F, Farnetani M, Di Bartolo R, Morgese G, Balestri P (2003) Epilepsy in neurofibromatosis 1. J Child Neurol 18(5):338-42.

Vogel KS, Klesse LJ, Velasco-Miguel S, Meyers K, Rushing EJ, Parada LF (1999) Mouse tumor model for neurofibromatosis type 1. Science 286(5447):2176-9.

Wallace MR, Marchuk DA, Andersen LB, Letcher R, Odeh HM, Saulino AM, Fountain JW, Brereton A, Nicholson J, Mitchell AL, et al (1990) Type 1 neurofibromatosis gene: identification of a large transcript disrupted in three NF1 patients. Science 249(4965):181-6.

Wang B, David MD, Schrader JW (2005) Absence of caprin-1 results in defects in cellular proliferation. J Immunol 175(7):4274-82.

Welch HC, Coadwell WJ, Stephens LR, Hawkins PT (2003) Phosphoinositide 3-kinase-dependent activation of Rac. FEBS Lett 546(1):93-7. Review.

Wilkerson LS, Touster O (1993) Biosynthetic and structural studies on Thy-1 in a rat neuronal tumor cell line. Arch Biochem Biophys 303(2):238-45.

Wrenn CC (2004) Social transmission of food preference in mice. Curr Protoc Neurosci. Chapter 8:Unit 8.5G.

Wu X, Kihara T, Akaike A, Niidome T, Sugimoto H (2010) PI3K/Akt/mTOR signaling regulates glutamate transporter 1 in astrocytes. Biochem Biophys Res Commun. 393(3):514-8.

Xu GF, O'Connell P, Viskochil D, Cawthon R, Robertson M, Culver M, Dunn D, Stevens J, Gesteland R, White R, et al (1990) The neurofibromatosis type 1 gene encodes a protein related to GAP. Cell 62(3):599-608.

Xu H, Gutmann DH (1997) Mutations in the GAP-related domain impair the ability of neurofibromin to associate with microtubules. Brain Res 759(1):149-52.

Yamagata Y, Jovanovic JN, Czernik AJ, Greengard P, Obata K (2002) Bidirectional changes in synapsin I phosphorylation at MAP kinase-dependent sites by acute neuronal excitation in vivo. J Neurochem 80:835-842.

Yang B, Steegmaier M, Gonzalez Jr LC, Scheller RH (2000) nSec1 binds a closed conformation of syntaxin1A. J Cell Biol 148:247-252.

Yonan AL, Alarcon M, Cheng R, Magnusson PK, Spence SJ, Palmer AA, Grunn A, Juo SH, Terwilliger JD, Liu J, Cantor RM, Geschwind DH, Gilliam TC (2003) A genomewide screen of 345 families for autism-susceptibility loci. Am J Hum Genet 73:886-897.

Young AW, Aggleton JP, Hellawell DJ, Johnson M, Broks P, Hanley JR (1995) Face processing impairments after amygdalotomy. Brain 118:15-24.

Young LJ (2002) The neurobiology of social recognition, approach, and avoidance. Biol Psychiatry 51(1):18-26.

Zacco A, Cooper V, Chantler PD, Fisher-Hyland S, Horton HL, Levitt P (1990) Isolation, biochemical characterization and ultrastructural analysis of the limbic system-associated membrane protein (LAMP), a protein expressed by neurons comprising functional neural circuits. J Neurosci 10:73-90.

Zafeiriou DI, Ververi A, Vargiami E (2007) Childhood autism and associated comorbidities. Brain Dev 29(5):257-72. Review.

Zanca A, Zanca A (1980) Antique illustrations of neurofibromatosis. Int J Dermatol 19(1):55-8.

Zang M, Hayne C, Luo Z (2002) Interaction between active Pak1 and Raf-1 is necessary for phosphorylation and activation of Raf-1. J Biol Chem 277(6):4395-405.

Zhang SC, Fedoroff S (1997) Cellular localization of stem cell factor and c-kit receptor in the mouse nervous system. J Neurosci Res 47(1):1-15.

Zeid JL, Charrow J, Sandu M, Goldman S, Listernick R (2006) Orbital optic nerve gliomas in children with neurofibromatosis type 1. J AAPOS 10(6):534-9.

Zhang SC, Fedoroff S (1997) Cellular localization of stem cell factor and c-kit receptor in the mouse nervous system. J Neurosci Res 47(1):1-15.

Zhang YY, Vik TA, Ryder JW, Srour EF, Jacks T, Shannon K, Clapp DW (1998) Nf1 regulates hematopoietic progenitor cell growth and ras signaling in response to multiple cytokines. J Exp Med 187(11):1893-902.

Zöller ME, Rembeck B (1999) A psychiatric 12-year follow-up of adult patients with neurofibromatosis type 1. J Psychiatr Res 33(1):63-8.

Zucker RS (1989) Short-term synaptic plasticity. Annu Rev Neurosci 12:13-31. Review.

CURRICULUM VITAE

John Paul Spence

Education

2004-2010
Ph.D. in Medical Neuroscience Program
Indiana University, Indianapolis, IN
Advisor, Anantha Shekhar, MD, PhD

1997-2000
B.S. in Biology, Indiana University, Bloomington, IN

Honors and Awards

2009
CTSI Travel Award, Indiana Clinical and Translational Science Institute (CTSI), Indianapolis, IN
2009
Funding to attend "Synapses: From Molecules to Circuits & Behavior" meeting, Cold Spring Harbor Laboratory, Cold Spring Harbor, NY
2008
Featured in: "A mouse model for autism" by Virginia Hughes, Simons Foundation Autism Research Initiative, New York, NY
2008
Hingtgen Travel Award (HTA), Indiana University School of Medicine, Department of Psychiatry, Indianapolis, IN
2000
Founder's Day Award, Indiana University, Bloomington, IN
1997-2000
Honor's Division Scholarship, Honors Division, Indiana University, Bloomington, IN
1997-2000
The Faculty Award, Indiana University, Bloomington, IN
1997
The Times Scholarship, The Times Newspaper, Munster, IN
1997
FCSLA Scholarship, Zenska Jednota, Beachwood, OH

Fellowships

2009-2010
Pre-doctoral Fellowship in Translational Research, Indiana Clinical and Translational Science Institute (CTSI), Indianapolis, IN

2008-2009
Pre-doctoral Fellowship in Translational Research, Indiana Clinical and Translational Science Institute (CTSI), Indianapolis, IN

Research and Training Experience

2001-2004
Research Technician, Molecular Biology and Alcohol Research, Department of Medicine, Indiana University School of Medicine, Indianapolis, IN
2000
Undergraduate Teaching Intern, "Genetics," Department of Biology, Indiana University, Bloomington, IN
2000
Undergraduate Teaching Intern, "Good Genes, Bad Genes," Department of Biology, Indiana University, Bloomington, IN
1999
Undergraduate Teaching Intern, "Biological Mechanisms," Department of Biology, Indiana University, Bloomington, IN
1999
Research Assistant, Eric Rasmusen, Kelly School of Business, Indiana University, Bloomington, IN

Technical Experience

Preparation and analysis of DNA:
PCR, sequencing, probe hybridization, minipreps, maxipreps, restriction digest, ligation, vector construction
Preparation and analysis of RNA:
Isolation of RNA, RT-PCR
Cell Culture:
Growth of various cell lines, transient transfection assays, luciferase and renilla assays
Surgical Procedures:
Catheter insertion (femoral artery)
Behavioral assessments:
Social behavior tests, elevated plus maze, open field test, forced swim test, olfactory habituation test

Publications

1. **Spence JP**, Molosh AI, Segu ZM, Goswami C, Zhu W, Li L, Mechref YS, Clapp DW, Shekhar. Neurofibromatosis type 1 (Nf1) gene deletion acting via p21-activated kinase 1 (Pak1) dependent mechanism selectively disrupts social memory formation and increases GABA inhibition in the amygdala. [In preparation]

2. **Spence JP**, Fitz SD, Eskay R, Carr LG, Heilig M, Shekhar A, Liang T. Selectively bred alcohol-preferring (P) and -nonpreferring (NP) rats show differences in response to restraint stress and corticotrophin-releasing hormone 2 receptor (Crfr2) expression. [Submitted ot Alcohol Clin Exp Res on September 5, 2010]
3. **Spence JP**, Liang T, Liu L, Johnson PL, Foroud T, Carr LG, Shekhar A (2009) From QTL to candidate gene: a genetic approach to alcohol abuse research. Curr Drug Abuse Rev 2(2):127-134.
4. Carr LG, Habegger K, **Spence JP**, Liu L, Lumeng L, Foroud T (2006) Development of congenic rat strains for alcohol consumption derived from the alcohol-preferring and nonpreferring rats. Behav Genet 36(2):285-90.
5. **Spence J**, Liang T, Foroud T, Lo D, Carr L (2005) Expression profiling and QTL analysis: a powerful complementary strategy in drug abuse research. Addict Biol 10(1):47-51. Review.
6. **Spence JP**, Liang T, Habegger K, Carr LG (2005) Effect of polymorphism on expression of the neuropeptide Y gene in inbred alcohol-preferring and -nonpreferring rats. Neuroscience 131(4):871-6.
7. Ehlers CL, **Spence JP**, Wall TL, Gilder DA, Carr LG (2004) Association of ALDH1 promoter polymorphisms with alcohol-related phenotypes in southwest California Indians. Alcohol Clin Exp Res 28(10):1481-6.
8. Liang T, Habegger K, **Spence JP**, Foroud T, Ellison JA, Lumeng L, Li TK, Carr LG (2004) Glutathione S-transferase 8-8 expression is lower in alcohol-preferring than in alcohol-nonpreferring rats. Alcohol Clin Exp Res 28(11):1622-8.
9. Carr LG, Habegger K, **Spence J**, Ritchotte A, Liu L, Lumeng L, Li TK, Foroud T (2003) Analyses of quantitative trait loci contributing to alcohol preference in HAD1/LAD1 and HAD2/LAD2 rats. Alcohol Clin Exp Res 27(11):1710-7.
10. Carr LG, **Spence JP**, Peter Eriksson CJ, Lumeng L, Li TK (2003) AA and ANA rats exhibit the R100Q mutation in the GABAA receptor alpha 6 subunit Alcohol 31(1-2):93-7.
11. **Spence JP**, Liang T, Eriksson CJ, Taylor RE, Wall TL, Ehlers CL, Carr LG (2003) Evaluation of aldehyde dehydrogenase 1 promoter polymorphisms identified in human populations. Alcohol Clin Exp Res 27(9):1389-94.
12. Foroud T, Ritchotte A, **Spence J**, Liu L, Lumeng L, Li TK, Carr LG (2003) Confirmation of alcohol preference quantitative trait loci in the replicate high alcohol drinking and low alcohol drinking rat lines. Psychiatr Genet 13(3):155-61.
13. Liang T, **Spence J**, Liu L, Strother WN, Chang HW, Ellison JA, Lumeng L, Li TK, Foroud T, Carr LG (2003) alpha-Synuclein maps to a quantitative trait locus for alcohol preference and is differentially expressed in alcohol-preferring and -nonpreferring rats. Proc Natl Acad Sci USA 100(8):4690-5.

Abstracts

1. **Spence JP**, Molosh AI, Zhu W, Michels EG, Dietrich A, Clapp DW, Shekhar A. p21-activated kinase 1 (Pak1) inactivation restores social learning and amygdala netwok deficits in a mouse model of Neurofibromatosis type 1 (NF1) (Society for Neuroscience, 2009)
2. **Spence JP**, Molosh AI, Michels EG, Dietrich A, Clapp DW, Shekhar A. p21-activated kinase 1 (Pak1) inactivation rescues social learning deficits in a mouse strain relevant to autism (Cold Spring Harbor Laboratory, 2009)
3. **Spence JP**, Michels EG, Dietrich A, Clapp DW, Shekhar A. p21-activated kinase 1 inactivation rescues social learning deficits in a mouse strain relevant to autism (IUPUI Research Day, 2009)
4. **Spence JP**, Dietrich A, Michels EG, Clapp DW, Shekhar A. NF1 mutation mediated p21ras activation selectively disrupts social learning/memory which is rescued by p21-activated kinase (Pak1) inactivation: Implications for the pathophysiology and treatment of autism spectrum disorders (American College of Neuropsychopharmacology, 2008)
5. **Spence JP**, Clapp DW, Shekhar A. Deletion of neurofibromatosis type 1 (Nf1) gene in mice leads to deficits in social learning (Society for Neuroscience, 2008)
6. **Spence JP**, Liu L, Foroud T, Carr LG, Shekhar A. Quantitative trait loci for body weight identified on chromosomes 3 and 4 in male inbred alcohol-preferring (iP) and -nonpreferring (iNP) rats (Research Society on Alcoholism, 2007)
7. Eriksson CJP, Lind PA, Carr LG, **Spence JP**, Wilhelmsen KC. ALDH1A1 polymorphism and alcohol addiction in Finnish populations (International Society for Biomedical Research on Alcoholism, 2006)
8. **Spence JP**, Liu L, Foroud T, Fitz SD, Sajdyk TJ, Carr LG, Shekhar A. The chromosome 4 QTL for alcohol consumption identified in alcohol-preferring and -nonpreferring rats also modulates body weight and anxiety-like behavior in males (Society for Neuroscience, 2005)
9. Carr LG, **Spence JP**, Alam I, Turner C, Sajdyk T, Liang T. A QTL for alcohol consumption in iP and iNP rats also influences bone mass, anxiety-like behavior and weight (Cold Spring Harbor Laboratory, 2005)
10. Carr LG, Liang T, **Spence JP**, Lumeng L, Li TK, Foroud T. Identifying genes underlying QTLs for alcohol preference in alcohol-preferring and -nonpreferring rats (International Society for Biomedical Research on Alcoholism, 2004)
11. Luczak SE, **Spence JP**, Carr LG, Hsueh AC, Wall TL. ALDH1A1 status relates to alcohol dependence in Chinese- and Korean-American college students (International Society for Biomedical Research on Alcoholism, 2004)
12. Carr LG, **Spence JP**, Taylor RE, Liang T. ALDH1 promoter polymorphism: genetic contribution to the predisposition for alcoholism in an African American population (International Society for Biomedical Research on Alcoholism, 2004)

13. Eriksson CJ, Yamamoto H, **Spence JP**, Carr LG. Role of alcohol- and aldehyde-dehydrogenase polymorphism in the protection of alcoholism in Finnish populations (Research Society on Alcoholism, 2004)
14. Ehlers CL, **Spence JP**, Wall TL, Garcia-Andrade C, Gilder DA, Carr LG. Associations between ALDH1A1 promotor polymorphisms, alcohol dependence and drinking behaviors in Mission Indians (Research Society on Alcoholism, 2004)
15. Liang TB, Habegger K, **Spence J**, Ellison JA, Lumeng L, Li TK, Carr LG. Glutathione-S- Transferase 8 expression is lower in alcohol-preferring than in -nonpreferring rats (Research Society on Alcoholism, 2004)
16. Carr LG, Habegger K, **Spence JP**, Liang TB, Liu LX, Lumeng L, Li TK, Foroud T. QTLs Contributing to Alcohol Preference in HAD1/LAD1 and HAD2/LAD2 Rats (Research Society on Alcoholism, 2003)
17. Liang TB, **Spence J**, Liu LX, Strother WN, Chang HW, Ellison JA, Lumeng L, Li TK, Carr LG. Alpha-synuclein expression is higher in alcohol preferring than alcohol-nonpreferring rats (Research Society on Alcoholism, 2003)
18. Liu L, **Spence J**, Habegger K, Lumeng L, Li TK, Foroud T, Carr LG. Quantitative trait loci influencing alcohol consumption in the high alcohol drinking and low alcohol drinking rats were confirmed in the replicate rat lines (Research Society on Alcoholism, 2003)
19. Liang T, **Spence JP**, Taylor R, Wall TL, and Carr LG. Expression and association study of human ALDH1 promoter mutations (Research Society on Alcoholism, 2002)